

ASD-TDR-62-787

AD-403713

**STUDIES OF
ROCKET NOISE SIMULATION WITH SUBSTITUTE GAS JETS
AND
THE EFFECT OF VEHICLE MOTION ON JET NOISE**

TECHNICAL DOCUMENTARY REPORT NO. ASD-TDR-62-787

MARCH 1963

Flight Dynamics Laboratory
Aeronautical Systems Division
Air Force Systems Command
Wright-Patterson Air Force Base, Ohio

Project No. 1370, Task No. 137005

(Prepared under Contract No. AF 33(616)-8201

by

Walter V. Morgan and Kenneth J. Young
The Boeing Company
Seattle 24, Washington)

Flight Dynamics Lab.

NOTICES

When Government drawings, specifications, or other data are used for any purpose other than in connection with a definitely related Government procurement operation, the United States Government thereby incurs no responsibility nor any obligation whatsoever; and the fact that the Government may have formulated, furnished, or in any way supplied the said drawings, specifications, or other data, is not to be regarded by implication or otherwise as in any manner licensing the holder or any other person or corporation, or conveying any rights or permission to manufacture, use, or sell any patented invention that may in any way be related thereto.

Qualified requesters may obtain copies of this report from the Armed Services Technical Information Agency, (ASTIA), Arlington Hall Station, Arlington 12, Virginia.

This report has been released to the Office of Technical Services, U.S. Department of Commerce, Washington 25, D.C., in stock quantities for sale to the general public.

Copies of this report should not be returned to the Aeronautical Systems Division unless return is required by security considerations, contractual obligations, or notice on a specific document.

FOREWORD

The research work in this report was performed by the Aero-Space Division, The Boeing Company, Seattle, Washington, for the Flight Dynamics Laboratory, Directorate of Aeromechanics, Deputy for Technology, Aeronautical Systems Division, Wright-Patterson Air Force Base, Ohio, under Contract Nr. AF33(616)-8201. This research is part of a continuing effort to obtain economic prediction methods to integrate acoustic analysis into the early design stage of flight vehicles which is part of the Air Force Systems Command's Applied Research Program 750A, the Mechanics of Flight. The Project Nr. is 1370 "Dynamic Problems in Flight Vehicles" and the Task Nr. is 137005 "Methods of Noise Prediction, Control, and Measurement". Davey Smith and later Phillip Hermes of the Flight Dynamics Laboratory were the Project Engineers.

This report has been authored by Walter V. Morgan and Kenneth J. Young. The research work was conducted under the supervision of Kenneth J. Young, Senior Group Engineer of the Acoustics Group, Aero-Space Division, The Boeing Company. The Project Leader was Walter V. Morgan. Primary technical assistance with all phases of the project, especially the test work and data processing, was given by James L. Walker. Other members of the Acoustics Group who made major contributions to this program include: Stanley C. Oas and Henry A. Kumasaka in processing and presenting the data and in editing of the report, Marion D. Lockleer in providing acoustic instrumentation and calibration, and David A. Bateman in designing and supervising fabrication of all mechanical test apparatus.

ABSTRACT

Part I -- The feasibility of using helium jets as a practical substitute for actual rockets in scale model acoustic tests was investigated by conducting an experimental program with four heated helium models. Sufficient evidence is presented to indicate that the substitute gas modeling concept is valid, i.e., simulation of rocket noise can be achieved if the essential rocket flow parameters are duplicated. Since it is not possible to duplicate all flow parameters simultaneously and still retain the essential feature of simplicity, some compromises must be made. The helium model which provided rocket exit values of Mach number, velocity, and static pressure, and near duplication of density performed best. This evaluation is based on agreement in sound pressure levels with a small solid propellant rocket.

Part II -- An investigation was made to determine the effect of flight vehicle motion on propulsion system noise which is propagated to parts of the vehicle located in the near field. Following the selection of a working hypothesis, experiments were performed using a 0.6-inch diameter heated air jet operating in a 16-inch diameter acoustically-treated wind tunnel. Experimental results compare favorably with predictions based on the hypothesis which explains the effect of vehicle motion by two separate factors: (1) the noise produced by a jet in motion is dependent upon the relative velocity between the jet and the air through which it moves; and (2) a shifting of the noise radiation pattern toward the rear occurs because of the combined effects of vehicle motion and the finite velocity of sound. A prediction method is developed which makes use of noise data from a stationary jet operated at a velocity corresponding to the relative jet velocity of a moving vehicle. These measured data are then translated by a calculated amount to account for the rearward shifting of the noise field due to motion.

PUBLICATION REVIEW

This report has been reviewed and is approved.

FOR THE COMMANDER:

Walter J. Mykytow
WALTER J. MYKYTOW
Chief, Dynamics Branch
Flight Dynamics Laboratory

TABLE OF CONTENTS

PART I: ROCKET NOISE SIMULATION WITH SUBSTITUTE GAS JETS

<u>Section</u>	<u>Page</u>
I. INTRODUCTION.	3
II. SELECTION OF EXPERIMENTAL CONDITIONS	4
A. Selection of Rocket Data	4
B. Selection of Significant Flow Parameters	4
C. Selection of Working Fluids	5
D. Flow Parameters of Model Solid Propellant Rocket and Helium Substitute Gas Model	6
III. APPARATUS, INSTRUMENTATION, AND OPERATING PROCEDURES	8
IV. RESULTS AND DISCUSSION	9
A. Far Field Results	9
B. Discussion of Far Field Results	10
C. Near Field Results	12
D. Discussion of Near Field Results	13
E. Summary of Performance	13
V. CONCLUSIONS	15
APPENDIX I	16

PART II. EFFECT OF VEHICLE MOTION ON JET NOISE

<u>Section</u>	<u>Page</u>
I. INTRODUCTION	45
II. HYPOTHESIS AND DISCUSSION	47
A. Hypothesis	47
B. Discussion	47
C. Procedure for Predicting Effects of Vehicle Motion	48
III. TEST APPARATUS, INSTRUMENTATION, AND PROCEDURES	49
A. Selection and Description of Apparatus	49
B. Instrumentation	50
C. Wind Tunnel Performance and Operation	51
IV. RESULTS AND DISCUSSION	53
A. Data Processing Method	53
B. Discussion	55
V. CONCLUSIONS	60
APPENDIX II	61
REFERENCES	92

LIST OF ILLUSTRATIONS

<u>Figure</u>	<u>Page</u>
PART I	
1. Flow and measurement systems for heated helium tests. . . .	22
2. Measurement locations for solid propellant rocket and heated helium tests	23
3. Test apparatus and microphone array for heated helium tests	24
4. Time variation of plenum pressure, plenum temperature, and sound pressure level during a heated helium test.	25
5. Sound pressure levels measured at 100 nozzle diameters radius vs. angle for the solid propellant model rocket and heated helium jets.	26
6. Representative far field sound pressure levels for the solid propellant model rocket and heated helium jets. . . .	31
7. Overall sound pressure levels measured at 100 nozzle diameters radius vs. angle for the solid propellant model rocket and heated helium jet Condition D.	32
8. Total radiated acoustic power levels of solid propellant model rocket and heated helium jets	33
9. Angle of half-power radiation vs. frequency for solid propellant model rocket and heated helium jets.	35
10. Near field sound pressure levels for the solid propellant model rocket and heated helium jets	36
11. Apparent source locations for one-third octave bands of noise as determined by microphones placed close to the exhaust	41
PART II	
12. Geometrical relationship between angles α and β for a jet in motion	65
13. Relationship between $(\beta - \alpha)$ and β for a jet in motion at various Mach numbers.	66
14. Schematic diagram of 16-inch wind tunnel assembly	67
15. Photograph of 16-inch wind tunnel assembly.	68

LIST OF ILLUSTRATIONS (Cont.)

<u>Figure</u>	<u>Page</u>
16. Assembled and exploded views of Bruel & Kjaer Type 4134 microphone with probe.	69
17. Model jet placement in wind tunnel and microphone locations used in obtaining noise data for both static and wind conditions	70
18. Frequency response of probe microphone with electrical equalization	71
19. Background noise in wind tunnel test section	71
20. Source locations for various frequency bands of noise generated by the 0.6-inch model jet.	72
21. Illustration of method of predicting the change in SPL at a location due to vehicle motion.	73
22. Comparisons of measured and predicted SPL versus frequency for various measurement stations	74
23. Measured vs. predicted values of noise reduction due to motion	84
24. Comparison of measured and predicted SPL versus station for the 8000 cps band (one-third octave)	85
25. Position shift of noise due to motion for various 1/3 octave frequency bands	86
26. Mathematical relationship between angles α and β for the moving vehicle situation	91

LIST OF TABLES

<u>Table</u>	<u>Page</u>
PART I	
I. Properties of selected gases	18
II. Flow parameters of solid propellant model rocket and heated helium jets	19
III. Sound pressure levels for heated helium jet Condition D. . .	20
IV. Summary of agreement of helium and rocket data	21
PART II	
V. Jet flow parameters and wind tunnel operating conditions . .	62
VI. Agreement of measured data with predicted values	63
VII. Estimated reduction in sound pressure level due to relative velocity effects	64

LIST OF SYMBOLS

A	cross-sectional area (ft ²)
a	acoustic velocity (ft/sec)
g	acceleration due to gravity (32.2 ft/sec ²)
M	Mach number, V/a or S/a
ND	Nozzle exit diameters
P	pressure (lb/in ²)
PWL	acoustic power level (db re: 10 ⁻¹³ watt)
R	gas constant (ft-lb/lb-°R)
S	vehicle (or wind) velocity (ft/sec)
SPL	sound pressure level (db re: 0.0002 microbar)
T	temperature (°R, unless otherwise noted)
V	jet velocity (ft/sec)
W	jet stream mechanical power: $\frac{1}{2} \frac{\dot{W}}{g} V^2$ (ft-lb/sec), or 0.021 $\dot{W} V^2$ (watts)
\dot{W}	rate of weight flow (lb/sec)
α, β	angles specifying receiver locations relative to noise source
γ	ratio of specific heats, c_p/c_v
ρ	density (lb/ft ³)

Subscripts and superscripts:

e	conditions at nozzle exit
t	total (plenum) conditions
*	conditions at nozzle throat for supersonic flow

PART I

ROCKET NOISE SIMULATION

WITH

SUBSTITUTE GAS JETS

I. INTRODUCTION

Scale model rockets are used during early design stages as a means of predicting the acoustic environment associated with flight vehicles. The concept of using heated helium as a substitute for actual rocket fuel for scale model acoustic testing was developed in the course of research performed under a previous USAF contract (Reference 1). The objective of Part I of the present study is to investigate the feasibility of such an approach.

The fluid which is exhausted by any full scale jet or rocket engine will be referred to as the "full scale gas" for that particular engine. Similarly, the fluid exhausted by any model jet or rocket will be referred to as the "model gas" for that particular model. If the model uses a gas which is different from the full scale gas for the engine being modeled, then the model will be considered to be using a "substitute gas".

The practical reasons for using substitute gas models are based on simplification of scale model techniques. Model testing with even small rocket engines requires extensive safety precautions. In addition, a failure of the rocket apparatus results in costly repairs and delays in the test program. The ability to conduct a model test with a convenient substitute gas results in considerable savings and advantages. These benefits appear as reduced costs of test facilities, apparatus, and operation through a reduction in the hazardous nature of the test and the time required for testing.

The use of substitute gases may also assist in providing an understanding of the theory of noise generation. For example, consider two similar experiments which have common values for a limited number of parameters. Then if the same noise field results in each case, it may be concluded that the parameters which are not duplicated either do not significantly affect the generation of noise or the effect of one parameter is compensated by an opposing effect of some other parameter. By use of substitute gases, the matching of parameters can be controlled more readily and a systematic sorting of the important variables may be accomplished.

The principle of using substitute gases applies equally well to all classes of jets, which include straight turbojets, afterburning turbojets, and liquid and solid rockets. However, because of the greater apparent savings, the practical emphasis will be placed on evaluating substitute gas models which might be used to simulate rockets.

It is assumed that the noise generated by any exhaust stream is primarily dependent upon stream parameters such as velocity, density, and Mach number which can basically be evaluated by the measurement of pressures and temperatures. This implies that the noise is not especially dependent upon inherent properties of the fluid being used, such as molecular weight and thermal capacity. This assumption is fundamental to the validity of substitute gas applications in acoustic scale model experiments.

Manuscript released by the authors 21 December 1962 for publication as an ASD Technical Documentary Report.

II. SELECTION OF EXPERIMENTAL CONDITIONS

A. Selection of Rocket Data

Conventional models which use actual rocket fuels and differ from their full scale counterparts only in size are known to duplicate full scale rocket noise quite well. Considerable acoustic data were available for a solid propellant rocket model*, having been obtained during a series of rocket firings conducted by The Boeing Company for research purposes. These rocket noise data included both near field and far field sound pressure levels generated by the rocket with an undeflected exhaust. Sufficient data were available to determine power level and directivity as a function of frequency, thus providing a convenient reference on which to establish the validity of the substitute gas model through correlation of experimental results. In addition, the same acoustic instrumentation used for the reference rocket data measurements could be used for the helium jet surveys, thus minimizing a possible error.

The reference model rocket used a single nozzle with an exit diameter of 2.33 inches; it produced 430 pounds of thrust for approximately one second. Data obtained for three firings of this configuration were sufficiently repeatable that only the average of the data from the three firings is reported. The rocket exhausted horizontally into a free field, the centerline of the exhaust being 26 nozzle exit diameters above the ground plane. Acoustic data were obtained in the far field at a radius of 100 nozzle diameters from the nozzle exit and in the near field along the jet boundary and forward of the nozzle.

B. Selection of Significant Flow Parameters

The initial step in design of an experiment is to select the parameters which are believed to be significant. In some instances it is not possible to simultaneously provide the desired values of all parameters. Then it is necessary to give preference to those believed most important or to perform successive experiments to observe relative effects. It is desired eventually to accumulate sufficient experimental evidence of the relative importance of the various parameters so that experiments may be designed on this basis. The present effort represents the beginning of this accumulation of experimental evidence.

Previous work on the subject of substitute gases reported in Reference 1 was based on the assumption that jet exit velocity, density, and Mach number were the most important parameters affecting noise generation. However, a thorough study of the subject must include the consideration of additional variables of possible significance. The additional variables considered are discussed below.

*The solid propellant was a standard composition of polybutadiene-acrylic acid and ammonium perchlorate with aluminum additive.

- (1) The work reported in Reference 1 was limited to ideally expanded jets. In the current study the possible effects of overexpansion of the nozzle are considered by including the static gas pressure at the nozzle exit as a variable.
- (2) For supersonic exhausts the exit velocity might be replaced by the acoustic velocity at the throat as a significant flow parameter.
- (3) It may be appropriate also to consider the viscosity of the gas since shear forces in fluids are dependent on viscosity.
- (4) Since the acoustic power radiated by rockets appears to be directly related to the jet stream mechanical power, it is appropriate to consider the stream power as a variable to be investigated.

C. Selection of Working Fluids

The main problem encountered in using a substitute gas to model a rocket is achieving the high exit velocities of rocket exhaust gases. Within a practical range of plenum pressures, exit velocities of only a few times the acoustic velocity are possible. It is therefore desirable that high acoustic velocity be a characteristic of the substitute gas to be used. Ease of handling the gas (absence of explosive or toxic properties) is also an important consideration, and finally the cost must be considered.

A comprehensive study of gases which might be useful in substitute gas models has been made, resulting in the information included in Table I. Not included in this table are gases which are deadly poisons (chlorine, phosgene, etc.) and those which are obviously much too expensive to consider using in quantity (krypton, xenon). The indications of hazards associated with these gases are intended as approximations only. More detailed information may be found in References 2 through 8. The decision as to whether a particular gas is safe to use must be made by the individual or group directly involved, because safety depends mostly on the availability of proper facilities and experience of the personnel.

The importance of Table I is that it shows only ten gases qualifying for widespread use on the basis of handling ease. These are the first ten of the listed gases. Of these it is next appropriate to determine which have acoustic velocities sufficiently high to allow their use at reasonably low temperature to achieve simulation of the rocket exit velocity.

Since the local velocity is the local acoustic velocity times the local Mach number, we may write

$$V = Ma = M \sqrt{\gamma g R T} \quad (1)$$

Selecting values of γ and R for a typical rocket, it is found that $\sqrt{\gamma R} = 7.8$. The quantity $\frac{\sqrt{\gamma R}}{7.8}$ has therefore been chosen to be called the

relative acoustic velocity. This is then an index as to how hot a gas must be in order to provide a desired acoustic velocity. For example, a gas having a relative acoustic velocity of 2 would have the same acoustic velocity as a rocket at just one-fourth of the absolute temperature. Although the temperature of concern is usually the exit temperature, the plenum temperatures can be used for the purpose of sorting out potentially useful gases. Taking 6000 °R as a typical rocket temperature, it may be seen that the velocities could be approximately matched by a gas heated to 1500 °R (the approximate limit of a simple burner) if it had a relative acoustic velocity of 2. Of the "safe" gases only helium qualifies. If the substitute gas could be heated to 3500 °R, gases with relative acoustic velocities of about 1.3 and greater could be included. Of the "safe" gases only neon and steam could then be considered in addition to helium, and for practical purposes steam can be eliminated because of the excessive pressures which would be required. Neon has no physical properties to make it preferable to helium, and it is more expensive. Helium therefore emerges as the clear choice for a substitute gas for modeling rockets. This conclusion might be altered if a less safe gas were to be seriously considered, if the full scale exhaust being modeled operated at significantly lower temperatures than conventional rockets, or if the exit Mach numbers or exhaust velocities of the substitute and full scale gas flows were permitted to be different by a large amount.

D. Flow Parameters of Model Solid Propellant Rocket and Helium Substitute Gas Model

Table II lists significant flow parameters of the solid propellant model rocket selected to provide reference data. Also listed in Table II are parameters of four helium flow conditions which were designed to have various flow parameters numerically equal to those of the model rocket.

In Reference 1 exit values of Mach number, density, and velocity were selected as being the most important parameters influencing noise generation. Limited experimental data presented there appeared to support this hypothesis as applied to turbojets and jets operating in the afterburning range. As a first attempt at making a substitute gas model of a rocket, the exit Mach number, density, and velocity were therefore selected to be the same as those for the solid propellant rocket. This is helium Condition A in Table II.

The work with substitute gas models reported in Reference 1 applies only to fully expanded flows; however, virtually all rockets produce overexpanded flow at the nozzle exit. A given rocket using a basic nozzle which varies only in the diameter of its exit will produce the same mass flow, and within a few percent the same sea level static thrust. It does not seem reasonable, therefore, to expect the noise to change by as large an amount as would be predicted by examining velocities and densities (or jet stream mechanical power) calculated for the exit. This effect for overexpanded exhausts has in fact been noted by NASA in Reference 9. It will be considered sufficient to note that the degree of over-expansion could logically have some influence on the noise generated.

For helium Condition A (Table II) the exit static pressure is significantly lower than for the model rocket. It is therefore noted that in one possibly important respect, helium Condition A is not the same as the model rocket. Of the four flow parameters (Mach number, density, velocity, and overexpansion as measured by exit pressure), it is possible to provide the desired values of only three at any one time unless the ratios of specific heats (γ) for the substitute and full scale gases are the same. Since γ for helium is quite different from the rocket value of γ , the elimination of overexpansion as a variable from the helium flow requires that one of the other parameters become a variable.

From the work of Reference 1 it was concluded that the effects on noise of varying density over a limited range were fairly predictable. Therefore, helium Condition B (Table II) was calculated differing from Condition A in that the exit density was allowed to increase so that the exit pressure would match the rocket value. If the noise generated is assumed proportional to the first power of density, the sound levels from Condition B will be 1.5 db too high.

The use of jet stream mechanical power, W , as an indication of the noise to be expected combines flow velocity and density in place of separate consideration of velocity and density effects. Helium Condition A matches the model rocket values of velocity and density and therefore has the same value of relative jet stream mechanical power (W_{rel}). Helium Condition C was also selected to provide the model rocket value of W_{rel} , but with neither velocity nor density at the rocket values. The Mach number and exit pressure were, however, maintained at the rocket values.

Some data have been collected which indicate that for supersonic flow the acoustic power generated is dependent upon a high power, possibly the eighth, of the acoustic velocity at the throat, a^* . The reason for considering this velocity as a possibly important parameter stems from the observation that most of the noise generated by supersonic exhausts seems to come from well downstream of the nozzle in the subsonic region of the jet. If it is assumed that there is no heat loss, the sonic velocity downstream of the nozzle is the same as the sonic velocity in the nozzle throat. For helium Condition C, a^* has the same value as for the model rocket. This happened coincidentally, that is, a helium model providing desired values of W , P_e and M_e can be found for any rocket, but usually a^* will then be different. As it turns out, Condition C can be interpreted to be testing the importance of either a^* or W_{rel} .

Helium Condition D, using a different nozzle, duplicated P_e and a^* . By almost any criterion Condition C would be expected to be a better model than D, but D serves a useful function in further separating possibly significant variables.

To summarize the helium conditions chosen: (1) Condition A is expected to produce noise different from the model rocket only because of different overexpansion, but this effect presently is not predictable; (2) Condition B is expected to produce the same noise as the rocket except that the density is high by an amount that might increase noise levels by about 1.5 db; (3) Condition C has erroneous velocity and density, these errors being in amounts which might cancel each other; (4) Condition D is related to the rocket only in that the sonic velocity at the throat and the degree of overexpansion are the same as for the rocket, so the resulting noise is not likely to be the same as for the rocket.

In addition to the above there are other helium conditions of interest. One of these would provide rocket values for all of the exit parameters believed important to the generation of noise except Mach number. However, the plenum temperature required would have been somewhat higher than was possible to attain with available facilities.

III. APPARATUS, INSTRUMENTATION, AND OPERATING PROCEDURES

Figure 1 shows schematically the apparatus used to produce the desired flow of helium and the instrumentation used to measure the flow and the resulting noise. The source of helium is bottles at 2200 psi pressure, each containing 213 standard cubic feet (approximately 2.2 pounds). Since the rate of flow possible from any cylinder is fairly small, 28 cylinders are manifolded together. Four large pressure regulators are operated in parallel to control the flow. The regulators provide a large volume flow at a pressure slightly below the pressure provided to the dome of the regulator. Bottled nitrogen controlled by a quick-acting valve and conventional regulator is used to supply the desired dome pressure. The regulator therefore acts as the main helium on-off valve as well as a pressure regulator. The discharge from the pressure regulators passes through a heat exchanger to a plenum and nozzle. Placement of the pressure regulators upstream of the heat exchanger is dictated by the inability of the regulator seals to withstand high temperatures. The pressure out of the regulators is maintained slightly higher than the desired plenum pressure to compensate for the small pressure drop across the heat exchanger.

The heat exchanger is of the cyclic storage type. Heated air passes through a large cylinder containing 221 thick-wall tubes of mild steel. Baffles position the tubes inside the cylinder and force the hot air to cross the outside surfaces of the tubes three times, assuring fairly even temperature distribution. The helium flow is in parallel through the tubes along a path separate from the heated air. Although this type heat exchanger is capable of continuous operation, it is used only in a transient manner, because relatively short duration helium flow is required. An advantage of the transient type operation is that shutting down the heated air flow prior to the helium test prevents any extraneous noise from the hot air exhaust.

Iron-constantan thermocouples inserted a few inches into each end of one of the helium flow tubes are used to determine the heat exchanger core temperature. The outputs of the thermocouples used for measuring the helium flow temperatures are recorded on an oscillograph and the corresponding temperatures are determined from standard tables. The helium plenum pressure is measured with a Statham pressure transducer and recorded on the oscillograph.

Locations of the microphones for the heated helium tests and for the solid propellant model rocket tests are shown in Figure 2. The noise data are recorded on magnetic tape. Playback of the data is through one-third octave band filters to a true rms graphic level recorder. One-third octave band filters are considered sufficiently narrow to detect any anomalies in the data. The helium weight flow which can be provided is not sufficient to operate a nozzle the same size as the

model rocket nozzle. A scale factor of 0.63 was chosen for the helium nozzle as a compromise between near maximum possible size and ease of data reduction. This scale factor requires exactly two one-third octaves shift in frequency. Measurements are made at scaled distances so that no corrections in sound levels are required to allow direct comparison of the helium and solid propellant rocket levels. The helium data which are reported, however, have all been shifted lower in frequency by the two-thirds octave required by the scale factor. The total acoustic power radiated by the smaller helium nozzles is, of course, lower than that radiated by the larger rocket nozzle. A correction of 4 db (assuming power proportional to nozzle area) is included in the reported helium jet acoustic power levels. The operating procedure for a typical heated helium test was as follows:

1. The pressure regulators were pre-set to the desired value. Typically the apparatus appeared as in Figure 3.
2. Hot air was supplied to the heat exchanger for a period of 3 to 15 minutes as necessary to heat the core to about 10° above the target temperature. This target temperature was in turn 20° to 50° above the desired helium plenum temperature.
3. Helium supply lines were opened, the pressure regulators then acting as the only helium valve.
4. At the time the thermocouples in the heat exchanger core indicated temperatures had decreased to the target values, a ten-second countdown commenced. At minus five seconds all recorders were started. At time zero, regulated pressure was applied to the domes of the main pressure regulators by opening the quick-acting valve. All recording channels were visually monitored for overloading. At plus two or three seconds the pressure to the domes was shut off, causing the main pressure regulators to close off the helium flow.
5. Necessary notations of attenuator settings, etc. were made, and then all recorders were turned off.
6. Valves of the helium supply bottles were turned off, and the pressure in the main supply lines was relieved.

Using this procedure it was possible to perform helium tests with various plenum conditions at an average rate of about three per hour. Three tests at each of the four helium conditions were conducted with indicated plenum temperature and pressure both within 3% of the target values. Complete data reduction was carried out for the three tests at each condition. For 95% of the data points, repeatability to within ±1 db was observed. Variations of temperature, pressure, and sound pressure level during one of the helium tests are shown in Figure 4.

IV. RESULTS AND DISCUSSION

A. Far Field Results

Far field overall and octave band sound pressure levels vs. angle for helium Conditions A, B, and C and the solid propellant rocket are given in Figure 5.

One-third-octave spectra for the above three helium conditions are compared with the rocket spectra at two locations in Figure 6. Sound levels for Condition D are presented separately in Figure 7 and Table III. The acoustic power level of each octave band for all helium conditions was computed from measured sound pressure level data; the results are presented in Figure 8.

The directivity of the noise for each helium jet condition and the rocket is shown by octave bands in Figure 9; this is presented as a means of simplifying and combining the information of Figure 5 and Table III. Since it is difficult to select by eye from Figure 5 a good representative value for the angle of maximum noise radiation, a graphical approach was used for finding the angle at which one-half of the acoustic power would be radiated forward (upstream) of that angle. This angle is referred to as the angle of half-power radiation. It is believed that this approach results in a more significant indication of directivity than by simply selecting the angle of maximum sound pressure level from Figure 5. This latter method gives too much weight to a single measurement which might have experimental error.

B. Discussion of Far Field Results

General trends of agreement with the rocket data are seen for helium Conditions A, B, and C in Figures 5, 6, 8 and 9. The agreement is best in the aft quadrant, where maximum noise is radiated. The major deviation of the helium data is that higher levels are consistently obtained in the forward quadrant. Each helium model differed from the rocket model in one or more possibly significant flow parameters; therefore, it is appropriate to investigate whether there are logical corrections which might be applied in each case. Since gross effects of jet parameters are usually observed more uniformly in the far field than in the near field, any proposed corrections should be applied first to the far field data.

The agreement of sound level data between helium Condition A and the solid propellant rocket, in general, is reasonably good; average values of root-mean-square deviations for fore and aft quadrants are 3.1 db and 1.8 db, respectively. The total radiated acoustic power of this model very nearly matches that of the rocket as shown in Figure 8 (a). Helium Condition A differed from the rocket primarily in having a low exit pressure and a high acoustic velocity at the throat. In view of the close agreement in power level, apparently no generally applied correction in the sound levels to account for these differences is appropriate. It may be seen in Figure 9 that the directivity of the noise for Condition A is shifted forward from that of the rocket at the higher frequencies. This result may possibly be due to the differences in either exit static pressure or throat acoustic velocity of Condition A.

The agreement of acoustic data for helium Condition B with that of the rocket is inferior to Condition A in the forward quadrant. The rms deviation there is 5 db while in the aft quadrant the deviation is 2 db which is comparable to that of Condition A. The octave band power levels of Condition B are about 2 db higher than those of the rocket as can be seen in Figure 8. Helium Condition

B duplicated the rocket values of Mach number, velocity, and exit pressure, but both the density and throat acoustic velocity were high. Assuming a first power correction is appropriate to account for the difference in density, all sound levels for Condition B should be decreased by 1.5 db. Applying this correction improves the agreement in sound pressure levels between Condition B and the rocket and makes the acoustic power level curves of the two nearly identical. (Condition B with the -1.5 db correction applied is called Condition B'.) The directivity of the noise for Condition B as shown in Figure 9 is shifted forward about 3° from that of the rocket at the higher frequencies. This shift, however, is less than for Condition A so possibly the duplication of exit pressure improved the agreement with the rocket.

The agreement of helium Condition C sound pressure levels with the rocket is fair, the rms deviation being approximately 4 db and 3 db in the forward and aft quadrants. Power level agreement between Condition C and the rocket is inferior to that of both Conditions A and B as may be seen in Figure 8. Neither velocity nor density was duplicated in Condition C, but these parameters were varied in such a way as to produce the same relative jet stream mechanical power as the rocket. The rocket values of Mach number, exit pressure, and throat acoustic velocity were also duplicated. Assuming the noise is proportional to the first power of density and the third power of velocity, the corrections to be applied to the acoustic data for Condition C are approximately -5 db for density and +5 db for velocity. On this basis it would be expected that helium Condition C would provide reasonable duplication of the rocket noise. When judged, however, by the far field criteria (SPL, PWL, and directivity), helium Condition C is inferior to Condition B'. Helium Condition C indicates an average shift in directivity of 4° in the aft direction when compared with the rocket (Figure 9). This directivity shift is possibly due to velocity or density differences which are not compensated for by maintaining the rocket value of mechanical power.

From Figure 8 (d) it can be seen that the acoustic power level for helium Condition D is much lower than that of the rocket. The design basis for Condition D was (1) to provide the same acoustic velocity as the rocket at the nozzle throat and (2) to provide the same nozzle exit pressure. It is apparent that these criteria alone are not adequate to design a substitute gas model. The exit Mach number for helium Condition D was much lower than for the rocket. At present there is no method available to correct for this difference. The density and velocity (and the jet stream mechanical power) were also different from the rocket values. Applying corrections for these parameters, again on the basis of first power of density and third power of velocity, a net of 7 db must be added to the acoustic power level for helium Condition D. (Condition D with the density and velocity corrections applied is called Condition D'.) With this correction included, the agreement in power level with the rocket is greatly improved, but it is definitely inferior to Condition B'.

Of the various helium conditions evaluated it is concluded that B' (Condition B with a -1.5 db correction for density) achieves the best simulation of the rocket noise in the far field. This conclusion is based on an overall evaluation of sound pressure levels, acoustic power levels, and directivity data.

In addition to evaluating the far field performance of the various helium models, it is desirable to explore possible causes for the general disagreement with the rocket at locations forward of the nozzle. There appears to be a definite possibility that the higher forward quadrant levels for Conditions A, B, B', and C are caused by reflections from building structure in the vicinity of the helium test area. Higher power is radiated at larger angles (e.g. 120°) relative to the forward jet axis than at smaller angles (e.g. 30°). If reflection from a wave is seen at the desired measurement position located at the smaller angle, then the reflected and incident pressures will combine to produce a higher sound level. A brief analysis of the present situation, considering the SPL differences and particular geometry involved, indicates that levels may be about 5 db high at the 30° measurement location; smaller increases are associated with measurement locations at larger angles up to 90°. Since the rocket tests were conducted at a different test site which was well removed from buildings, the reference rocket data are not believed to contain this type of error. It appears, then, that a large part of the forward quadrant deviations of the helium data relative to the rocket might be explained by the effect of reflections.

C. Near Field Results

One-third octave band sound pressure levels for all near field microphone locations for the rocket and helium Conditions A, B, and C are plotted in Figure 10 (a-i). Octave band data for helium Condition D are presented in tabulated form only (Table III). Because the condenser microphones used at locations close to the exhaust were limited in response at the high frequency end of the spectrum, only the data in the frequency range 160-10,000 cps are reported. The higher frequency capability of the M-213 crystal microphone would have been preferred, but the approximately 140-160 °F. temperature limitation on these microphones was considered to be too low in view of the proximity to the exhaust.

Figure 11 shows the apparent source locations, as a function of frequency, for the four helium models and the solid propellant rocket as determined from the near field data. These curves were obtained by cross-plotting the data of Figure 10 into a form which shows sound pressure level versus distance along the exhaust and forward of the nozzle. The apparent source location was determined by taking the mid-location of the region where the sound pressures were down 3 db from the highest level measured.

D. Discussion of Near Field Results

General trends in agreement with the near field rocket levels are seen for helium Conditions A, B, and C (Figure 10, a-i). In contrast with the far field situation, there is no strong tendency for the helium levels to be higher than those of the rocket for locations forward of the nozzle.

For helium Condition A the agreement of near field sound pressure levels with the rocket is reasonably good, except for microphone locations 8 and 9 (Figure 10, h and i). An average value of rms deviation computed for all near field locations is about 3.5 db, this figure being strongly influenced by the poor agreements at the two far downstream positions. Location of the low frequency sources in the jet compared to the rocket is only fair as indicated in Figure 11.

Sound pressure levels for Condition B are in closer agreement with the rocket, the rms deviation averaging slightly over 2 db for all nine near field locations. Application of the -1.5 db correction for density to the SPL data for Condition B does not significantly change the near field agreement. The apparent source locations for Condition B are on an average closer to those of the rocket than for Condition A; however, they do not appear to be distributed over as large a region of the jet as are the rocket sources.

The near field agreement of sound levels for Condition C with that of the rocket is comparable to that of Condition B and B'. The apparent source locations for Condition C also exhibit a similar distribution in the jet as shown in Figure 11.

Helium Condition D shows a distribution of apparent source locations greatly different from that of the rocket. This feature eliminates any hope that application of a general correction in SPL to Condition D will succeed in making it a satisfactory model for simulating rocket noise.

It is concluded that the best simulation of near field rocket noise is achieved with helium Conditions B, C, and B' (B corrected for density) and that there is little significant difference between these three conditions on an overall basis. The reflection problem discussed for the far field data does not occur in the near field because the ratio of incident to reflected pressure is much higher in the case of the near field.

E. Summary of Performance

Overall performance of the various helium models is summarized in Table IV by showing deviations from the reference rocket for both near and far field criteria. Rank orders of agreement with the rocket for the helium conditions are indicated along with root-mean-square deviations from the rocket values.

Condition B' clearly ranks highest in its overall ability to achieve simulation of rocket noise. This appears to be a reasonable result because Mach number, velocity, and static pressure were duplicated, and density was accounted for by a small correction. Condition B ranks second best, but there is no reason to consider using this condition without the correction for density.

Helium Conditions A and C appear to rank next in their overall ability to achieve rocket simulation; Condition A, however, is better in the far field, and Condition C is better in the near field. Condition A lacks the duplication of the rocket static pressure which Conditions B and B' provide. Condition C fails to duplicate both velocity and density by rather large amounts; however, in effect, compensating corrections for velocity and density are applied by maintaining the relative jet stream mechanical power at the rocket value.

Condition D clearly ranks lowest of all the helium models. Failure to duplicate three important parameters (Mach number, velocity, and density) obviously explains the lack of simulation. Application of SPL corrections to account for differences in velocity and density (Condition D') makes the agreement with the rocket better for far field locations. These corrections, however, do little to improve the near field agreement apparently because the source locations of the rocket are not duplicated. Conditions D and D' are considered to be unacceptable models.

In summarizing the performance of the helium models, a brief discussion of the significance of the deviations from the rocket values is in order. Experience in making sound measurements around rockets and jets (full scale and model) has shown that some inconsistencies appear in the data in almost any measurement program. For example, at one or more microphone positions, sound levels may appear incompatible with the remainder of the data, or a few frequency band levels may be displaced from an otherwise smooth SPL versus frequency curve. Whether these discrepancies are caused by instrumentation difficulties, faulty technique, lack of free field conditions, faulty operation of the rocket or jet, or other causes, they can usually be reduced considerably by additional testing which is designed to investigate the specific problem. Inconsistencies, which are often more noticeable with cross plotting, are apparent in both the helium and the rocket data. The problem is magnified in the present study because the helium data are necessarily being compared with reference rocket values which may themselves include experimental error. The inconsistencies frequently tend to disappear, however, if all the test data are viewed as a whole rather than individually. For example, the mean deviation in SPL from the rocket computed for all near field measurement locations for Condition B' is -0.8 db; whereas, the average value of rms deviation is about 3 times as large, and individual frequency bands of specific test points show deviations up to ± 7 db.

V. CONCLUSIONS

The substitute gas model technique shows good potential for becoming a practical method for experimentally investigating rocket noise. Sufficient evidence for helium models is presented to indicate that the substitute gas modeling concept is valid, i.e., if the essential flow parameters are duplicated, rocket noise simulation can be achieved. The principal problem is in providing simultaneously the desired values for the essential parameters, or in determining appropriate sound pressure level corrections for unavoidable deviations from these desired values.

Of the four helium models tested, the model which provided the rocket values of Mach number, velocity, and exit pressure, and near duplication of density performed best. This evaluation is based on agreement of sound pressure levels with the reference rocket in both the near and far field. A small correction to account for the difference in density is required.

Limitations of the present helium model data are (1) lack of sufficient information to design an optimum substitute gas model, (2) lack of adequate near field high frequency data to define the region at and beyond the peak of the spectrum, and (3) larger sound pressure level deviations from the rocket values than desired at some measurement locations.

Further investigations could result in (1) quantitative determination of the effects of varying the different gas flow parameters, (2) selection of a near optimum design for a substitute gas model of a given rocket, and (3) substantial evidence required to verify the ability of the substitute gas model to duplicate rocket noise under a variety of conditions, i.e., at numerous near and far field locations throughout the frequency range of interest for various nozzle and deflector configurations.

APPENDIX I

PROCEDURE FOR CALCULATING SUPERSONIC

HELIUM FLOW PARAMETERS FOR SUBSTITUTE GAS EXPERIMENTS

The fact that helium is very nearly an ideal gas allows its flow parameters to be readily calculated. Reference 10 lists important ratios of area, pressure, etc. by increments of 0.01 in Mach number for supersonic helium flow. These ratios and the perfect gas law are sufficient to allow calculation of any helium flow parameter of interest; however, the following equations will simplify the calculation. In some of the equations constants have been introduced in order to be consistent with the dimensional system used throughout this report (see List of Symbols). In other cases numerical values have been assigned to physical constants for helium in order to simplify use of the equations.

$$a = \sqrt{\gamma g R T} = 143.8 \sqrt{T} \quad (2)$$

$$a^* = 124.5 \sqrt{T_t} \quad (3)$$

$$\rho = \frac{144 P}{R T} = 0.372 \frac{P}{T} \quad (4)$$

The additional equation

$$\rho^* = 0.6495 \rho_t \quad (5)$$

may be useful when the problem is to evaluate weight flow and only the plenum conditions are known.

The nozzle size will in general be limited by the rate of helium flow which can be provided with the required plenum conditions. It is therefore important to evaluate the rate of weight flow

$$\dot{w} = \rho A V = \frac{30.2 A^* P_t}{\sqrt{T_t}} \quad (6)$$

The latter expression utilizes the quantities which are most generally useful.

Since jet stream mechanical power is customarily expressed in watts, it may be evaluated as

$$W = 0.021 \dot{w} v^2 = 0.021 \rho A V^3 \quad (7)$$

The usual problem in designing a substitute gas flow experiment using helium will start with a complete description of the flow for the rocket to be modeled. It is possible to duplicate all of the rocket parameters simultaneously only if the ratios of specific heats are the same for both gases.

Since the ratio of specific heats is much higher for helium than for any practical gas which it may be desired to model, it is necessary to compromise on the values for one or more flow parameters.

It is usually possible and convenient to pre-select the Mach number of the flow. If this is done, a tabulation should be made of the ratios P/P_t , ρ/ρ_t , T/T_t , A^*/A , and V/a^* from reference 10.

Once the Mach number and nozzle area ratio are determined, the exit pressure is simply the plenum pressure multiplied by the tabulated pressure ratio, unless the flow separates from the nozzle. Separation does not occur if the exit pressure is at least 0.4 of the local ambient pressure. It may be possible to use lower exit pressures, but it would be necessary first to measure pressures in the nozzle in order to detect the possible occurrence of flow separation.

The exit velocity is the Mach number times the exit acoustic velocity. Once a Mach number is chosen, velocity is determined by temperature alone. Density is dependent on both temperature and pressure.

Illustration No. 1: Given M_e and V_e for a helium model.

1. Find a^* from tabulated value of V/a^* .
2. Calculate T_t by equation (3).
3. Select P_e ; find P_t from tabulated value of P/P_t .
4. Calculate ρ_t by equation (4); evaluate ρ_e from tabulated value of ρ/ρ_t , and then determine ρ^* by equation (5).
5. Evaluate the rate of weight flow by equation (6), selecting nozzle size in the process.

(Steps 3 and 4 above could readily be interchanged.)

Illustration No. 2: Given M_e and P_e for a helium model.

1. Find P_t from tabulated value of P/P_t .
2. Select a value of ρ_e ; evaluate T_e from equation (4).
3. Evaluate T_t from tabulated value of T/T_t .
4. Determine a^* from equation (3).
5. Find V_e from tabulated value of V/a^* .

(At step 2, the procedure could as well be reversed to first select a velocity, and then find the necessary temperature and density.)

Illustration No. 3: Given V_e and P_e for a helium model.

1. Select ρ_e ; evaluate T_e by equation (4).
2. Determine a_e from equation (2).
3. Determine M_e as V_e/a_e .
4. Tabulate the appropriate ratios from reference 10, and proceed with evaluating other quantities required.

Table I. Properties of selected gases.

Gas	Chemical Symbol	Specific Heat, Constant Pressure, c_p , Btu/lb-°R	Specific Heat Ratio γ	Gas Constant R , ft-lb/lb-°R	Relative Acoustic Velocity $(\sqrt{\gamma R / 7.68})$	Inflammability Limits, % Lower Upper	Auto-Ignition Temperature of, °F	Toxicity
Solid Rocket	-	0.65	1.12	54.2	1.00	-	-	-
Helium	He	1.251	1.66	387.0	3.26	-	-	None
Neon	Ne	0.2450	1.67	76.5	1.45	-	-	None
Steam	H ₂ O	*0.485 **0.474	1.30	85.9	1.39	-	-	None
Nitrogen	N ₂	0.2477	1.404	55.2	1.13	-	-	None
Air	0.79 N ₂ , 0.21 O ₂	0.2414	1.404	53.3	1.11	-	-	None
Oxygen	O ₂	0.2178	1.401	48.3	1.05	-	-	None
Argon	A	0.1253	1.668	38.7	1.03	-	-	None
Nitrous Oxide	N ₂ O	0.2004	1.309	35.1	0.87	-	-	Slight
Carbon Dioxide	CO ₂	0.1989	1.304	24.9	0.865	-	-	None
Freon-12	CCl ₂ F ₂	0.1437	1.17	12.78	0.495	-	-	None
Hydrogen	H ₂	3.389	1.41	768.0	4.22	4.0	74.2	None
Methane	CH ₄	0.5931	1.31	96.4	1.44	5.0	15.0	None
Ammonia	NH ₃	0.5232	1.31	91.0	1.40	16.0	25.0	Moderate
Carbon Monoxide	CO	0.2478	1.404	55.2	1.13	12.5	71.5	High
Acetylene	C ₂ H ₂	0.3832	1.26	59.4	1.11	2.50	80.0	Slight
Nitric Oxide	NO	0.231	1.38	51.4	1.08	-	-	High
Ethylene	C ₂ H ₄	0.3592	1.255	54.7	1.06	2.75	28.60	None
Ethane	C ₂ H ₆	0.3881	1.22	51.5	1.01	3.0	12.5	None
Hydrogen Sulfide	H ₂ S	0.2533	1.32	45.5	0.995	4.3	46.0	Moderate
Propane	C ₃ H ₈	0.473	1.15	35.1	0.85	2.3	7.3	None
Propylene	C ₃ H ₆	0.371	1.145	36.8	0.84	2.00	11.10	None
Butylene	C ₄ H ₈	0.3595	1.11	27.4	0.71	1.65	9.95	None
Sulfur Dioxide	SO ₂	0.1516	1.29	23.6	0.71	-	-	High
Butane	C ₄ H ₁₀	0.395	1.09	26.6	0.69	1.86	8.1	None

Approximate acoustic velocity relative to the acoustic velocity of a typical rocket exhaust at the same temperature.
Concentration limits in percentage by volume in air at ambient temperature and pressure at which ignition and combustion will occur in the presence of a spark or flame.
Temperature at which inflammable concentrations of the gas will self-ignite and sustain combustion in the absence of a spark or flame.
For information in greater detail on toxic effects of these gases consult references 2-8.
*212°F, 1 atmosphere. **440°F, 1 atmosphere.

TABLE II. Flow parameters of solid propellant model rocket and heated helium jets.

Flow Parameter	Unit	Symbol	Solid Propellant Rocket	Helium Condition			
				A	B	C	D
Plenum pressure	psia	P_t	635	239	349	349	44
Plenum temperature	$^{\circ}R$	T_t	6000	1560	1560	750	750
Exit Mach number		M_e	3.12	<u>3.12</u>	<u>3.12</u>	<u>3.12</u>	1.6
Exit velocity	ft/sec	v_e	8600	<u>8600</u>	8600	5980	4630
Exit density	lb/ft ³	ρ_e	0.0065	<u>0.0065</u>	0.0095	0.0196	0.0086
Exit static pressure	psia	P_e	9.4	6.43	<u>2.4</u>	<u>2.4</u>	<u>2.4</u>
Acoustic velocity at nozzle throat	ft/sec	a^*	3420	4910	4910	<u>3420</u>	<u>3420</u>
Relative jet stream mechanical power	megawatts/in ² (exit area)	W_{rel}	0.61	<u>0.61</u>	0.88	<u>0.61</u>	0.12
Total jet stream mechanical power	megawatts	W	2.6	1.03	1.5	1.03	0.21
Thrust	lbs	F	430	162	250	248	52
Weight flow	lb/sec	\dot{w}	1.67	0.66	0.965	1.38	0.484
Viscosity at exit	lb/ft-sec $\times 10^{-6}$	η_e	30	11.0	11.0	6.7	11.0
Exit temperature	$^{\circ}R$	T_e	3600	370	370	180	370
Nozzle exit diameter	in	D_e	2.33	1.47	1.47	1.47	1.50
Nozzle area expansion ratio		A_e/A^*	10	3.25	3.25	3.25	1.20

Note: Helium jet flow parameters which are numerically equal to the corresponding solid propellant model rocket flow parameters are underlined.

Table III. Sound pressure levels for heated helium jet Condition D.

Frequency Band (cps)	150- 300	300- 600	600- 1200	1200- 2400	2400- 4800	4800- 10K	10K- 20K	20K- 40K
Angle Relative to Nozzle Axis	Far Field Survey - (100 Nozzle Diameters)							
30°	96.0	103.0	110.0	116.5	120.5	119.0	115.0	109.0
50°	97.0	104.5	111.5	119.0	121.5	119.0	116.5	113.0
70°	98.0	104.5	112.0	119.5	121.5	120.5	119.0	116.0
90°	99.0	106.0	114.0	120.0	124.0	124.5	121.5	117.0
100°	99.0	107.5	115.5	122.0	126.0	128.0	124.5	118.0
110°	100.0	109.0	118.0	125.5	130.0	130.0	126.5	121.0
120°	103.5	114.0	124.5	131.5	133.0	130.0	126.0	122.5
130°	106.0	118.0	127.0	131.0	132.0	128.5	124.0	117.5
140°	111.0	119.5	125.0	127.5	128.5	126.0	121.0	116.0
150°	113.0	121.0	125.5	126.5	126.0	122.5	118.5	113.0
170°	112.0	121.0	123.0	124.0	123.0	120.0	-	-
Test Location	Near Field Survey							
1	104.0	111.5	120.0	126.0	129.0	129.5	-	-
2	109.0	115.5	123.5	129.0	132.5	134.0	-	-
3	117.0	124.0	130.0	136.5	142.0	146.5	-	-
4	131.5	134.0	140.5	147.5	154.0	157.5	-	-
5	137.5	140.0	145.0	151.5	154.0	151.5	-	-
6	134.5	140.0	145.0	149.0	146.5	142.0	-	-
7	130.0	135.5	137.0	133.0	132.0	131.0	-	-
8	122.0	127.0	128.5	129.5	130.0	128.5	-	-
9	119.5	125.5	129.5	131.0	130.0	127.0	-	-

Table IV. Summary of agreement of helium and rocket data.

Values shown in the table indicate rms deviations of the helium test data from the rocket data. Numbers in parentheses () indicate rank order of the agreements among the various helium conditions.

	Helium Condition					
	A	B	B' 1	C	D	D' 2
<u>Far Field Criteria</u>						
SPL forward of nozzle	3.1 db (1)	4.9 db (5)	3.7 db (3)	4.0 db (4)	5.6 db (6)	3.4 db (2)
SPL aft of nozzle	1.8 db (2)	1.9 db (3)	1.5 db (1)	3.0 db (4)	7.5 db (6)	3.9 db (5)
Octave band power levels	1.4 db (2)	2.0 db (3)	0.7 db (1)	2.3 db (4)	7.6 db (6)	3.4 db (5)
Directivity angle	4.7° (4)	2.4° (1)	2.4° (1)	4.1° (3)	3.3° (2)	3.3° (2)
<u>Near Field Criteria</u>						
SPL forward of nozzle	3.2 db (4)	2.4 db (1)	2.8 db (2)	3.0 db (3)	6.0 db (5)	6.0 db (5)
SPL aft of nozzle	3.8 db (4)	2.2 db (3)	2.0 db (2)	1.9 db (1)	13.0 db (6)	10.0 db (5)
Source location	4.2 ND (3)	2.6 ND (1)	2.6 ND (1)	2.8 ND (2)	13.6 ND (4)	13.6 ND (4)
Overall rank	(3)	(2)	(1)	(3)	(5)	(4)
1	Condition B' is Condition B with - 1.5 db applied to correct for the difference in density between Condition B and the rocket.					
2	Condition D' is Condition D with + 7.0 db applied to correct for the difference in density and velocity between Condition D and the rocket.					

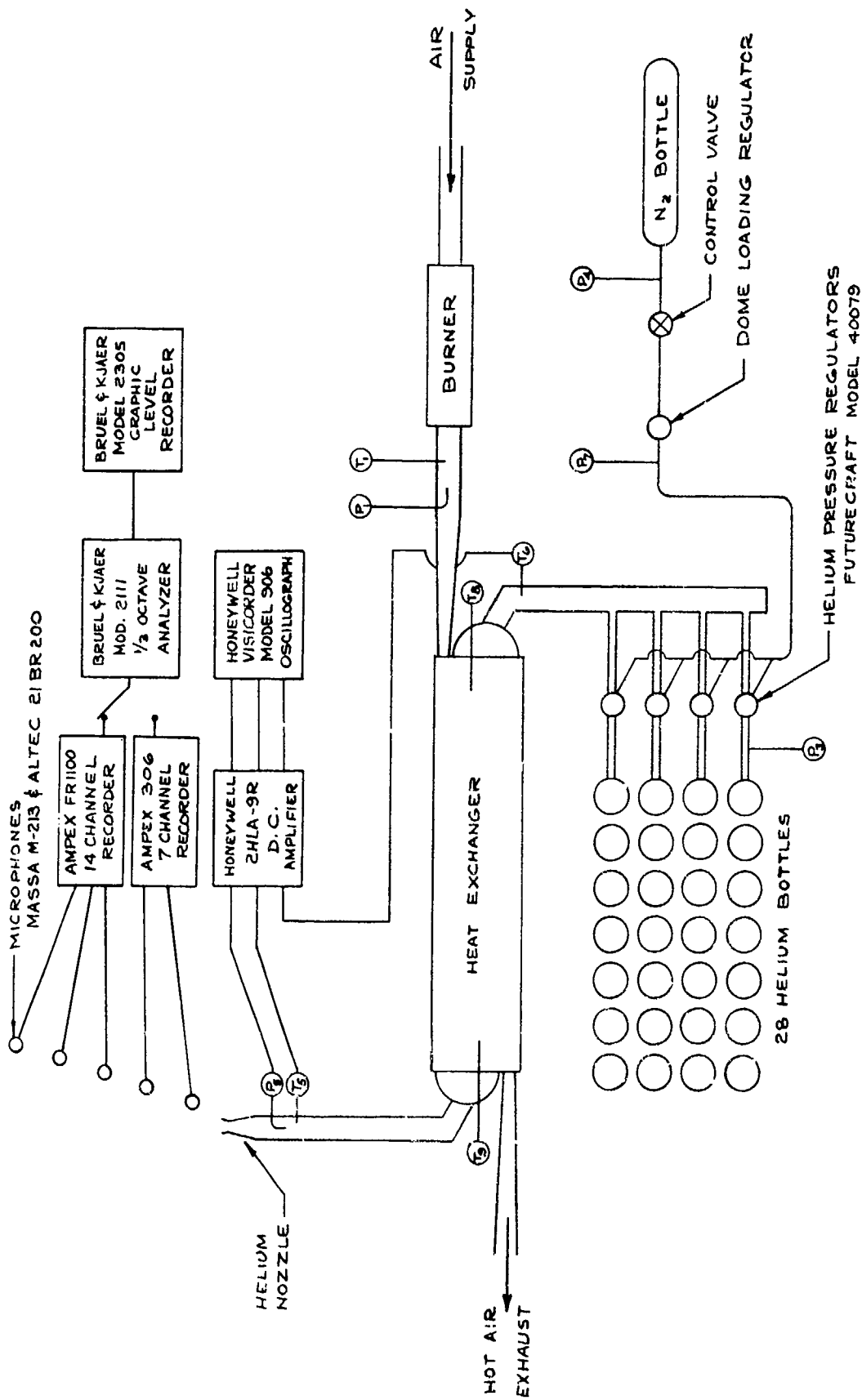
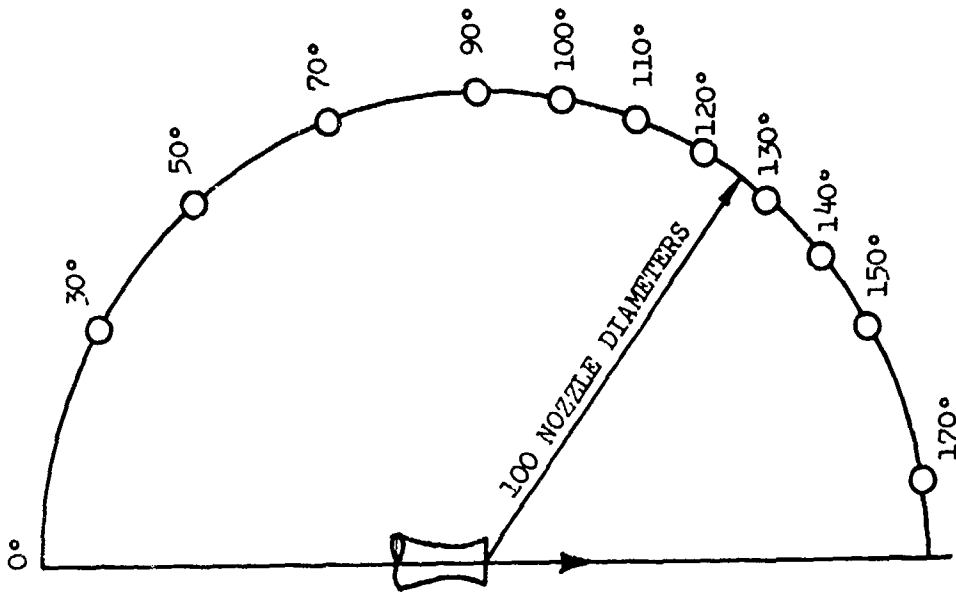
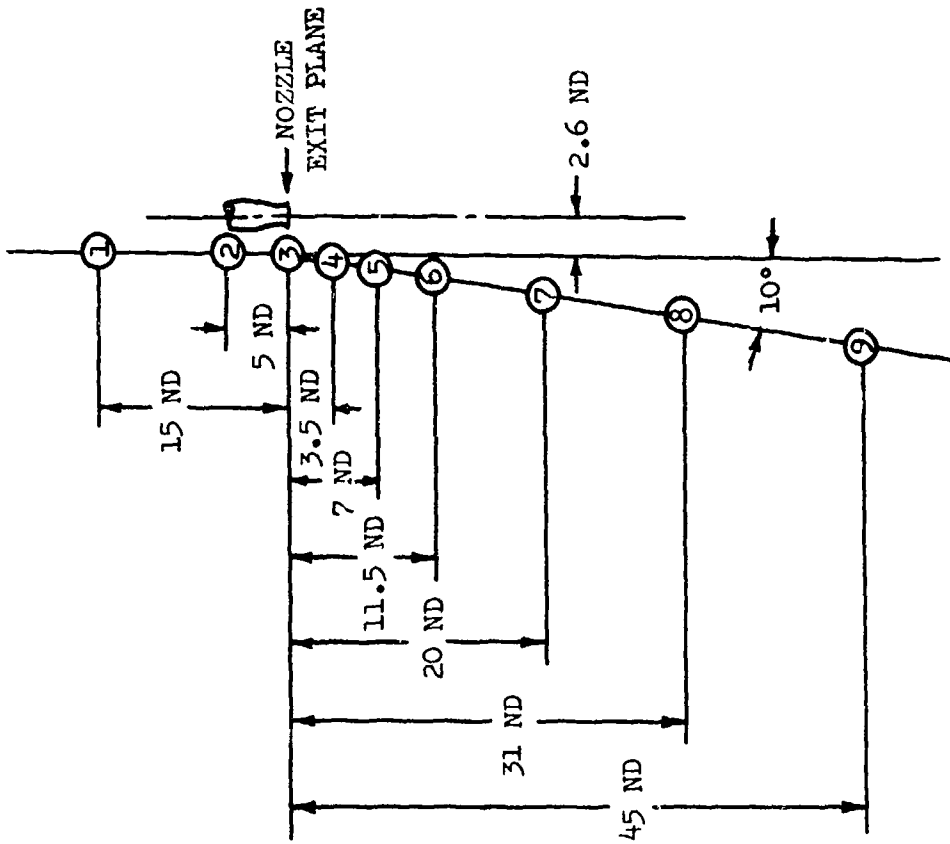


Figure 1. Flow and measurement systems for heated helium tests.



(b) Far Field



(a) Near Field

Figure 2. Measurement locations for solid propellant rocket and heated helium tests.

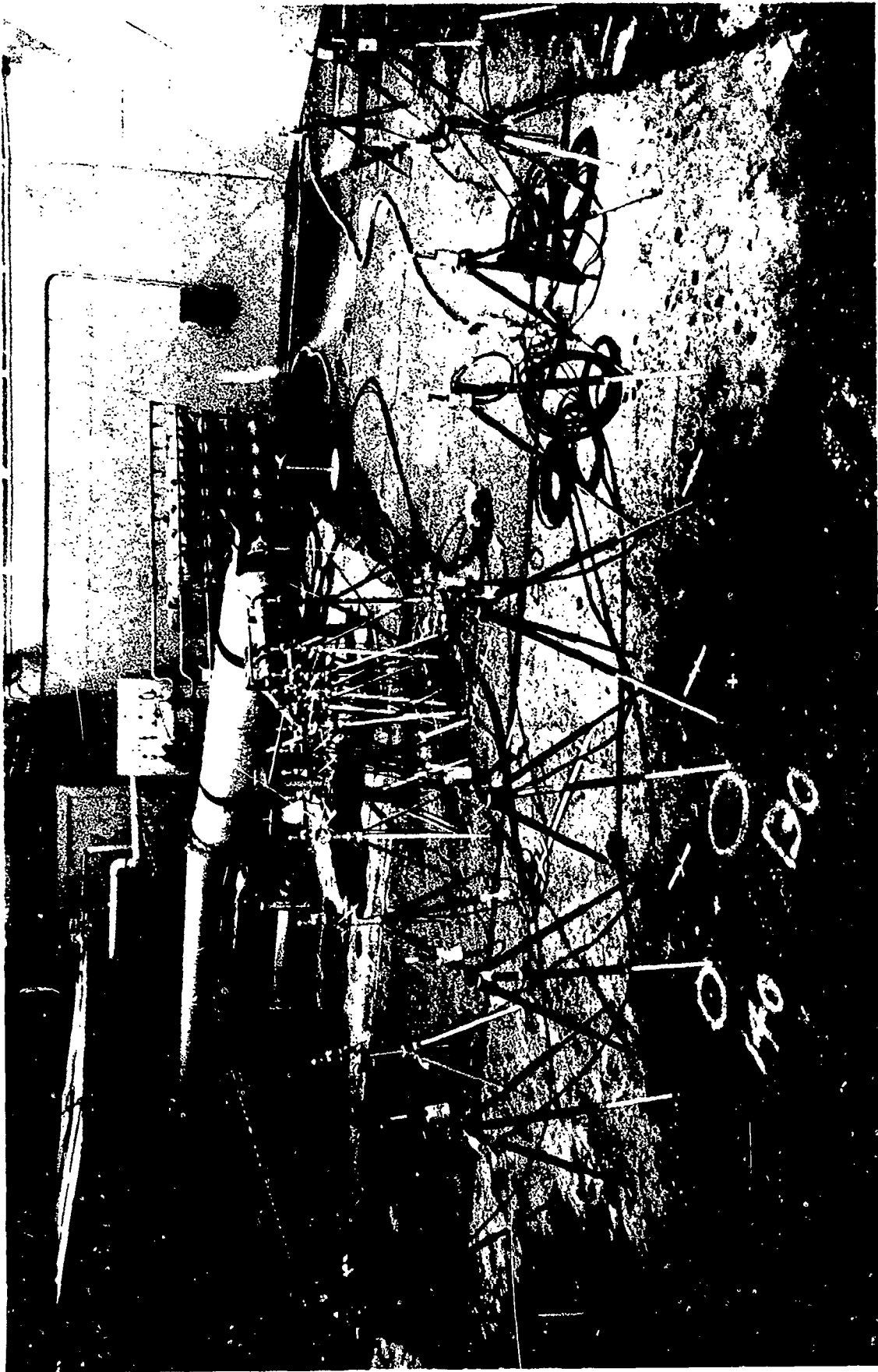


Figure 3. Test apparatus and microphone array for heated helium tests.

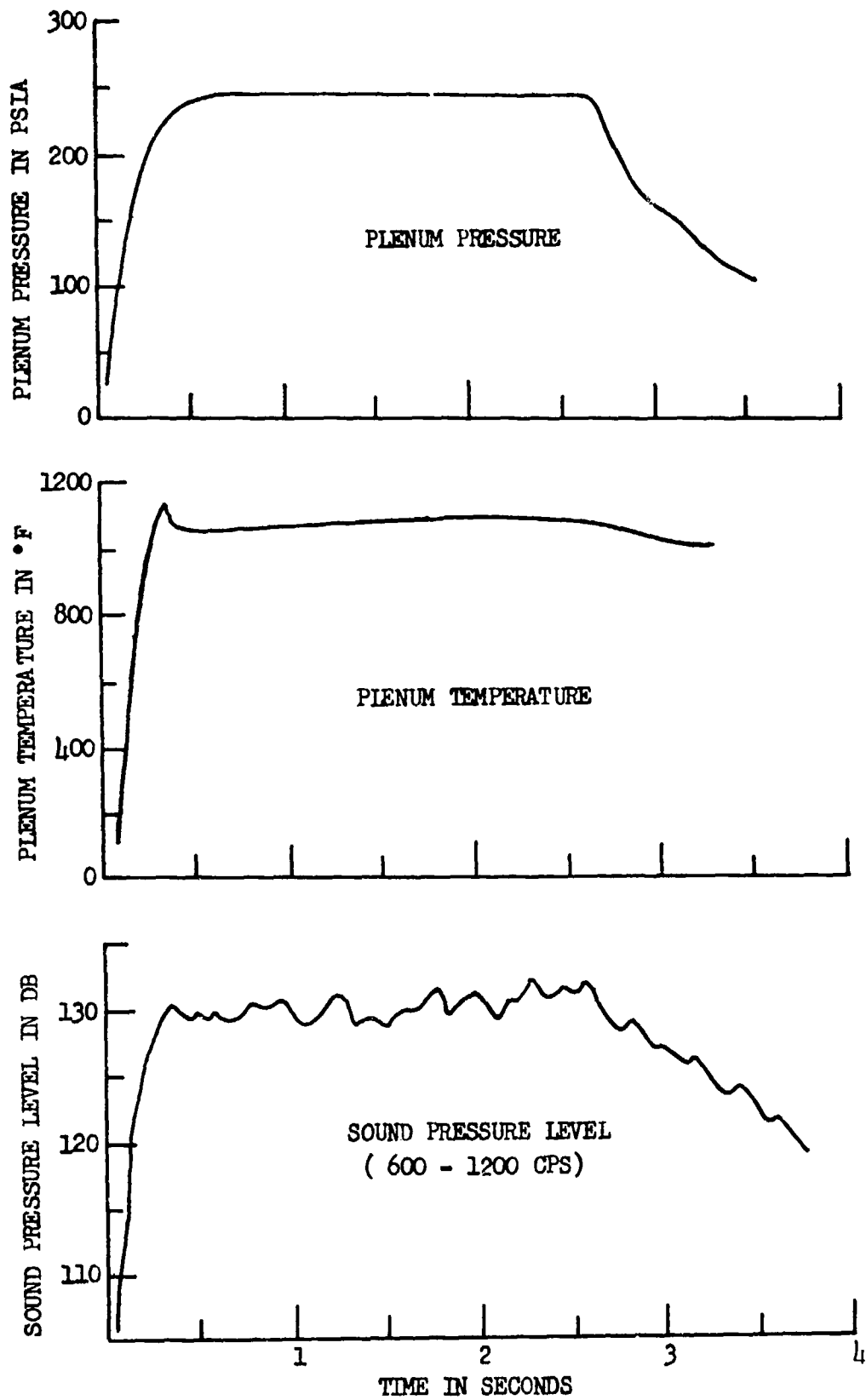
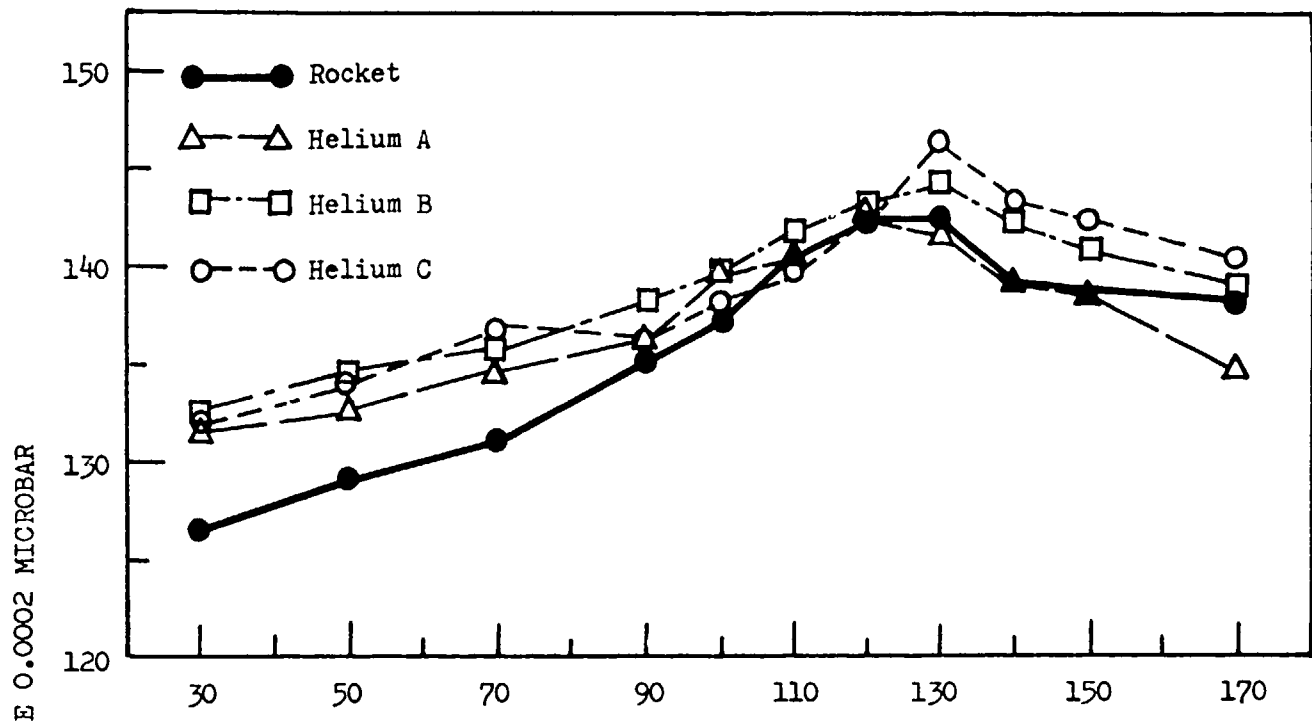
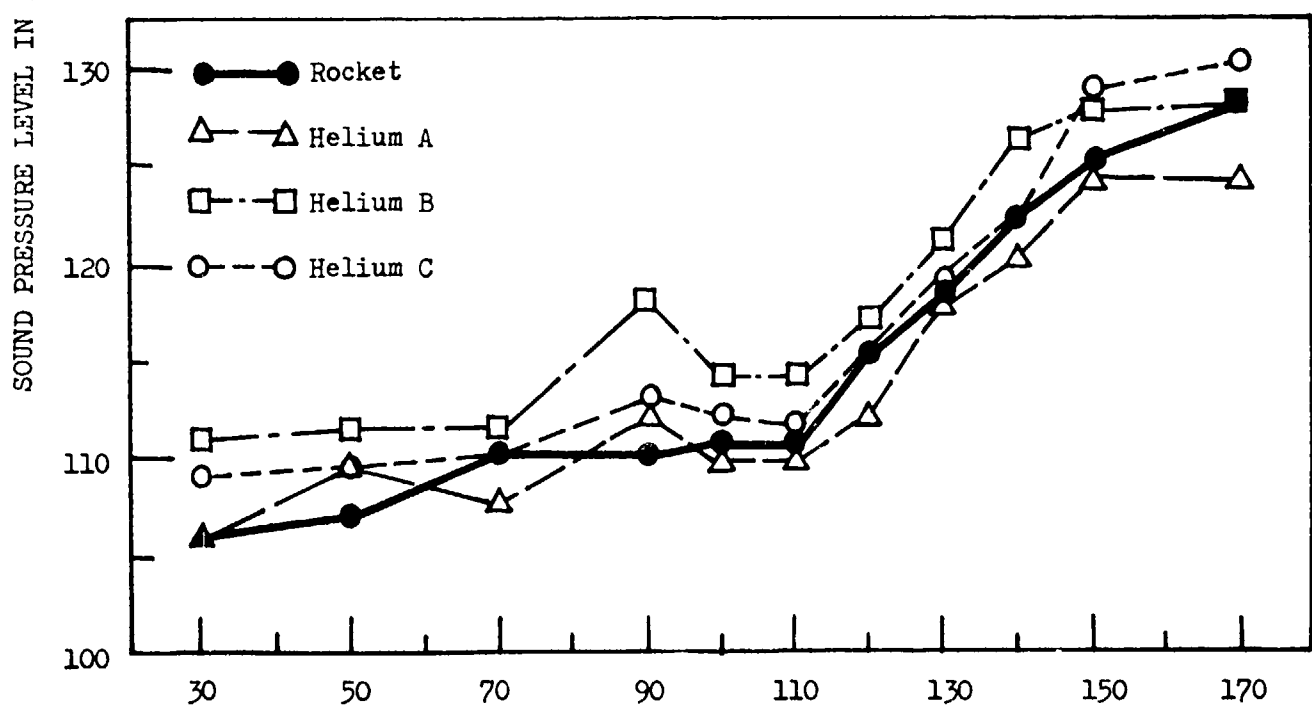


Figure 4. Time variation of plenum pressure, plenum temperature, and sound pressure level during a heated helium test.



(a) Overall



ANGEL θ IN DEGREES FROM FORWARD JET AXIS

(b) 150-300 cps

Figure 5. Sound pressure levels measured at 100 nozzle diameters radius vs. angle for the solid propellant model rocket and heated helium jets.

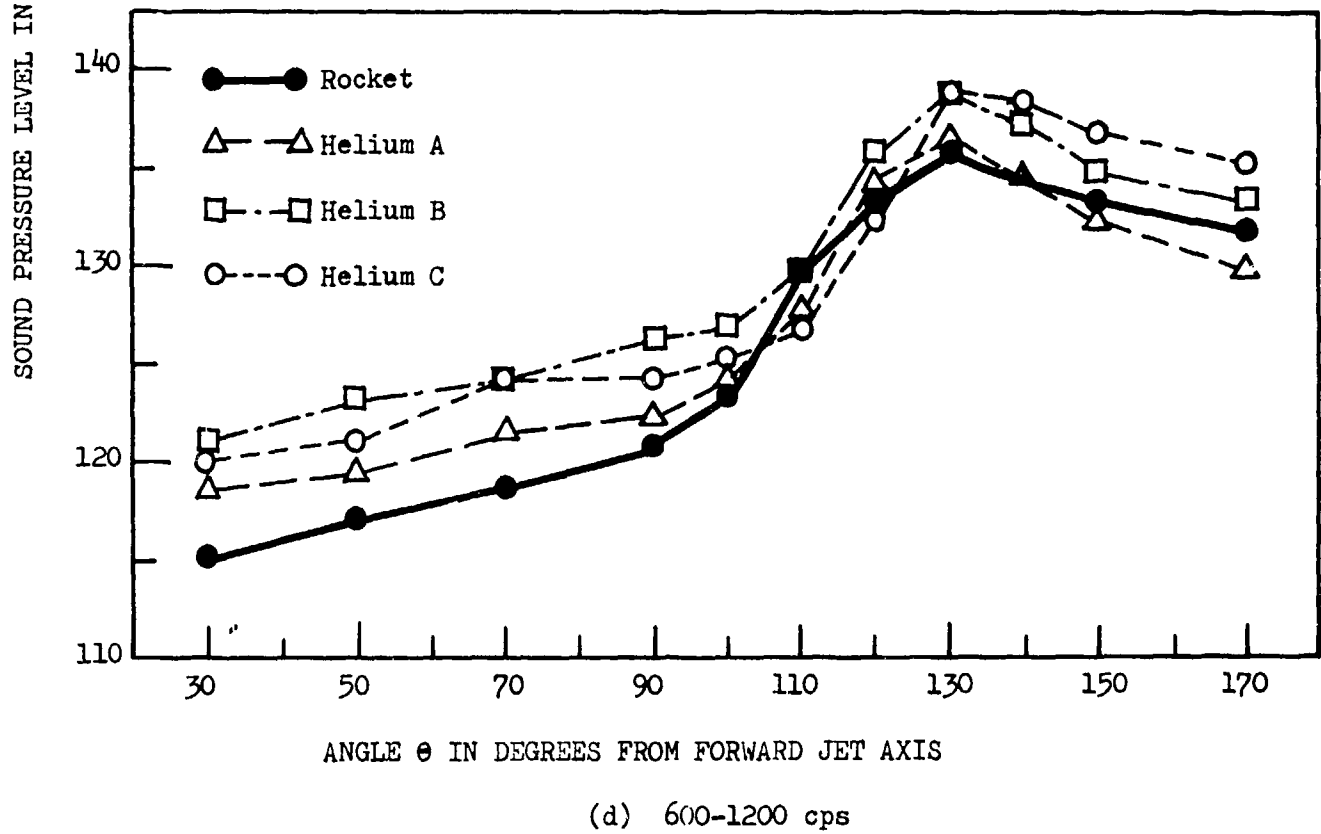
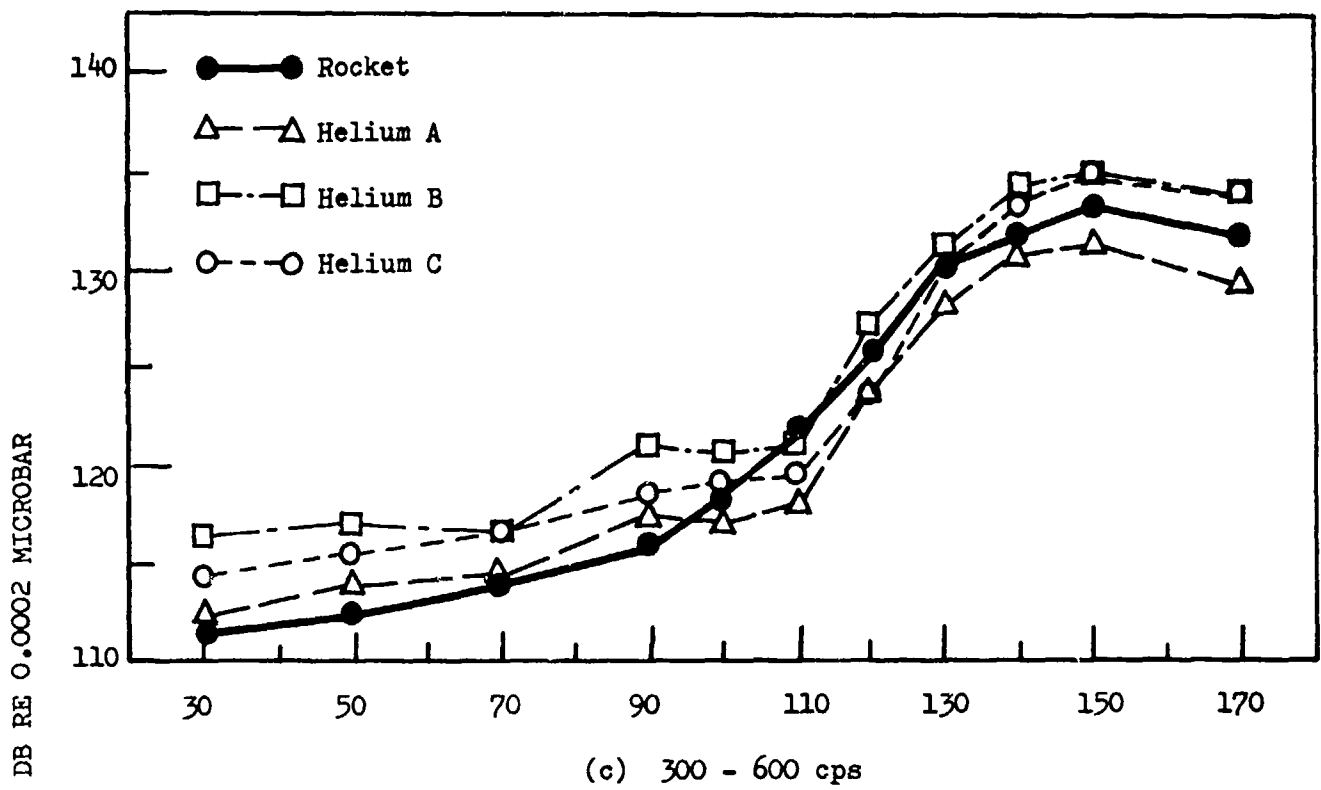


Figure 5. Continued.

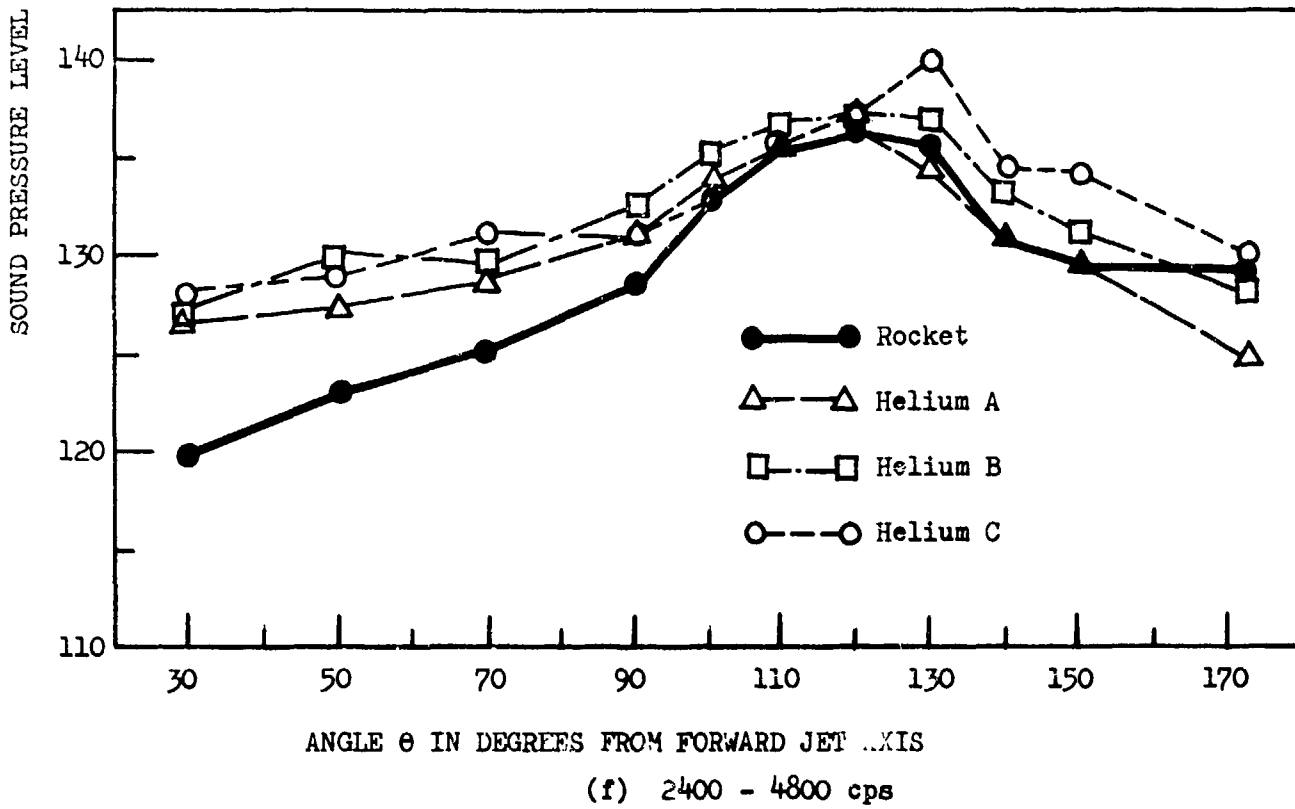
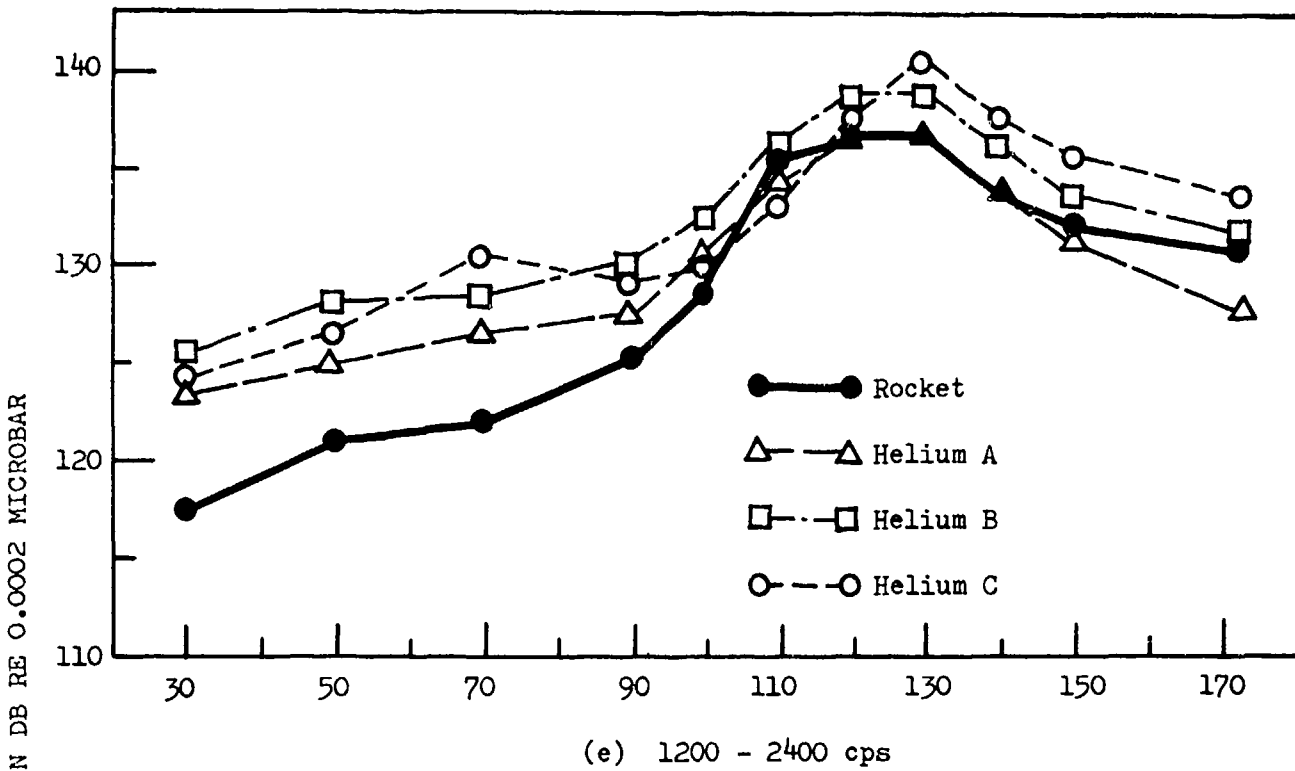


Figure 5. Continued.

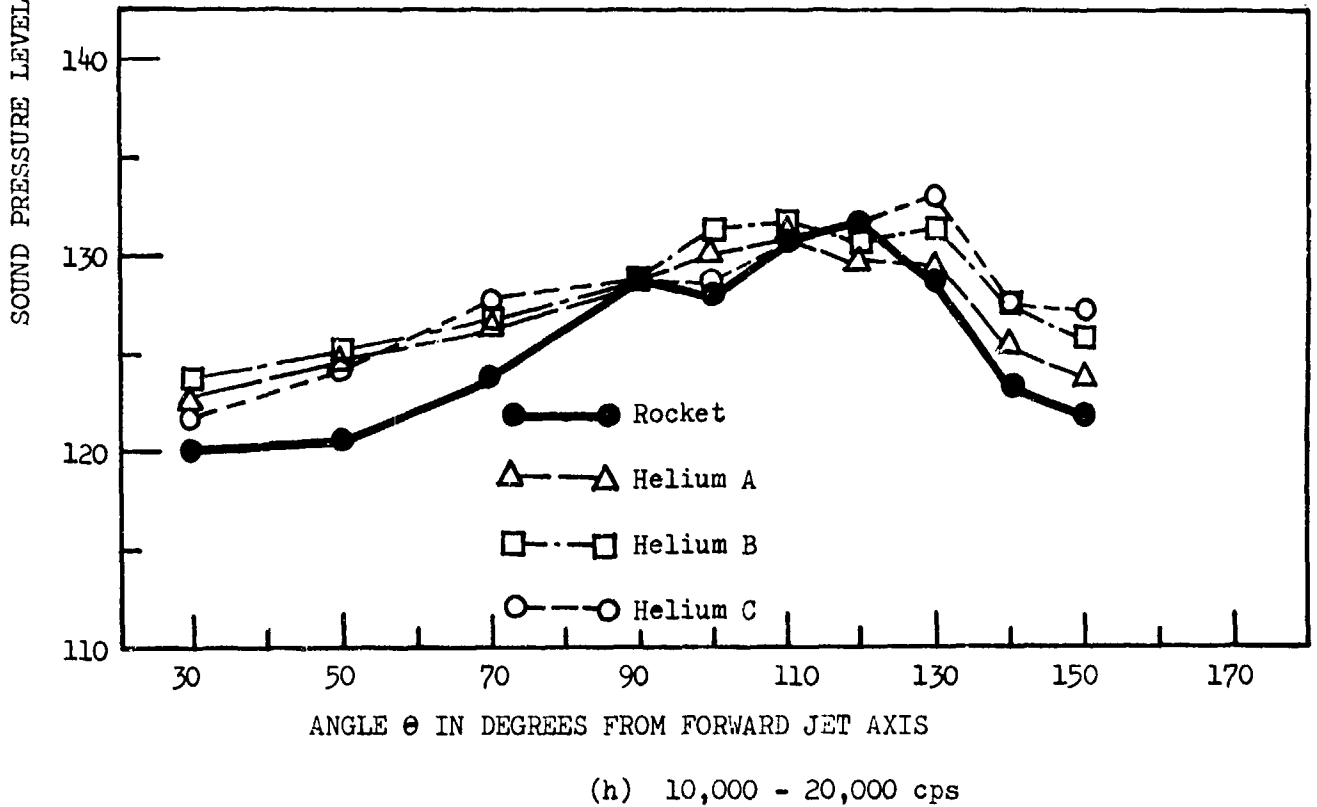
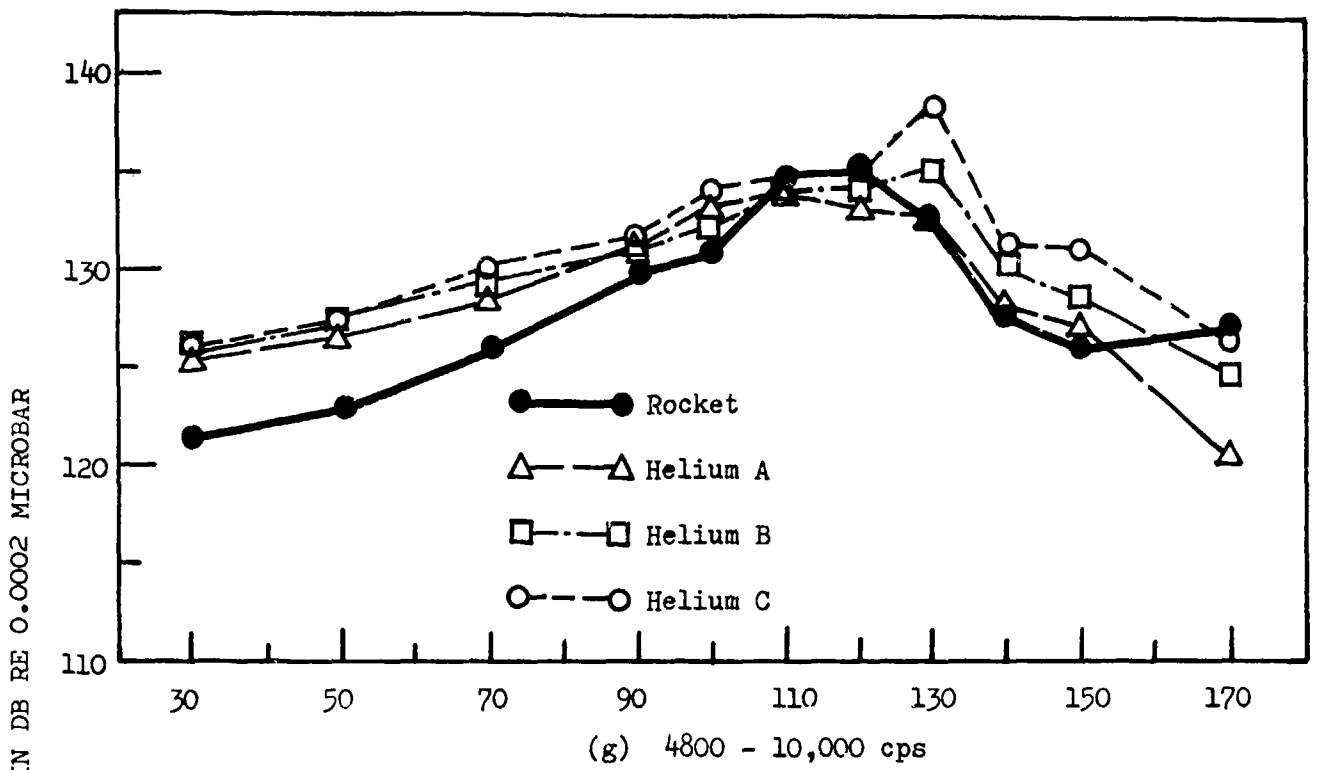


Figure 5. Continued

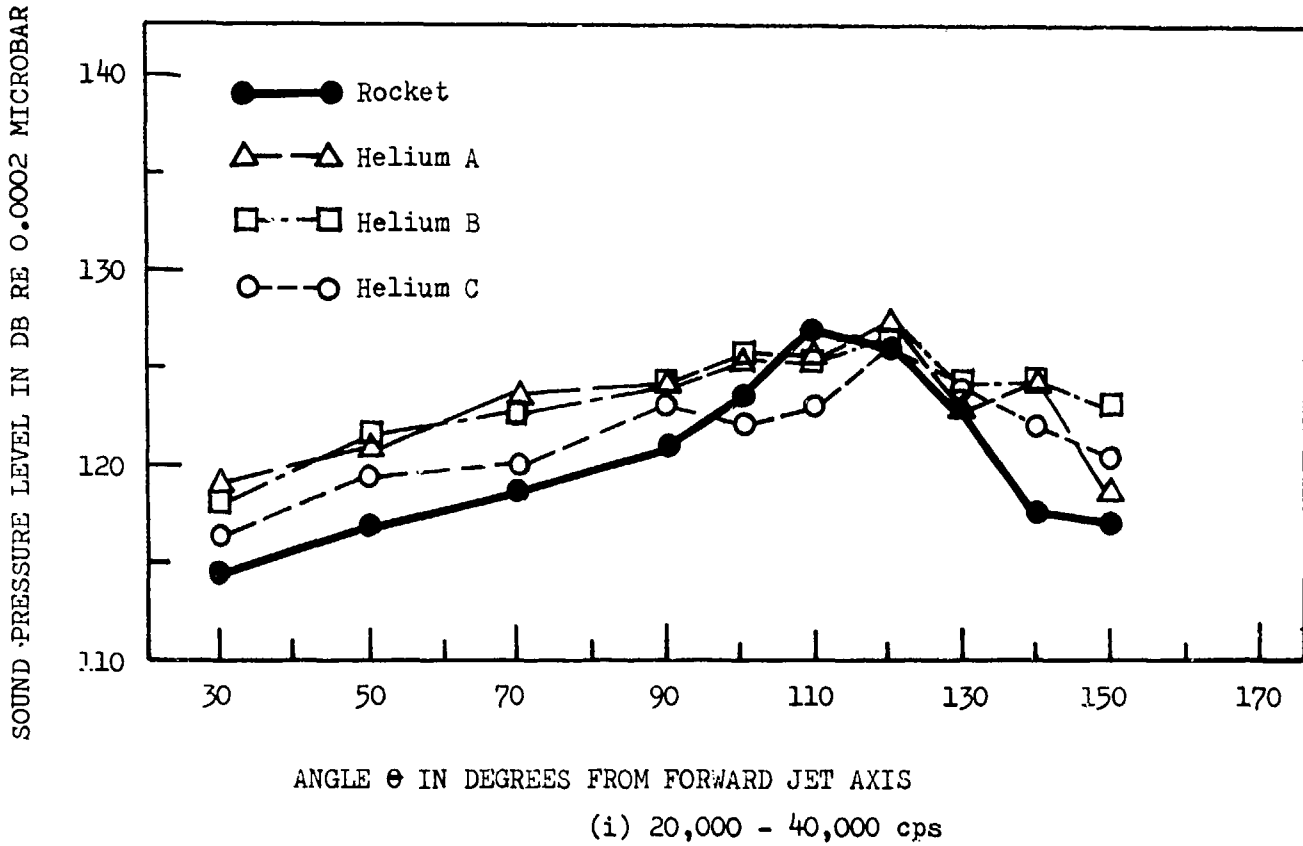
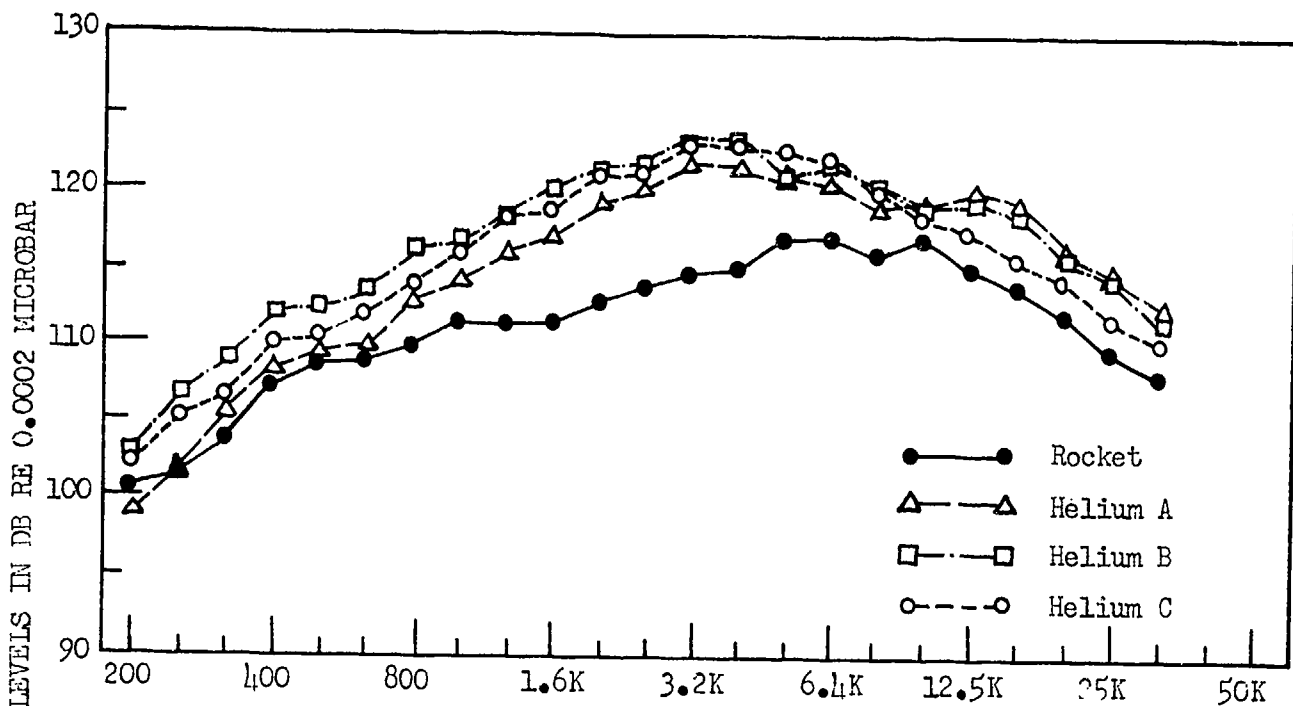
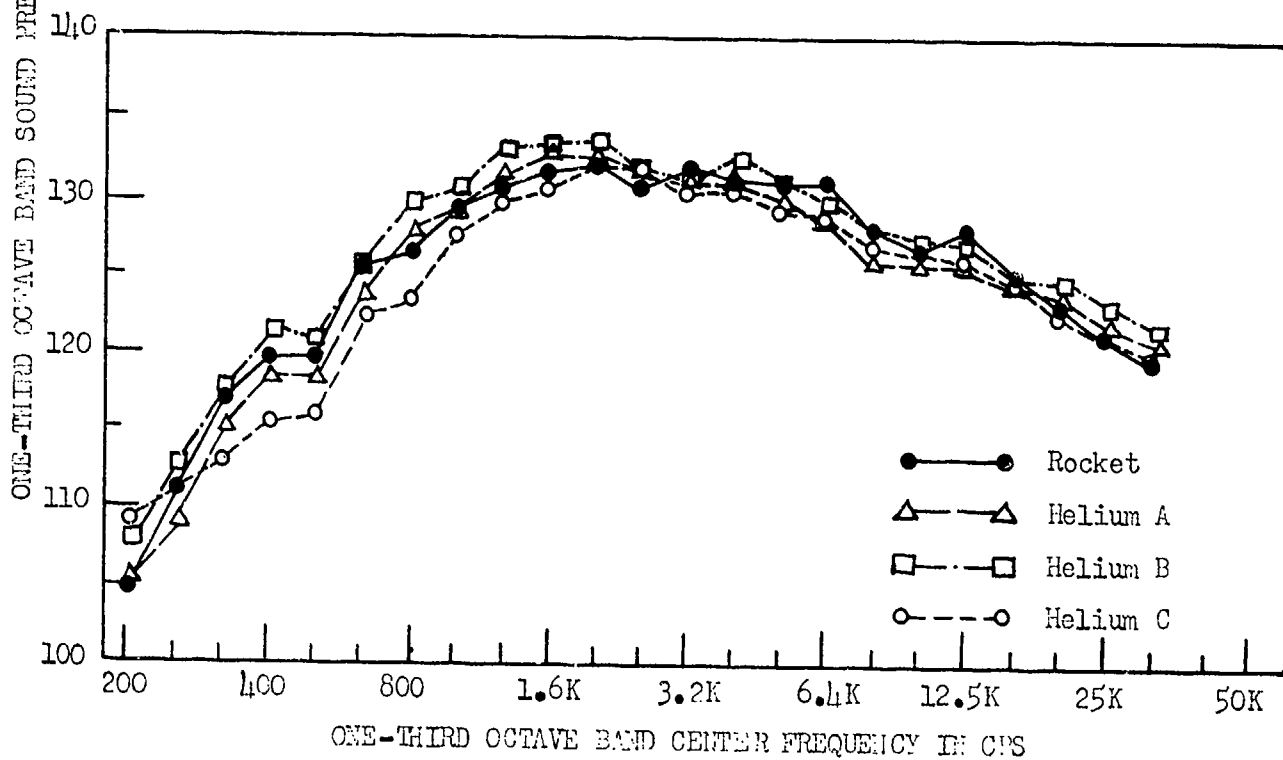


Figure 5. Concluded.



(a) 30° far field point at 100 ND radial distance.



(b) 120° far field point at 100 ND radial distance.

Figure 6. Representative far field sound pressure levels for the solid propellant model rocket and heated helium jets.

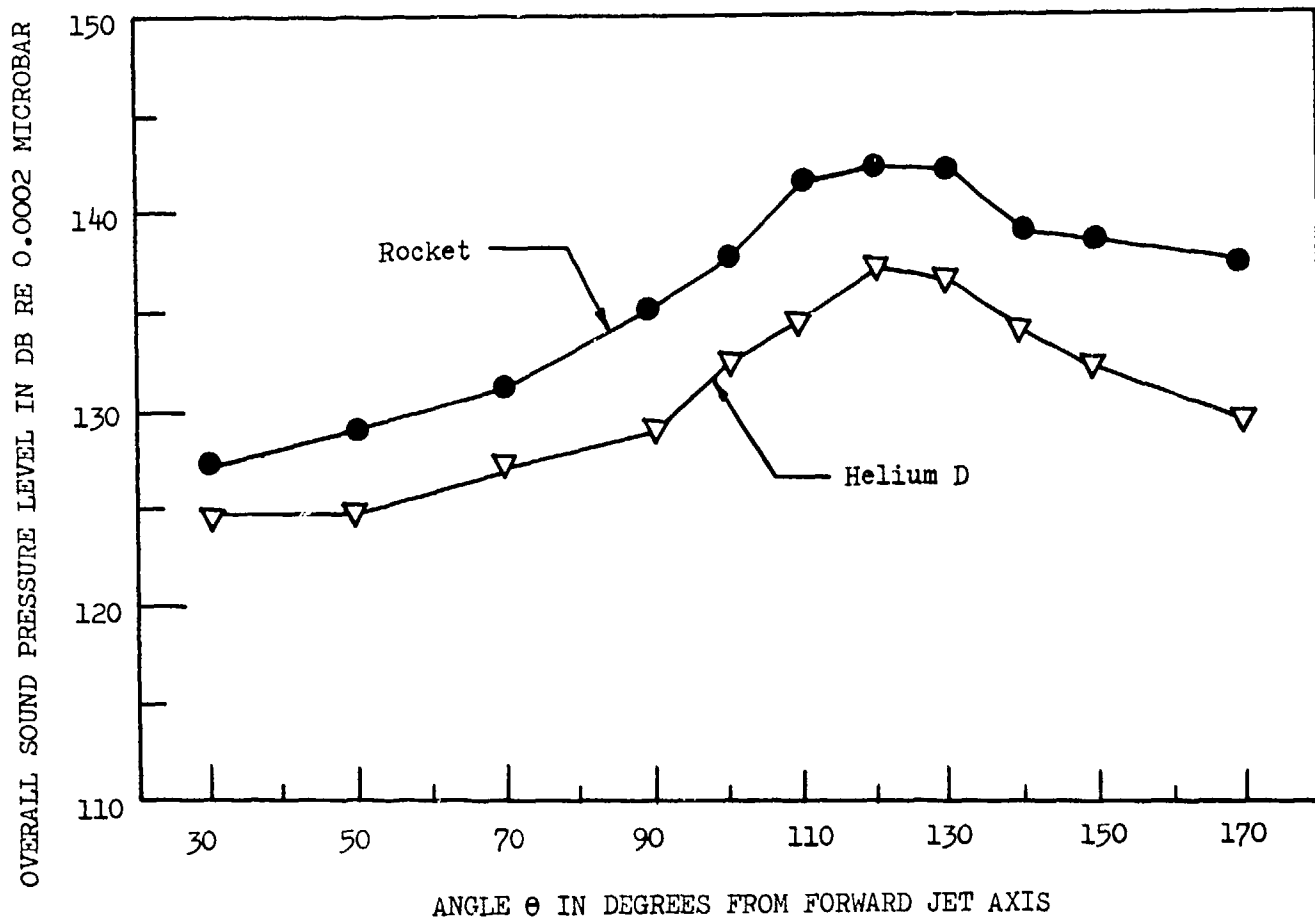
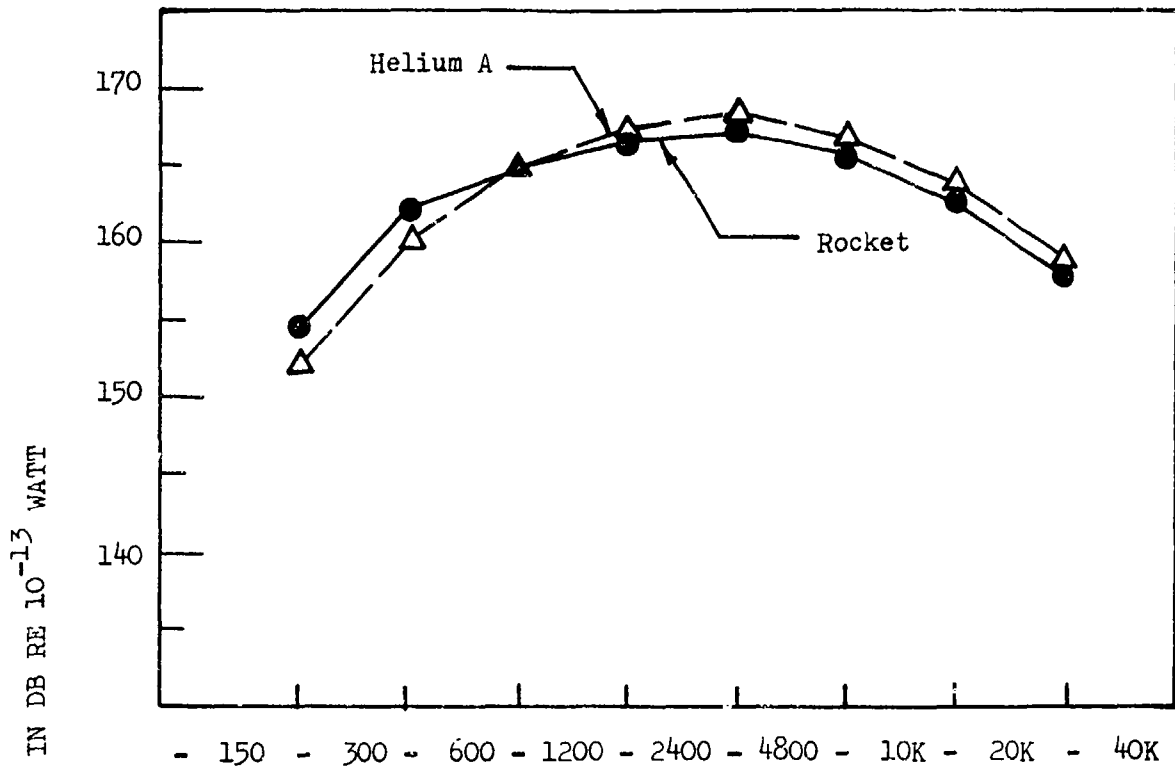
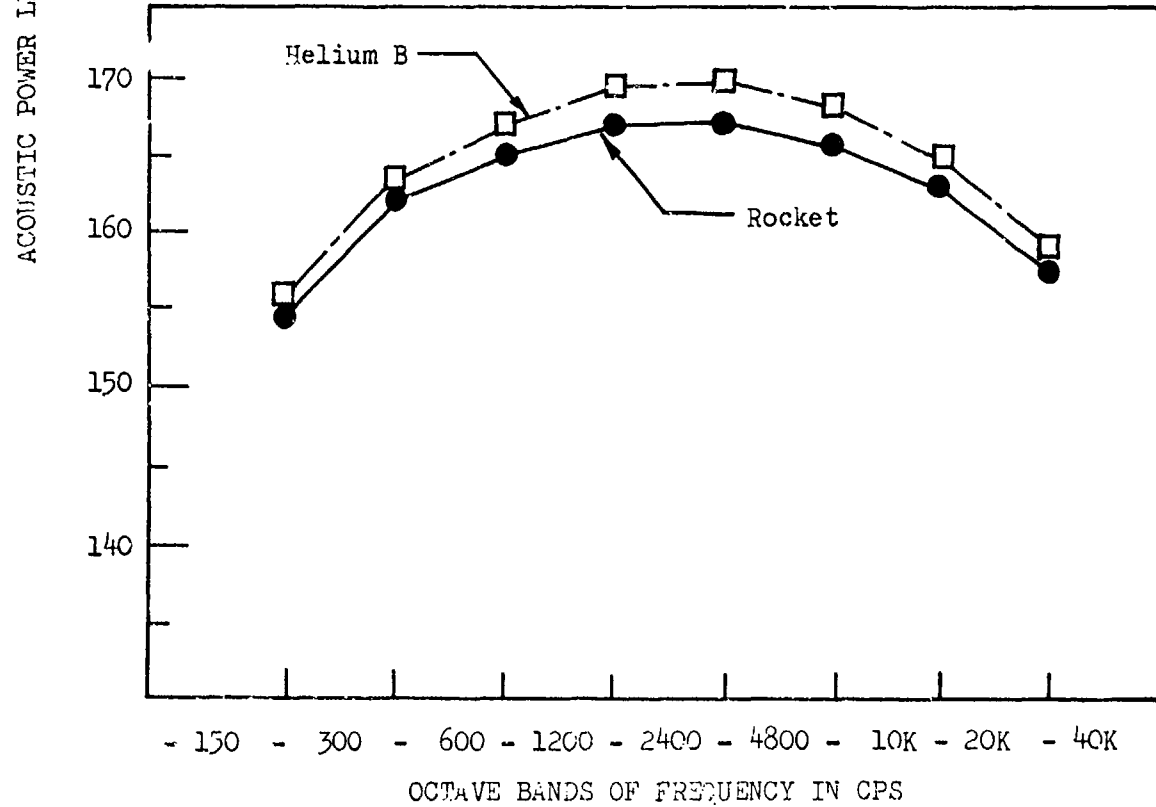


Figure 7. Overall sound pressure levels measured at 100 nozzle diameters radius vs. angle for the solid propellant model rocket and heated helium jet Condition D.



(a) Helium A vs. solid rocket



(b) Helium B vs. solid rocket

Figure 8. Total radiated acoustic power levels of solid propellant model rocket and heated helium jets.

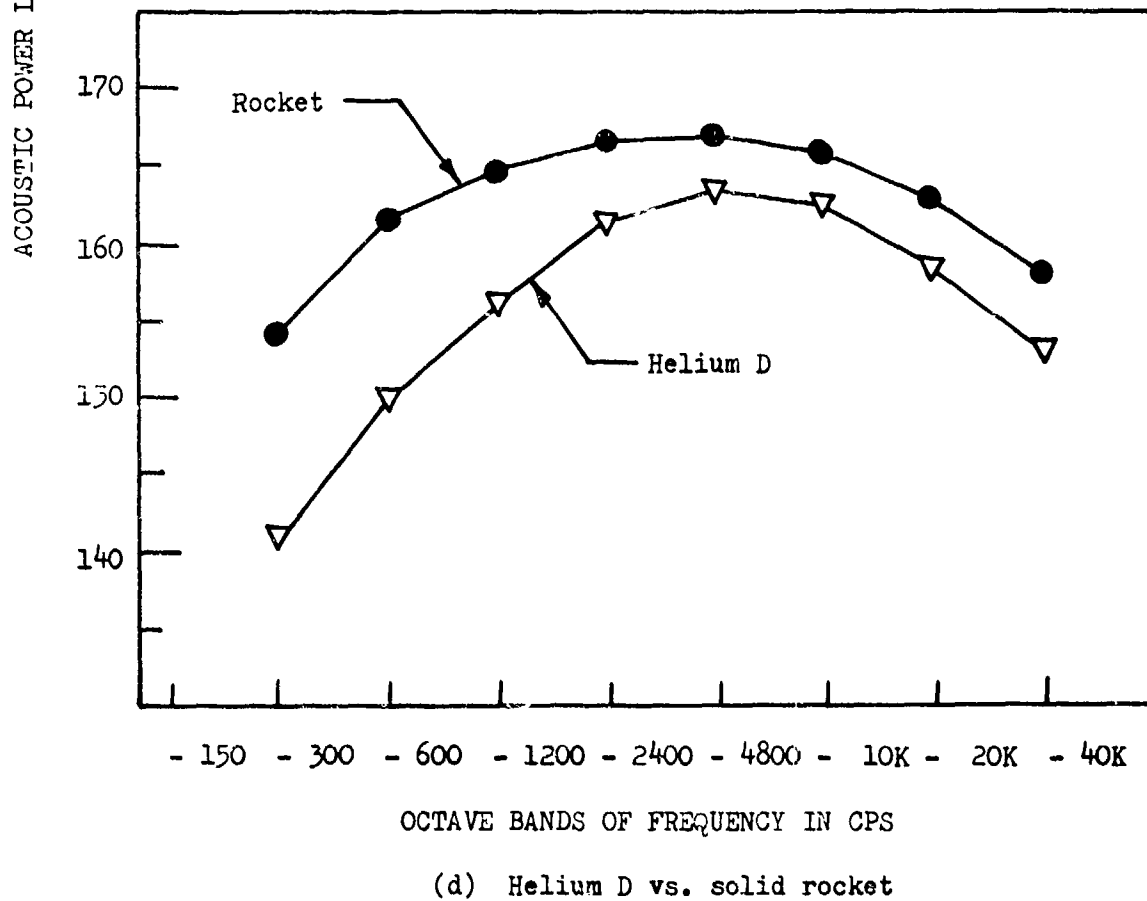
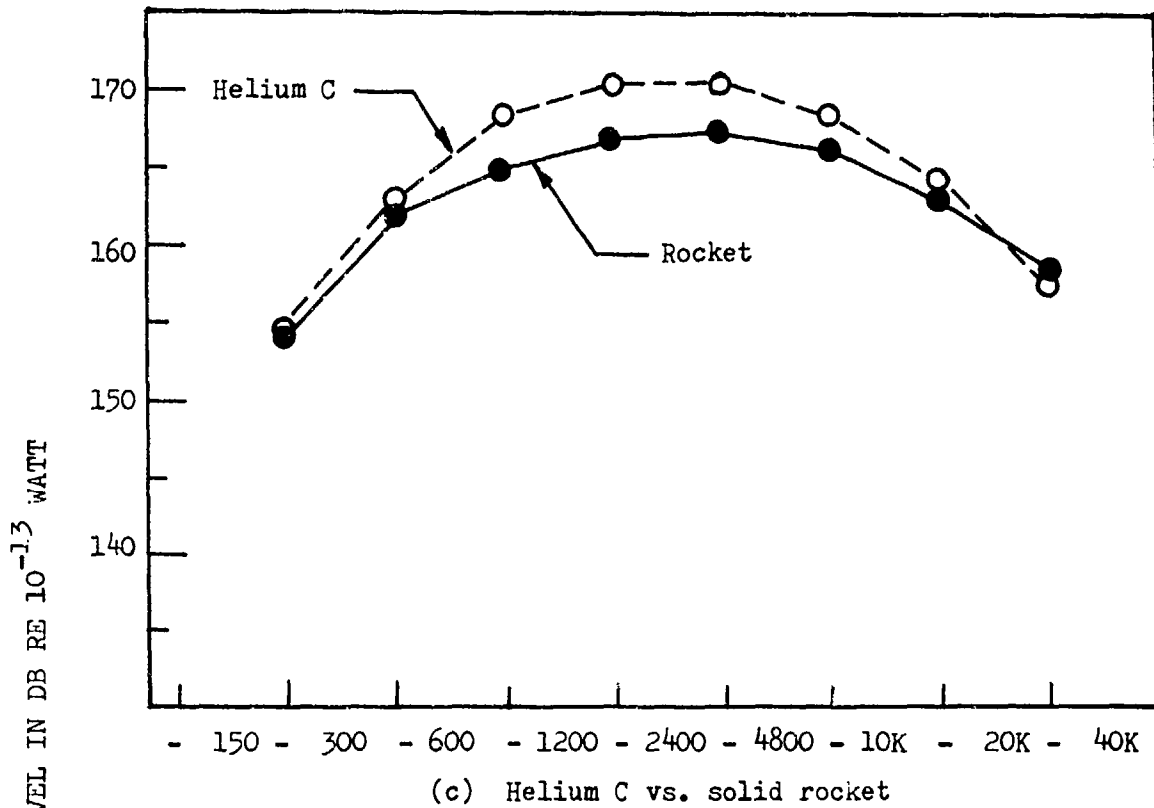


Figure 8. Concluded.

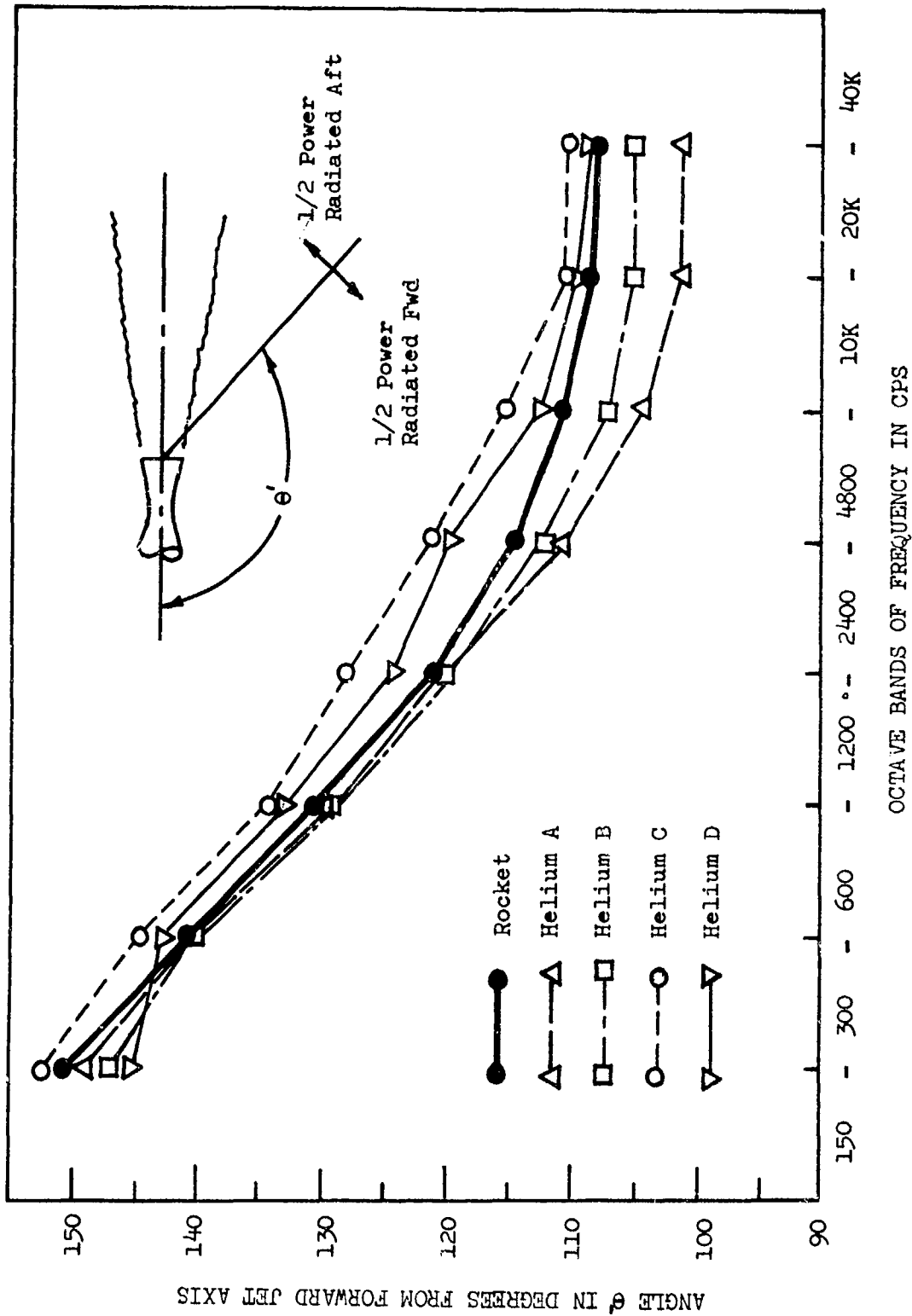
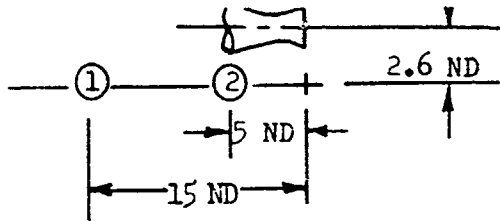
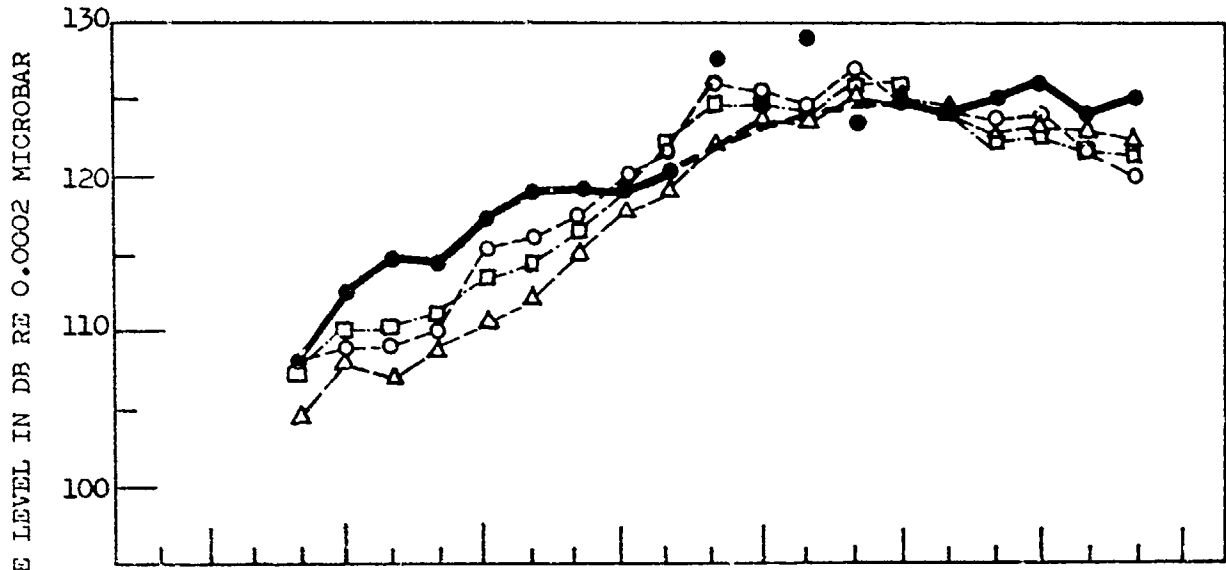


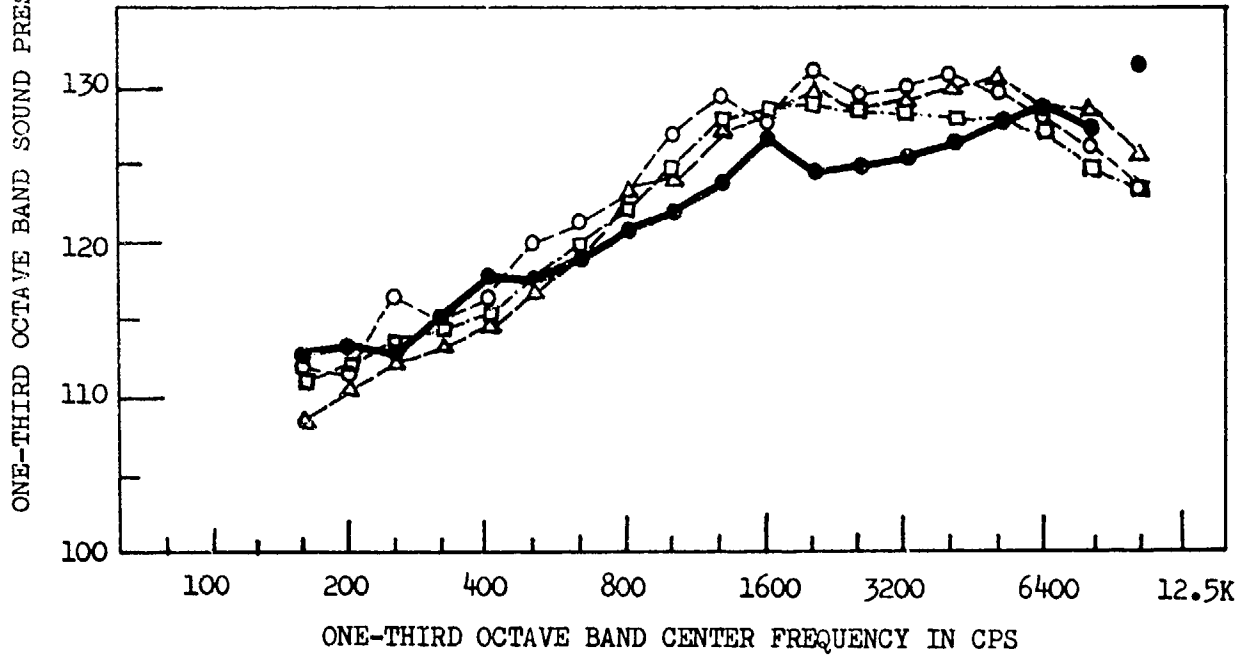
Figure 9. Angle of half-power radiation vs. frequency for solid propellant model rocket and heated helium jets.



△ ——— △ Helium A
 □ ——— □ Helium B
 ○ ——— ○ Helium C

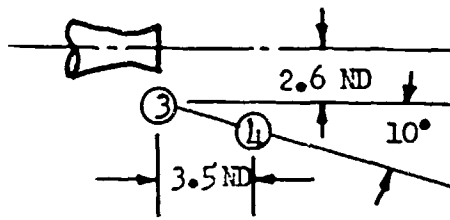


a. Test Location 1

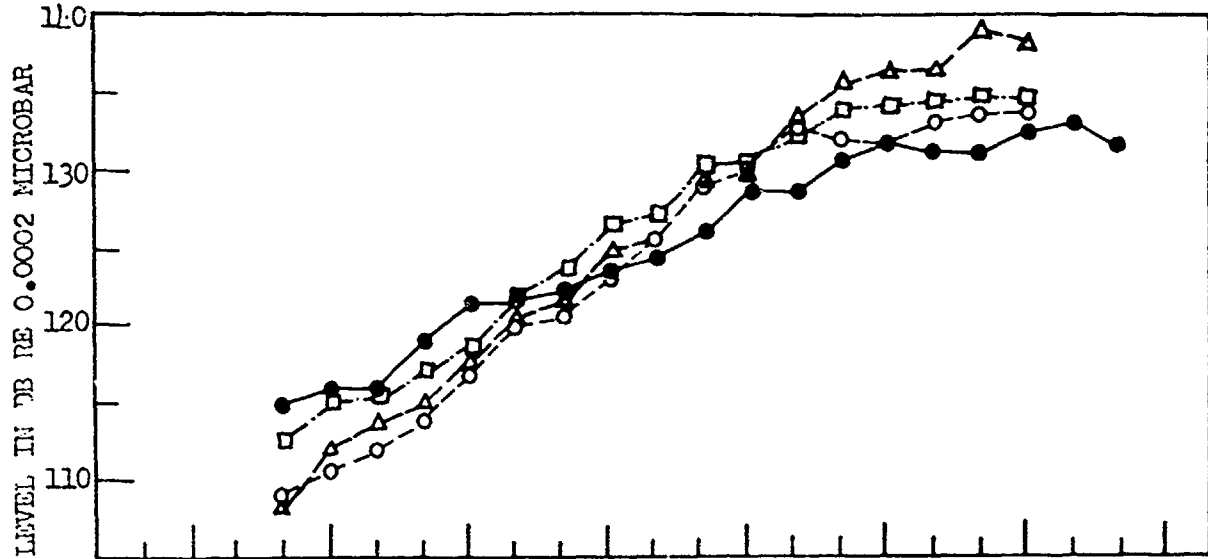


b. Test Location 2

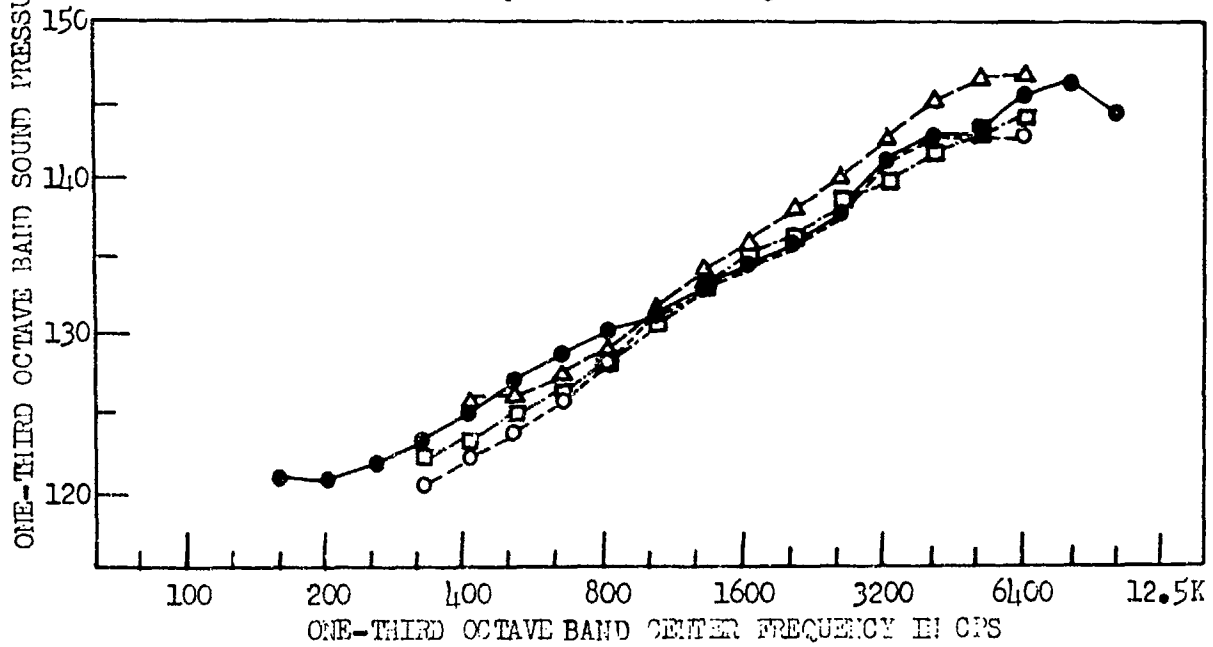
Figure 10. Near field sound pressure levels for the solid propellant model rocket and heated helium jets.



- Rocket
- △—△ Helium A
- Helium B
- Helium C

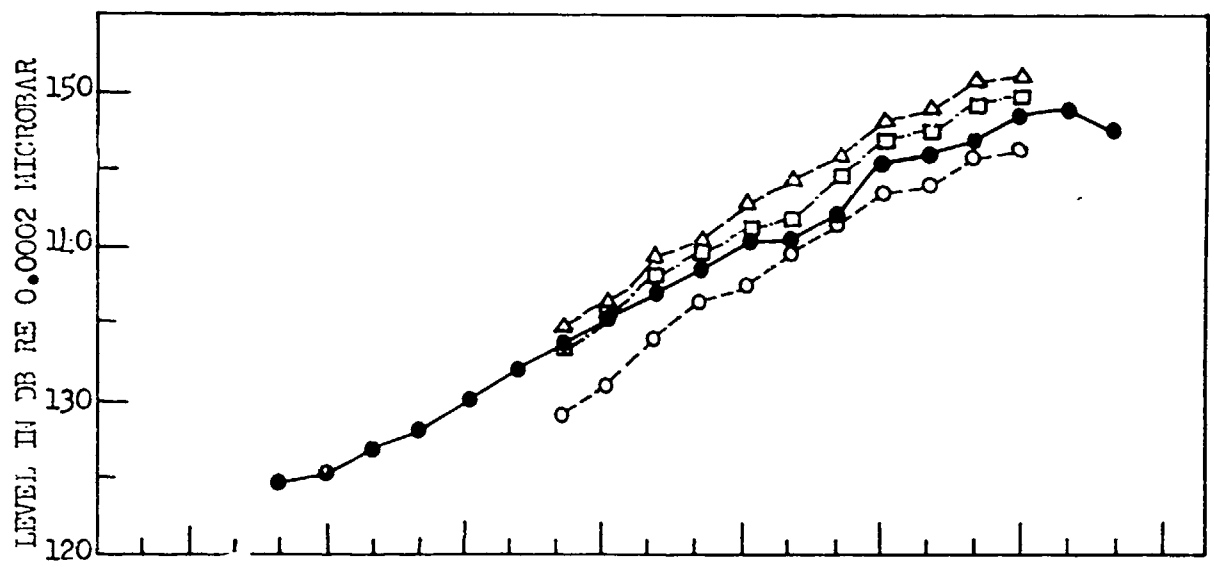
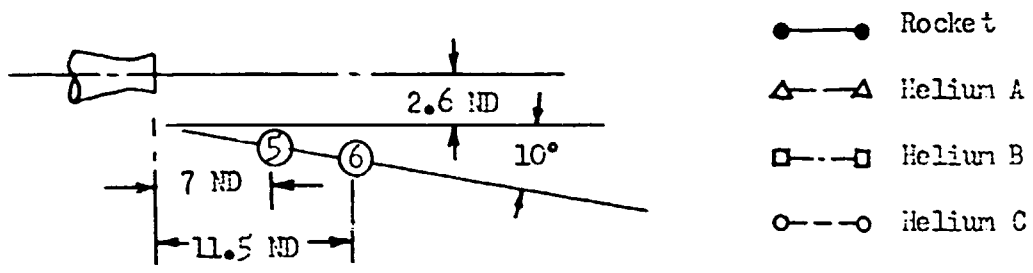


c. Test Location 3

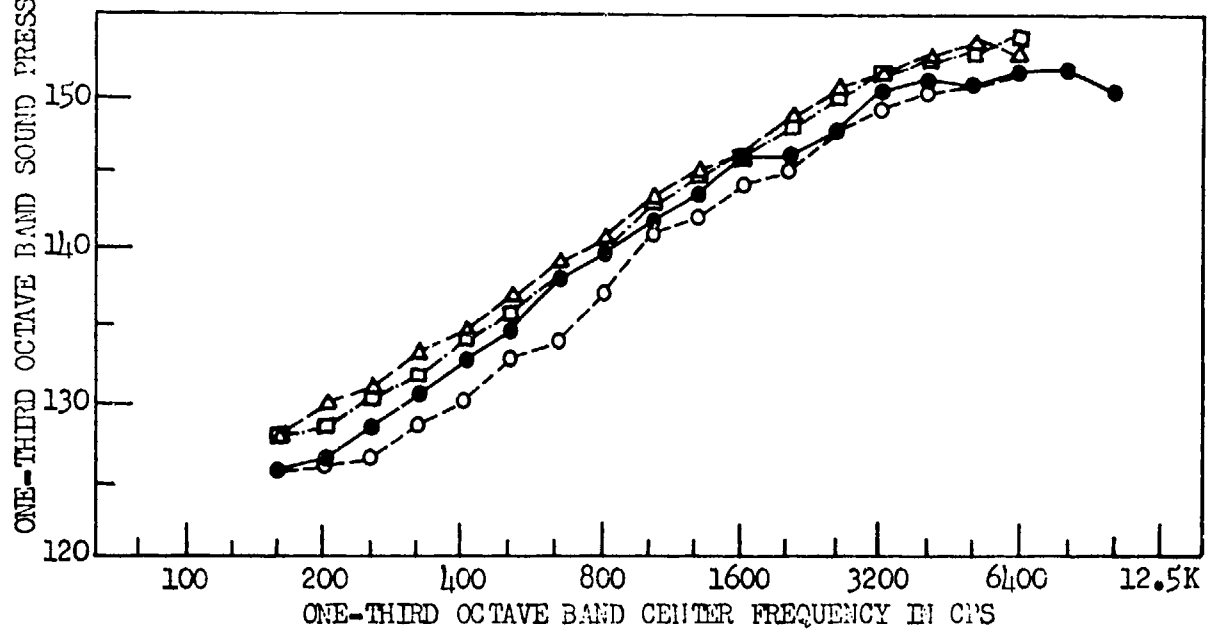


d. Test Location 1

Figure 10. Continued.

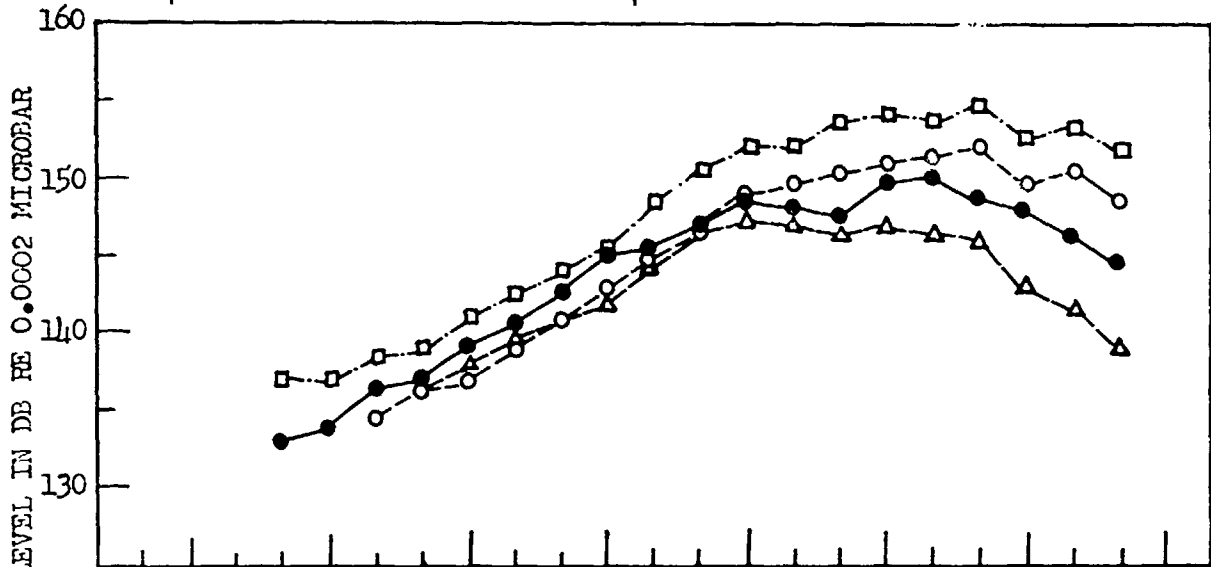
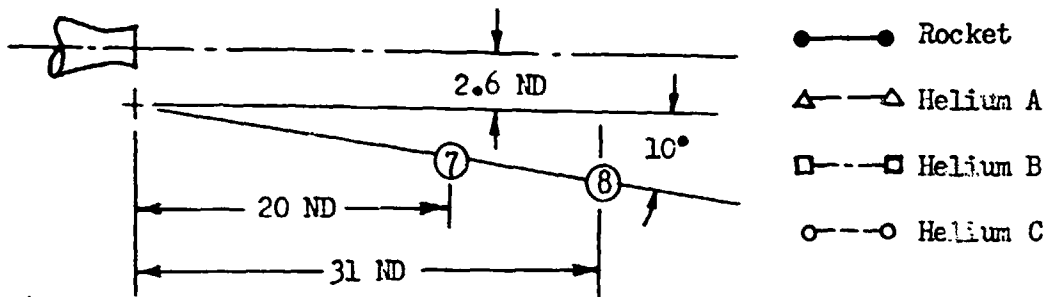


e. Test Location 5

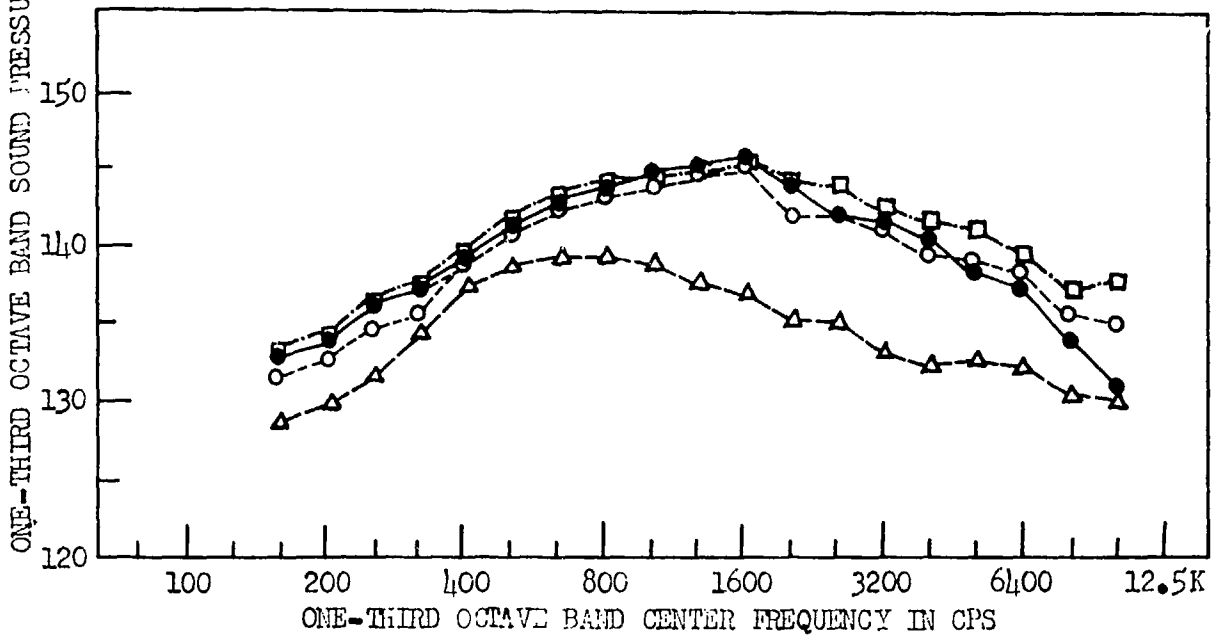


f. Test Location 6

Figure 10. Continued.

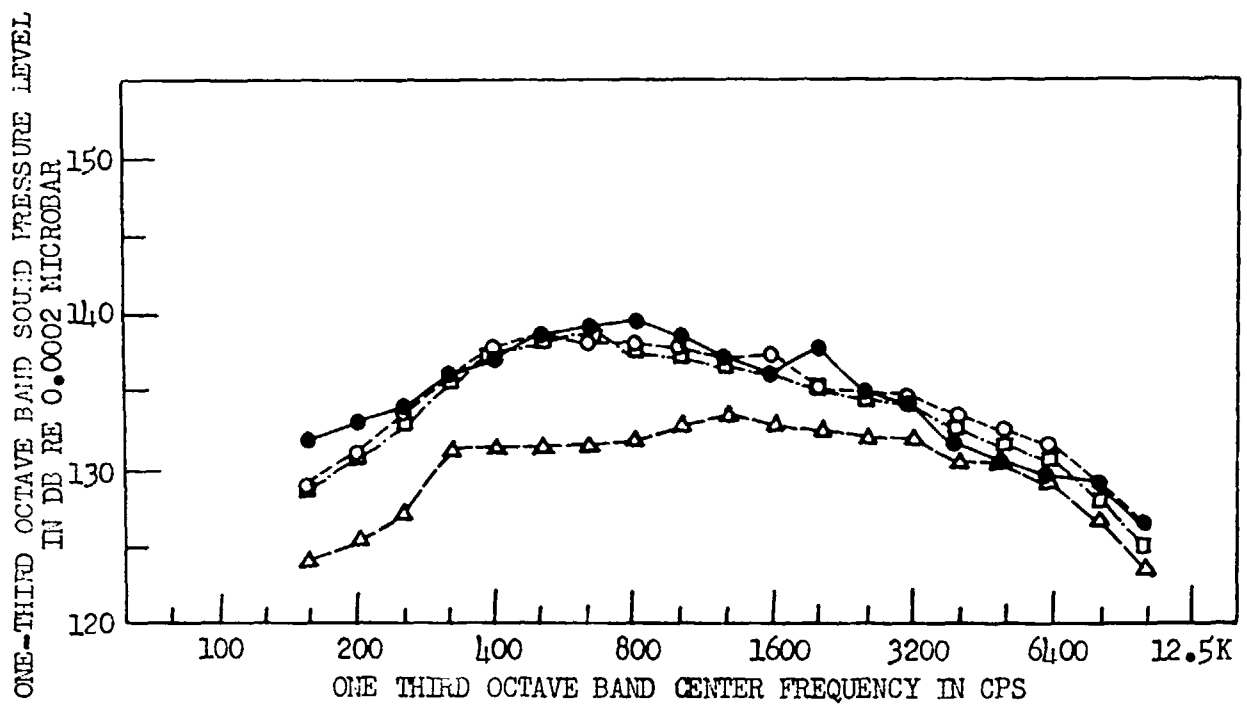
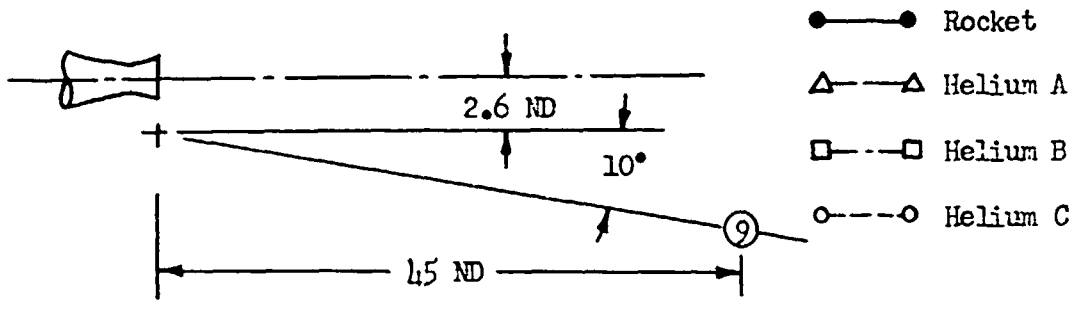


g. Test Location 7



h. Test Location 8

Figure 10. Continued.



i. Test Location 9

Figure 10. Concluded.

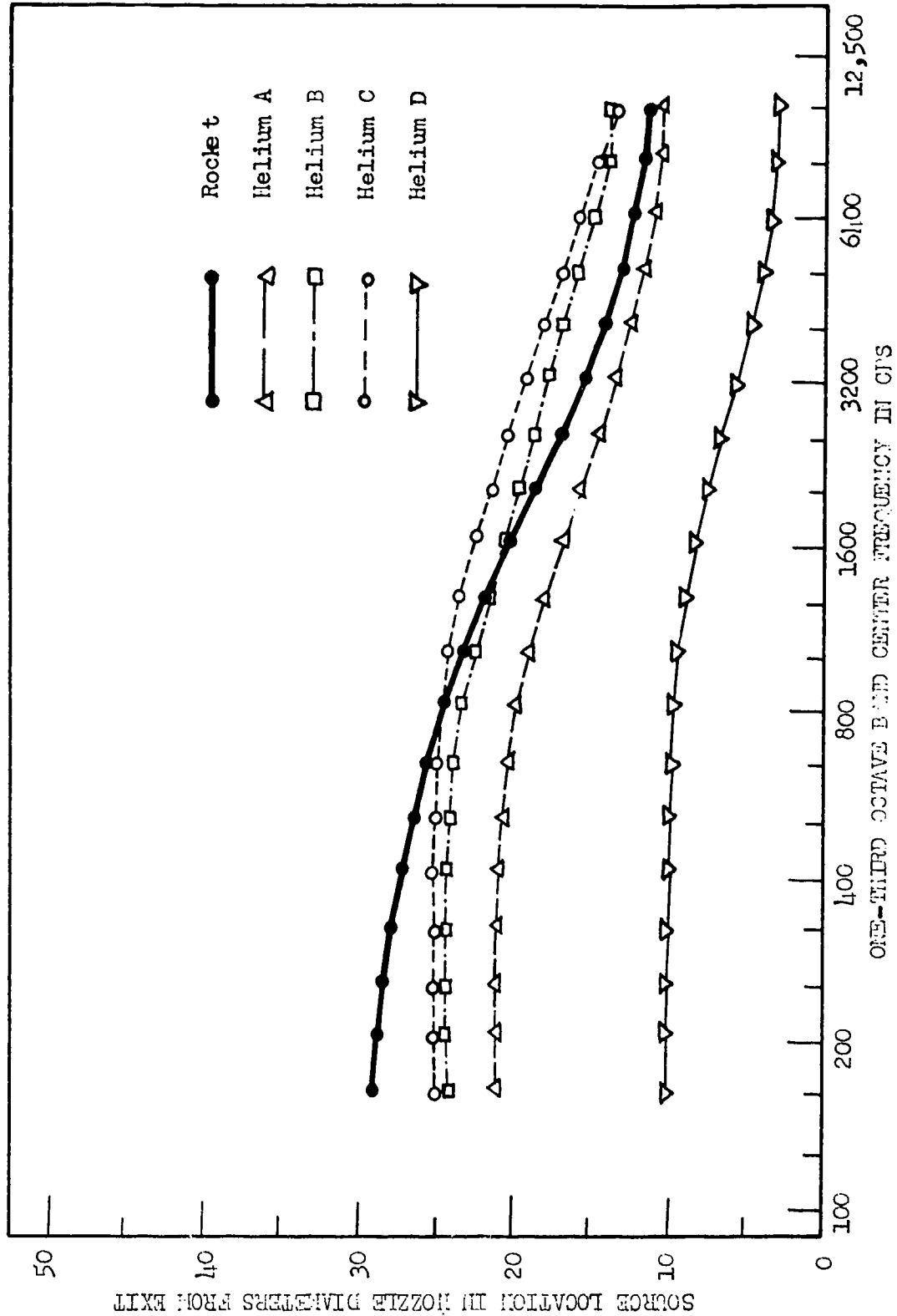


Figure 11. Apparent source locations for one-third octave bands of noise as determined by microphones placed close to the exhaust.

PART II
EFFECT OF VEHICLE MOTION
ON
JET NOISE

I. INTRODUCTION

In recent years a concerted effort has been made to investigate the basic mechanism of noise generation by aerodynamic flow. To a large extent, the results of these investigations have been applied to stationary jet and rocket engines. However, for a more complete study of noise fields associated with flight vehicles, the effects of vehicle motion must also be considered. Relatively little progress has been made in obtaining sufficient experimental data which substantiate existing theories on the effects of motion. It has been difficult to obtain measurements of the type required to substantiate such theories during the course of normal flight test programs because of such problems as: (1) extraneous noise from additional engines, (2) changing engine and flight conditions, (3) extraneous noise from the vehicle boundary layer and noise generated by turbulence around the microphone.

The purpose of this program is to investigate the effects of flight vehicle motion on propulsion system noise which is propagated to parts of the vehicle located in the near field of the jet or rocket engine. The major emphasis is placed on obtaining controlled experimental data which can be compared with theory.

The approach taken in this investigation was as follows:

1. A study was made of the various methods which might be used for theoretically predicting the effects of motion on noise. Following this study, a working hypothesis was developed.
2. A survey was made of various approaches which might be used for measuring the effects of motion experimentally. A scale model jet operating in a small wind tunnel was selected as the best approach.
3. A limited experimental program was conducted to obtain noise data at various operating conditions of the wind tunnel and jet.
4. Experimental results were then compared with those predicted by theory.

A literature survey was initially made of previous work related to the general subject of motion effects on noise. The more pertinent features as revealed by this survey are summarized below.

In the general development of the theory of noise generation from aerodynamic sources, Lighthill¹¹ shows that convection of quadrupole sources increases the noise radiated in the direction of convection. This is introduced as a plausible explanation for the fact that the noise radiated from a jet is greater in the downstream direction than in the upstream direction.

Ostreicher¹² develops equations for the sound field from sources of a general multipole nature which are moving with subsonic speed in a viscous compressible gas.

A general procedure for referring the data observed at a point on the ground to the noise emitted by an airplane during a fly-by is presented by Cole, et al.¹³ Taken into account are the difference in time of emission and observation, inverse square loss, sound absorption in the atmosphere, and Doppler effect. This method permits evaluation of the acoustic power generated by a moving jet.

Reference is made by Powell¹⁴ to theoretical work on the influence of an axial motion of external air flow on the spreading characteristics of a jet. Similarity considerations result in the following conclusions for the region immediately downstream of the nozzle, all expressed relative to the situation when external air flow is absent: (1) the power generated per unit length along the axis is reduced, and the region of generation is extended because the jet itself is extended; (2) the characteristic frequency generated at any given station is increased; (3) the power generated at any particular frequency is decreased, but the rate of change of power generation with frequency is unchanged. Similar but tentative results are described for the region well downstream of the jet core.

Franken, et al.¹⁵, estimated the effect of motion on jet noise by assuming a model which is a simple source attached to the vehicle. This leads to the result that for an attached source, motion of the vehicle tends to increase sound levels in the direction of motion. In the absence of supporting experimental data, Franken¹⁶ later concluded that the analytical method related to sources not attached to the vehicle as suggested by Powell¹⁷ is more reasonable. Franken then derived a relationship between the angle of propagation from the source to a receiver attached to the vehicle when the vehicle is in motion and the corresponding angle when there is no vehicle motion. This results in a general procedure for estimating the change to be expected in a noise field due to vehicle motion.

In reference 17 Powell considers the specific case of noise radiated directly forward, as to a rocket vehicle from the rocket exhaust. It is suggested that the noise on the moving vehicle decreases because of two effects: (1) the total acoustic power decreases as the third power of the relative exhaust velocity, and (2) an inverse square type of loss occurs because of the increased distance that the sound must travel between the source and the receiver located on the vehicle, i.e., the receiver moves away from the source.

Williams¹⁸ derives a method of calculating the noise field generated by a jet by considering the convection of eddies in the flow and the effects of external flow. An equation results which defines a correction factor to be applied to the noise field measured in the absence of external flow to allow for the presence of external flow. Thus at a particular point in the static noise field generated by a stationary vehicle, a correction expressed in decibels for the effect of vehicle motion can be calculated if there is given the ambient speed of sound, the vehicle velocity, the jet velocity relative to the vehicle velocity, and the eddy convection velocity expressed as a fraction of the jet exit velocity. (The practical usefulness and experimental verification of this expression is limited by lack of knowledge of values to assign to the eddy convection velocity.)

Eldred¹⁹ has shown that a receiver attached to a vehicle is expected to receive different noise for varying vehicle velocities. An expression is derived relating the angle of propagation from source to receiver when the vehicle is stationary to the corresponding angle when there is vehicle motion. This expression is mathematically equivalent to that derived by Franken.

II. HYPOTHESIS AND DISCUSSION

A. Hypothesis

Based on the methods suggested by Franken¹⁶, Powell¹⁷, and Eldred¹⁹, a working hypothesis has been developed which is considered to best explain the effects of vehicle motion on jet noise. This hypothesis consists of two parts as stated below:

1. Generation -- The noise generated by a jet exhaust is a function of the relative jet velocity only, i.e., the noise generated by a jet with exhaust velocity V_1 which is in motion at velocity S is identical to the noise generated by a stationary jet with exhaust velocity $V_2 = V_1 - S$.
2. Propagation -- During the time that the noise is propagating away from the source, a receiver attached to the vehicle is moving through the noise field and therefore receives noise which would have passed forward of the receiver had the vehicle been stationary.

Referring to Figure 12, the angle β specifies the direction of a receiver at point R relative to the source at time t_0 . The noise radiated from the source at time t_0 travels at the finite velocity of sound and reaches the moving receiver at a later time t_1 . At time t_1 , the receiver is at a new position R' and therefore intercepts noise which was radiated from the source at t_0 , not at the angle β , but at a smaller angle α . The relationship between the angles α and β is given by the following:

$$\tan \beta = \frac{\sin \alpha}{\cos \alpha - M} \quad (8)$$

(The derivation of this equation as presented by Eldred¹⁹ is shown in Appendix II.) The relationship $(\beta - \alpha)$ vs. β is plotted in Figure 13 for various values of Mach number.

B. Discussion

The validity of the above hypothesis is dependent upon two assumptions: (1) that jets with the same relative jet velocity are dynamically similar and therefore generate the same noise, and (2) that a far field type of radiation can be applied to the near field outside the hydrodynamic region of the jet. It is appropriate to consider these assumptions separately in greater detail.

Noise Generation -- It is essential to distinguish between changes in the radiated noise field which result from changes in exhaust flow parameters and those which are due to vehicle motion. It is therefore necessary that flow parameters which influence noise generation have essentially constant values with changing vehicle velocity, or to somehow account for the changes in the noise field when the desired values of these parameters cannot be maintained as constants.

Jet exhaust noise from a stationary jet is generated by turbulence resulting from shear forces produced by the high speed exhaust stream in the surrounding atmosphere. The intensities of these shear forces are directly related to the velocity of the jet relative to the surrounding air. It is reasonable to assume that when a jet is moved through the surrounding air in a direction opposite to the jet flow, the jet noise power will be reduced because of decreased shear action. Relative exit velocity ($V - S$) of a moving jet is therefore assumed to be equivalent to jet exit velocity (V) in the stationary situation. This assumption is made by Powell in Reference 17; likewise, in a number of other references relative velocity is used as a significant parameter.

Noise Propagation -- References 16 and 19 describe the effect of vehicle motion on the propagation of noise from a jet exhaust, i.e., a receiver attached to the vehicle moves through the noise field. Since this method assumes the source of a particular frequency to be located at a particular point (in contrast to an extended region in the jet), it is basically applicable to the far field. It is desired, however, to apply this method to the near field outside the hydrodynamic region of the jet. The hydrodynamic field cannot be expected to behave like the far field. It appears, however, that the hydrodynamic field considerations are not applicable beyond about five nozzle diameters from the jet; by restricting the receiver to locations outside this boundary, this complication can be disregarded.

The approximate source location of each frequency band of interest can be determined experimentally by measuring noise levels along the jet exhaust boundary and determining the region where the maximum noise levels in that band are observed. By this method an apparent point source for that band of noise in the exhaust can be determined to a probable accuracy of one or two nozzle diameters. For a receiver located beyond eight nozzle diameters from the apparent point source, the source-receiver angular relationship can be reasonably approximated. The only limitation on the ability of a near field experiment to verify the propagation convection effect is the fact that the sources appear to the receiver to be distributed over finite regions. This, however, does not seem to be a prohibitive limitation.

Franken¹⁶ and Eldred¹⁹ both point out that a change in wave-length may be expected at any receiver for any particular frequency when there is vehicle motion. This is not caused by a Doppler frequency shift, but instead it results from a change in the effective propagation velocity only. This effect is not of immediate concern in the current study as it is a refinement in defining the noise field secondary in importance to determination of magnitude and frequency.

C. Procedure for Predicting Effects of Vehicle Motion

The general procedure for predicting the effect of motion on noise in accordance with the previously stated hypothesis is first to account for the effect of reduced relative velocity and then to shift the noise field obtained for the stationary case aft by a calculated amount. A step-by-step procedure is outlined for predicting the sound pressure level which will occur at a

specific vehicle location in a particular frequency band for a particular Mach number by using measured noise data from a stationary engine test.

1. For a given stationary jet, obtain the jet exhaust velocity (V_1) and the density ratio (ρ_e/ρ_a).
2. From the given vehicle velocity (S), calculate the relative jet velocity ($V_2 = V_1 - S$).
3. Operate the stationary jet at the relative jet velocity (V_2) of (2) above and at the density ratio of (1) above. Locate the apparent source of the frequency band of interest by measuring the sound pressure level along the jet boundary and determining the point where a maximum occurs.
4. Determine β (azimuth from source to receiver) for the receiver location of interest (R) from consideration of the geometry alone (Figure 12).
5. From the given vehicle Mach number (M), determine α from Figure 13 or by calculation of Equation 8.
6. Locate a microphone at R' at azimuth α and at the same perpendicular distance from the jet axis as R.
7. Operating the jet as in (3) above, measure the noise at R' in the frequency band of interest. The hypothesis predicts that this is the noise that will be found at the location of interest (R) when the jet specified in (1) above is moving at the given Mach number.

In practice the above procedure may be readily modified so that one stationary engine run serves the functions of (1) determining the source locations of all frequency bands and (2) measuring sound pressure levels on any line parallel to the jet axis. Then by interpolation, predictions can be made for all frequencies of interest at many locations for a given vehicle velocity. One stationary run is necessary for each desired vehicle velocity.

The experiments reported here were all performed in a wind tunnel instead of using a moving vehicle. Although separate mathematical derivations may be made from either viewpoint, the expected results are the same. Throughout the remainder of this report the wind tunnel test results are presented as being applicable to either situation.

III. TEST APPARATUS, INSTRUMENTATION, AND PROCEDURE

A. Selection and Description of Apparatus

A number of existing facilities were evaluated for possible use in determining the effect of vehicle motion on jet noise. These included jet airplanes, a rocket sled, and large wind tunnels. However, each of these were ruled out on the basis of excessive background noise, high operating costs, or difficulty in providing suitable instrumentation.

The apparatus selected for use on this program was a 16-inch diameter induction wind tunnel. The basic features of this apparatus can best be described using Figure 14. The propulsive source was the plant supply of

compressed air which was introduced through an annular injector downstream of the test section. The injector design was based on the work of Knowler and Holder²⁰. The downstream position of the injector allowed the introduction of a sonic block to prevent the noise from the propulsive system from reaching the test section. In order to minimize background noise, an attempt was made to match the size of the sonic plug to airflow at high velocities. The injector introduced air at an angle of 10° to the tunnel axis. The injector slot width was variable up to a maximum of 0.33 inches. The width normally used was 0.25 inches as this resulted in the optimum relationship between tunnel efficiency and low background noise.

To minimize the problem of reverberation effects anticipated in such a small test section, the tunnel wall was made of sound absorptive material. Fiberglas PF-615, a 6 lb/ft³ board, was cut into annular rings whose inside and outside diameters were 16 inches and 24 inches, respectively. Forty-eight 1-inch rings were placed side by side, with occasional one-eighth inch thick aluminum rings for strength, to form the test section wall. A partial vacuum was applied to the plenum surrounding the Fiberglas wall to pull air radially out of the test section through the Fiberglas to minimize the boundary layer and associated noise in the test section.

The jet noise source was a heated air jet, 0.6 inch in diameter, introduced through the tunnel inlet. A conical nozzle of 10° half angle convergence was used as a compromise between the best internal flow and minimum external wake.

A probe microphone (described in Section III-B following) was mounted on a sting projecting through the sonic plug. Adjustment of the axial position of the microphone was made externally by rotating a rod running through the strut. This linkage was completed by a rack on the sting and gears contained within the plug.

Part of an existing exponential horn with a 10 cps cutoff was adapted to serve as a diffuser. The maximum diameter of this section was 48 inches. The average half-angle of expansion was about 3.5°.

A photograph of the assembled apparatus is shown in Figure 15. Only a small part of the diffuser is visible in this photograph.

B. Instrumentation

The two basic requirements of the microphone to be used with this program were that it have a sufficiently low self-noise level and that it be able to measure frequencies high enough to include a significant portion of the model jet spectrum.

To minimize microphone self-noise in the wind stream, laminar flow at the pressure-sensing position was considered to be necessary. This could only be provided by using a cylindrical body to contain the microphone. Descriptions of only two previous instances of success with this type arrangement could be

found in the literature.^{19, 21} In both cases the dimensions of the microphone and housing were so large that diffraction effects limited excessively the upper frequency at which useful data could be obtained. The conclusion reached was that it would be necessary to use a probe microphone.

The probe microphone as it was inserted in the wind tunnel is shown in Figure 16. Four 0.0135-inch holes are drilled in the tip near the point of tangency to the main probe tube. The main tube is 10 inches long, with a 3/16-inch outside diameter and 0.065-inch wall thickness. The probe tube was connected to a Bruel and Kjaer Type 4134 condenser microphone with the UA 0040 Probe Kit. The small plastic washer included with this kit was used to improve the frequency characteristics, but a small slot was first cut across the face of the washer so that the microphone would be vented. Small tufts of steel wool were used near each end of the probe tube to damp the major tube resonances. The conical housing was attached rigidly to the probe at the front end, but soft rubber material for vibration isolation was placed between the microphone vacuum-tube cathode follower case and the conical housing. Similar material was placed on the cable for a short distance downstream of the cathode follower.

An equalizing circuit was placed after the cathode follower. The frequency response of the probe microphone utilizing this equalizer is shown in Figure 18 for one-third octave bands. This calibration was performed by comparing the probe microphone with a standard Bruel and Kjaer Type 4133 microphone, both being exposed to the broad band noise from a small jet operated outdoors. This should be considered as only an approximate calibration. However, because only changes due to the effect of motion were to be determined, this method was considered satisfactory. The corrections implied by the frequency response shown in Figure 18 have been applied to all reported data. No data are reported above 12,500 cps, however. Without the equalizing circuit, the response of the probe microphone would have been down approximately 24 db at 12,500 cps relative to 1000 cps instead of 1 db down as shown.

C. Wind Tunnel Performance and Operation

Performance -- A rake consisting of three calibrated static pressure pickups and five total pressure pickups was arranged so that it could be positioned at various locations in the tunnel test section. An additional static pressure pickup located in the downstream portion of the test section was monitored during all tests. Static pressure taps were also placed in the wall opposite the plug.

The surveys which were made with these pickups indicated that the total pressure was atmospheric down to within a short distance forward of the plug. The Mach number at any location could therefore be obtained by measuring the static pressure, calculating the pressure ratio as the ratio of static to atmospheric pressure, and reading the Mach number corresponding to this ratio as tabulated in Reference 22. At any given station in the test section, the wind velocity was constant up to within one-half inch of the walls. The velocity along the axis of the tunnel increased somewhat with downstream station. At a nominal Mach number of 0.62, the Mach number increased from about 0.60 at the most forward station used to 0.64 at the most downstream station used. At this

and all other velocities used, the value reported is the average velocity in the test section. At Mach numbers lower than 0.62 the change in velocity with axial position was proportionately less. Eliminating the vacuum-induced flow approximately doubled the variation noted in axial velocity.

The weight flows of air in the injector supply line and the vacuum line were determined using an approximate method described by Ower.²³ The ratio of weight flow through the tunnel test section to weight flow through the injector varied from about 7 at a test section Mach number of 0.12 to 2.5 for a test section Mach number of 0.62.

Figure 17 shows the placement of the 0.6-inch diameter jet nozzle in the wind tunnel and the 13 stations at which sound level measurements were made. The background noise level at one station in the test section is presented in Figure 19. Background noise was measured while operating the jet with unheated air at the same velocity as the wind tunnel flow (zero relative velocity). This background noise was nearly independent of location throughout the central part of the test section. At a Mach number of 0.62, eliminating the vacuum-induced flow increased the background noise by about 2 db at all frequencies. The maximum vacuum-induced flow which could be provided was about 3 lbs/sec. It is believed that two or three times this flow would have been necessary to reduce the boundary layer noise substantially.

Wind Tunnel and Jet Operation -- The mechanics of predicting noise in the presence of vehicle motion consist of obtaining measurements at specific locations in the absence of vehicle motion and then translating these data to new positions based on vehicle motion considerations. The stationary condition required is a jet exhaust velocity numerically equal to the relative exhaust velocity for the motion condition to be predicted. The set of jet conditions intended to be representative of a typical straight turbojet engine are given in Table V as Conditions 1 through 3. The set of Conditions 4 through 6 maintains the relative exhaust velocity constant. This second set is useful in providing additional conditions from which to make comparisons and is not intended to be representative of actual engine operating conditions. The noise data measured for the stationary jet Conditions 9, 10, and 11 are translated in accordance with predicted propagation effects to establish the predicted sound pressure levels for the moving jet Conditions 1, 2, and 3, respectively. Condition 7 supplies the reference noise data for the stationary 1860 fps jet.

Condition 12 serves as the base line for another series using Conditions 4 through 6. In this series a different reference stationary jet is used for each of Conditions 4 through 6. Condition 9 serves as the reference for Condition 4, and Condition 8 is the reference for Condition 5. Since a stationary jet with an exit velocity of 2070 fps was not included among the measured data, a noise spectrum for a 2070 fps jet was estimated at each measurement location by extrapolating measured data from Conditions 7 through 12. These estimated data serve as reference data for Condition 6. The small difference in density ratio for Conditions 4 through 6 was taken into account by a correction of 0.5 db.

The desired adjustments between jet density and velocity were made by varying the temperature, pressure, and Mach number of the jet. The velocities were the highest which could be used with a convergent nozzle and a 1100°F temperature limitation. Although a convergent-divergent nozzle could have been used at higher pressures and Mach numbers without producing screech, a different convergent-divergent nozzle would have been required for each jet condition at each tunnel velocity.

To obtain the required acoustic data, the microphone was first positioned. The model jet was then started and stabilized operation was achieved. The tunnel was then set to the desired velocity, and a spectrum of one-third octave band levels was obtained by use of a graphic level recorder. The tunnel was shut down, the microphone moved (usually with the jet still running), and the procedure repeated.

Data for determining the source locations of the various frequency bands (required for application of the prediction method) were obtained by placing a microphone at various positions along the jet boundary. Data were taken for all jet operating conditions from 1190 to 1860 fps inside the wind tunnel without tunnel air flow.

IV. RESULTS AND DISCUSSION

A. Data Processing Method

Using the data in absence of vehicle motion (Conditions 7 through 11 in Table V), predictions of the noise expected with vehicle motion are made. Each of these stationary conditions corresponds to a condition measured in the presence of vehicle motion in that it has the same relative velocity (e.g. Condition 10 and Condition 2). A shift in position is all that needs to be applied to the stationary data at the corresponding relative velocity. This shift depends on Mach number and angular location; therefore, the source location of the particular frequency band of interest must be known. Figure 20 shows the source locations for the particular jet used in this investigation.

An illustration of the method used in this study to make sound pressure level predictions for the conditions for which wind tunnel data were obtained is given in the following example.

Consider a jet operating at 1860 fps and moving with the vehicle at a velocity of 670 fps (Mach 0.62). It is desired to predict from static noise data the sound pressure levels during motion in a one-third octave band centered about 8000 cps for a number of stations all located 8 nozzle diameters to the side of the jet axis. Station 20, which is located 20 nozzle diameters aft of the nozzle, is considered first in the following example:

1. The relative velocity is 1190 fps (1860 - 670); this is Condition 11 in Table V.
2. From Figure 20, the source location for 8000 cps for a jet of 1190 fps is 2.4 nozzle diameters aft of the nozzle.

3. The azimuth β in relation to the source (jet exhaust direction is 180°) is determined as follows:

$$\beta = \tan^{-1} \frac{8}{-20 + 2.4} = 155.5^\circ$$

4. From Figure 13, $\beta - \alpha$ is found to be 15° for Mach 0.62; therefore $\alpha = 140.5^\circ$.
5. The station for the static jet where the sound pressure level is the same as for Station 20 in the moving case becomes

$$\frac{8}{\tan 140.5^\circ} + 2.4 = 12.1$$

6. Sound pressure levels for the one-third octave band centered about 8000 cps are plotted versus station for the 1190 fps stationary jet condition in Figure 21.
7. The sound pressure level is read at Station 12.1 from the 1190 fps stationary jet curve (Figure 21) and then shifted aft to Station 20.
8. By following the above procedure (steps 3-7) at other stations, a predicted curve of sound pressure level versus station for the 1860 fps jet moving at Mach 0.62 can be drawn. For reference, the curve of the stationary 1860 fps jet is also shown in Figure 21.

By use of the method outlined above, the data were processed for all frequency bands and for all Mach numbers. This resulted in information to make plots of predicted sound pressure levels versus frequency at a given station. Comparisons of these data were then made at each station with measured results obtained in the wind tunnel and also with the measured stationary full-velocity jet data; these comparisons are shown in Figure 22 (a-e).

Obtaining a sufficient signal-to-noise ratio was a problem in many cases, particularly for the high wind tunnel velocities which with resulting low relative jet velocities constituted combinations of low signal and high background noise. It was necessary, therefore, to exclude a large portion of the data because of inadequate signal-to-noise ratio (3 db or less) relative to the tunnel background noise. In less severe cases corrections have been applied to the data. Corrections applied to measured levels based on the signal-to-noise ratio noted were as follows:

Greater than 12 db	No correction applied
6 to 12 db	Data corrected (-1.5 to -0.5 db)
3 to 6 db	Data corrected (-3.0 to -1.5 db) Data in this range marked with line through the plotting symbol (ϕ)
Less than 3 db	Data discarded

In summary, very little reliable data were obtained where the jet sound pressure levels were low, for example, at low frequencies (below 1000 cps), at high wind tunnel velocities (above Mach 0.32), or at stations forward of the nozzle.

B. Discussion

Scale Model Frequencies -- Because of the small jet nozzle used in this experimental program, the frequencies are, of course, very high relative to a full size engine. For example, a 22-inch turbojet engine operating at a velocity of 1860 fps would generally have its spectrum peak in the 150 to 600 cps range. By application of scaling principles, the 0.6-inch model jet correspondingly should peak at 5,500 to 22,000 cps. An examination of the static jet curves in Figure 22 shows this to be true. The upper frequency limit of the microphone and probe combination prevented observance of this spectrum peak in a few cases.

Comparison of Predicted and Measured Levels -- The general agreement with theory is easily seen for a Mach 0.32 condition in Figure 22d, where moderately large SPL reductions from the static condition are expected. For example, at Stations 12, 16 and 20, 6 to 12 db reduction was predicted and 5 to 10 db reduction was measured.

The agreement between predicted and measured values is apparently poorest at the Mach 0.22 condition shown in Figure 22b. At Stations 16 and 20, where the static jet levels were highest, 4 to 11 db reduction was predicted, but only 1 to 5 db reduction was measured.

The highest wind tunnel velocity for which any jet noise levels were measurable above the background was Mach 0.62; data for this condition are shown in Figure 22e. At Station 20 measured reductions of 17 to 20 db compared favorably with predicted reductions of 15 to 19 db. At the other stations for which data were obtained above the background noise the measured reductions were somewhat greater than predicted.

Except for very few cases (1%), the predicted moving jet sound pressure levels for all frequency bands at all stations never exceeded by more than one decibel those for the static jet at the same station. This prediction was verified by measurement also where less than 2% of the measured values in motion were more than one decibel above those for the static jet. It is significant to note that there is no general trend of increasing sound levels with motion at positions forward of the nozzle as would have been predicted by some of the earlier theories. The agreement of measured levels with those predicted by the present theory is much worse at the forward stations than for positions aft of the nozzle.

The general trends of the predicted motion effects shown in Figure 22 appear to be confirmed by the results from the experimental program; however, the magnitudes of the deviations in some instances are somewhat disappointing. In order to summarize the extent of the agreement and to compare the subject method with other simpler approaches, Table VI has been prepared. This table shows the

percentage of the measured noise data obtained in the wind tunnel that agreed within ± 2 decibels of the predicted values. All of the measured data from Figure 22 were used in making this analysis, i.e., all stations and all frequency bands.

In Method 1 the measured sound levels at each station from the full-velocity static jet are used with no corrections, i.e., this method assumes the effect of motion to be negligible. As might be expected the agreement between predicted and measured sound levels gets progressively worse as the vehicle Mach number is increased, thus demonstrating the need for some type of correction.

Method 2 uses measured noise data from a static jet operating at reduced velocity corresponding to flight relative velocity, but no correction is made for the shift in position caused by motion as required by the second part of the present hypothesis. With this method the agreement gets progressively worse with increased Mach number, but it is significantly better than Method 1 where no correction is applied.

Method 3 represents the present approach which utilizes measured data from a reduced velocity static jet and also accounts for a position shift for the motion effect. There appears to be no general trend in agreement with increasing Mach number as was noted for Methods 1 and 2. For over 98% of the 369 individual sets of values compared, Method 3 gave values within ± 6 decibels of those measured in the wind tunnel.

In Method 4 the reduced relative velocity is taken into account by means of calculation based on the 8th power of relative velocity. No corrections are applied for a shift in position. This method is identical to Method 2 except that reduced relative velocity levels are estimated from the levels measured for a full-velocity static jet rather than being measured for the lower relative velocity condition. Use of this method appears to produce no trend in agreement with Mach number. The use of the 8th power of relative velocity for all locations and frequencies is justified only on the basis of simplicity. If this method were to be used in practice, velocity exponents appropriate to a specific location and frequency should be used.

From inspection of Table VI, it can be seen that Method 3 yields better agreement than Method 2 for four out of the five conditions shown; thus it is seen that the correction for position shift resulted in an improvement. The very simple approach of Method 4 appears to give results almost as good as the complex approach of Method 3. It should not be concluded, however, that Method 4 will apply equally well in all situations. For example, if the method is applied to rockets the eighth power dependence on relative velocity would probably have to be changed to a third power dependence. This lower exponent coupled with the smaller percentage change in relative velocity (because of the high exit velocity of the stationary rocket) would then make the position shift the predominant factor governing the SPL changes due to motion. It would be desirable to verify this experimentally with a high velocity (above 7500 fps) jet or rocket in a wind stream. This could be accomplished by use of a small heated helium jet as described in Part I of this report.

Past experience in working with jet noise has shown that most consistent data are generally found near the peak of the spectrum. For the model jet used in this program, the upper four 1/3 octave bands (center frequencies at 6.4, 8, 10, and 12.5 kcps) are considered to be representative of the spectrum peak. The correlation between measured and predicted values of noise reduction caused by motion is shown in Figure 23 for these frequency bands. Although there is considerable data scatter, the measured data tend to follow the predicted values.

Position Shift -- The shift in position of the noise field caused by vehicle motion is not obvious in the plots of SPL versus frequency in Figure 22. To observe this effect more readily, a different type presentation is required as shown in Figure 24. In this figure an 1860 fps jet operating in a Mach 0.32 wind is considered. According to the hypothesis, the effects of motion are determined in this case by operating a static jet at an exit velocity of 1505 fps and by making a noise measurement at a specified forward position determined by calculation. In Figure 24 the calculated rearward shifting of the noise field for an 8000 cps source can be seen. The measured data for an 1860 fps jet operated in a Mach 0.32 wind stream are shown for comparison. It is apparent that the measured and calculated plots of SPL versus position are quite similar. The measured values are slightly higher, but the peaks occur at the same station. This particular condition and frequency band was selected for illustration because it was one of the better examples. However, a shift of position occurs at all frequencies and at all test conditions. The position shift is not readily apparent in some cases because of unexplained variations in level which tend to obscure the shift.

To permit quick analysis of the position shift effect for various motion conditions, Figure 25 (a-e) presents curves of SPL versus station for (1) the measured static relative-velocity jet, (2) the measured full-velocity jet in motion, and (3) the predicted full-velocity jet in motion. The peaks of these curves have been normalized to separate the shift in position from the unexplained shift in sound pressure level.

Analysis of the curves of measured data in Figure 25 indicates the following:

1. Without exception, all curves shift downstream.
2. For a given jet and wind tunnel condition the shifts are greater for the more downstream positions.
3. The Mach 0.32 data show greater shifts than the Mach 0.22 data. The Mach 0.62 data are somewhat inconclusive as to the magnitude of the shift because of lack of data; however, they appear to fit the trend of increased shift with Mach number.

Qualitatively, then, the shift in position caused by motion is behaving as predicted, i.e., in direction, in trend with position, and in trend with Mach number. Quantitatively, the experimental results appear to be in reasonable agreement with theory. In general, the actual shift appears to be somewhat greater than predicted, except for the 1860 fps jet at Mach 0.22 which produced much less position shift than expected. Also, this particular condition did not produce the expected drop in sound pressure level as noted in Figure 22b. This raises the question of a possible error in wind tunnel velocity for this particular jet condition because the other Mach 0.22 condition shown in Figure 24a

produced shifts in reasonable agreement with theory. (However, a check of the records for this particular experimental run did not reveal any obvious errors.)

Overall Evaluation of Hypothesis -- On a qualitative basis the experimental results are consistent with the two motion effects predicted by the hypothesis; i.e., noise reductions associated with reduced relative velocity and downstream shifting of the noise field are both observed. However, on a quantitative basis, the agreement of experimental results with theory is not sufficient to completely confirm the hypothesis. It is reasonable to assume that a combination of small experimental errors could account for at least some of the deviations observed, e.g., a 3% error in jet velocity determination will cause a one decibel change in sound pressure level. In the absence of any conflicting trends with theory or gross inconsistencies between measured and predicted values in general, it is tentatively concluded that the hypothesis is fundamentally valid.

Airplane Flight Results Compared -- It is desired to compare results predicted by theory with those obtained from airplane flight. Unfortunately very little of the already small quantity of available flight data can be used because of (1) the presence of boundary layer noise, (2) unknown flight and engine conditions, (3) multiple engine operation and (4) lack of ground-measured static data at the appropriate reduced relative velocity conditions. In order to make a good comparison, preferred flight conditions are those which will be expected to produce a large change in noise so that motion effects can be easily observed.

Noise measurements made in two aft compartments of the XB-47 airplane²⁴ showed large reductions in sound pressure level for a flight condition of Mach 0.77 at 15,000 feet altitude compared to ground measurements made at the same engine compressor speed. Average noise reduction values are shown below for three low frequency bands where boundary layer noise did not affect the results.

75 - 150 cps	22 db
150 - 300 cps	17 db
300 - 600 cps	12 db

It is not possible to make an accurate prediction of the noise reduction for the above case because no noise data along the outside of the fuselage are available from static runs at reduced engine power settings which correspond to the lower relative velocity in flight. Qualitatively, however, the measured results appear to be in reasonable agreement with theory. For example, at Mach 0.77 the relative velocity would be reduced to about 55% of the static jet velocity; this would cause a large reduction in acoustic power generated (21 db if V^6 is assumed to apply). The jet directivity effects caused by reduced relative velocity and forward motion would modify the results, but these effects are difficult to evaluate because of the lack of static data for the reduced velocity condition.

Method Applied to Various Propulsion Systems -- Application of the general method described in this report to various type engines and vehicles can be expected to produce a wide variation in the SPL changes caused by motion.

Approximations of the predicted change in noise caused by the change in relative velocity with motion are given in Table VII. (This table does not account for the shift in position of the noise radiation pattern with motion.) The velocity dependence terms, which have been assumed for illustrative purposes only, are shown below; these are based on directivity considerations.

	<u>Aft of Nozzle</u>	<u>Forward of Nozzle</u>
Turbojets	v^8	v^4
Afterburning turbojets	v^8 below 1860 fps; v^6 for 1860 to 2500 fps	v^4
Rockets	v^3	v^3

The smaller values of noise reduction shown in Table VII for rockets relative to turbojets are caused by two factors: (1) the percentage change in relative velocity is smaller because of the high rocket exit velocity and (2) the velocity exponent is smaller. Because of the small noise level change due to these two factors, it appears unnecessary to require noise data from a reduced velocity static run when it is desired to predict the effect of motion on rocket noise. The principal requirement, then, for making a prediction is the availability of full-velocity noise data at various locations of interest. These noise data can be conveniently provided by use of a scale model rocket. The expected result for positions forward of the nozzle would be rapidly decreasing noise levels as the vehicle velocity approaches Mach 1.0 due to the shift in noise radiation pattern. Aft of the nozzle, the rocket noise could increase or decrease depending upon the particular location and velocity relationship. For turbojets, an increase in noise aft of the nozzle does not generally occur because the relative velocity effect predominates over the effect caused by the shift in the noise pattern.

5. CONCLUSIONS

The evidence presented in this report tends to confirm the hypothesis that the effect of vehicle motion on jet noise can be explained by two separate factors: (1) the noise produced by a jet in motion is dependent upon the relative velocity between the jet and the air through which it moves; and (2) a shifting of the noise radiation pattern toward the rear occurs because of combined effects of vehicle motion and the finite velocity of sound.

The specific method developed for predicting effects of motion on jet noise is workable. However, since it requires the use of either measured or estimated noise data for various power conditions for a stationary engine, the success of the method is dependent upon the availability and accuracy of the appropriate stationary engine data.

Application of the method to various classes of flight propulsion systems indicates that the relative importance of the two factors contributing to the motion effect changes as the exhaust velocity of the power plant is increased. For turbojet vehicles the general effect of motion is large reductions in noise mainly because of reduced relative velocity. When similar motion is applied to vehicles equipped with the higher jet velocity afterburners or ramjets, the noise reductions will be smaller. The effect produced by the shifting of the noise radiation pattern then becomes more significant. For rocket vehicles the effect of relative velocity change is almost insignificant compared to the effect of the shift in the noise radiation pattern. For a vehicle with a tail-mounted rocket the noise on the vehicle is always reduced relative to the static condition; however, for a forward-mounted rocket, the noise on the vehicle could increase or decrease with motion depending upon the particular relationship of vehicle velocity and location. These general effects can be investigated for specific cases by the method outlined in this report.

APPENDIX II

EFFECT OF MOTION ON PROPAGATION OF SOUND

The following derivation has been reported by Eldred.¹³ Minor changes have been made in designating certain symbols to be consistent with the terminology of this report.

The moving vehicle situation is depicted in Figure 26. The receiver, which is initially at point R at the time t_0 , is attached to the vehicle, which moves at a constant velocity S, or Mach number $M = S/a$ through the stationary medium. Consider that the sound radiated at time t_0 reaches a point R' at time t_1 , $(t_1 - t_0)$ seconds after the sound was radiated. During this propagation time the receiver has moved from R to the point R', a distance equal to $Ma(t_1 - t_0)$.

The distance which the sound must travel in the stationary medium to reach the moving receiver is given by

$$r' = a(t_1 - t_0) \quad (9)$$

The distance which the receiver has moved in the time interval $t_1 - t_0$ is

$$Ma(t_1 - t_0) = r' \cos \alpha - r \cos \beta \quad (10)$$

where β is the angle (measured from the direction of vehicle motion) which relates the receiver to the source in the coordinate system moving with the vehicle, and α is the angle of noise radiation from the source to the moving receiver.

Substituting r' for $a(t_1 - t_0)$ in equation (10),

$$r' (\cos \alpha - M) = r \cos \beta \quad (11)$$

Since the perpendicular distance between the vehicle longitudinal axis and both R and R' is constant,

$$r' \sin \alpha = r \sin \beta \quad (12)$$

Dividing equation (12) by equation (11) and transposing,

$$\tan \beta = \frac{\sin \alpha}{\cos \alpha - M}$$

shown previously as equation (8). The relationship $(\beta - \alpha)$ versus β is plotted in Figure 13 for various values of Mach number.

Table V. Jet flow parameters and wind tunnel operating conditions.

Condition Number	Wind Tunnel			Model Jet				ρ_e/ρ_a
	M	S (ft/sec)	ρ_a (lbs/ft ³)	P_t/P_a	T_t (°F)	V_e (ft/sec)	ρ_e (lb/ft ³)	
1	0.22	245	0.0747	2.175	960	1860	0.0331	1615
2	0.32	355	0.0726	2.19	950	1860	0.0322	1505
3	0.62	670	0.0636	2.275	900	1860	0.0282	1190
4	0.22	245	0.0747	1.74	1055	1645	0.0293	1400
5	0.32	355	0.0726	1.88	1070	1755	0.0285	1400
6	0.62	670	0.0636	2.44	1100	2070	0.0249	1400
7	0	0	0.0765	2.16	970	1860	0.0339	1860
8	0	0	0.0765	1.97	940	1725	0.0339	1725
9	0	0	0.0765	1.81	910	1615	0.0339	1615
10	0	0	0.0765	1.685	885	1505	0.0339	1505
11	0	0	0.0765	1.38	820	1190	0.0339	1190
12	0	0	0.0765	1.575	860	1400	0.0339	1400

Table VI. Agreement of measured data with predicted values.

Values shown in the table indicate the percentage of measured SPL data which agree within ± 3 decibels with SPL values predicted by various methods (see text); numbers in parentheses indicate the percentage of data which agree within ± 6 decibels. The sample consists of all measured SPL data shown in Figure 22 (a-e), i.e., for all frequency bands and all measurement locations.

Vehicle Mach number	0.22	0.22	0.32	0.32	0.62
Jet velocity	1645	1860	1725	1860	2070
Wind tunnel velocity	245	245	355	355	670
Number in sample	97	107	71	72	22
<u>Prediction method</u>					
1. Use measured full-velocity static jet only (no corrections)	51	71	25	23	0
2. Use measured relative-velocity static jet (no correction for position shift)	62	63	50	53	35
3. Use measured relative-velocity static jet with correction for position shift	71 (100)	52 (97)	65 (99)	85 (100)	41 (91)
4. Use estimated relative-velocity static jet based on: $(V_1 - S) / V_1^8$	61	69	62	65	59

Table VII. Estimated reduction in sound pressure level due to relative velocity effects.

	Aft of nozzle		Forward of nozzle	
	Mach 0.5	Mach 0.9	Mach 0.5	Mach 0.9
Turbojets (1860 fps)	12 db	26 db	6 db	13 db
Afterburning turbojets (2500 fps)	6 db	15 db	4 db	9 db
Rockets (7500 fps)	1 db	2 db	1 db	2 db

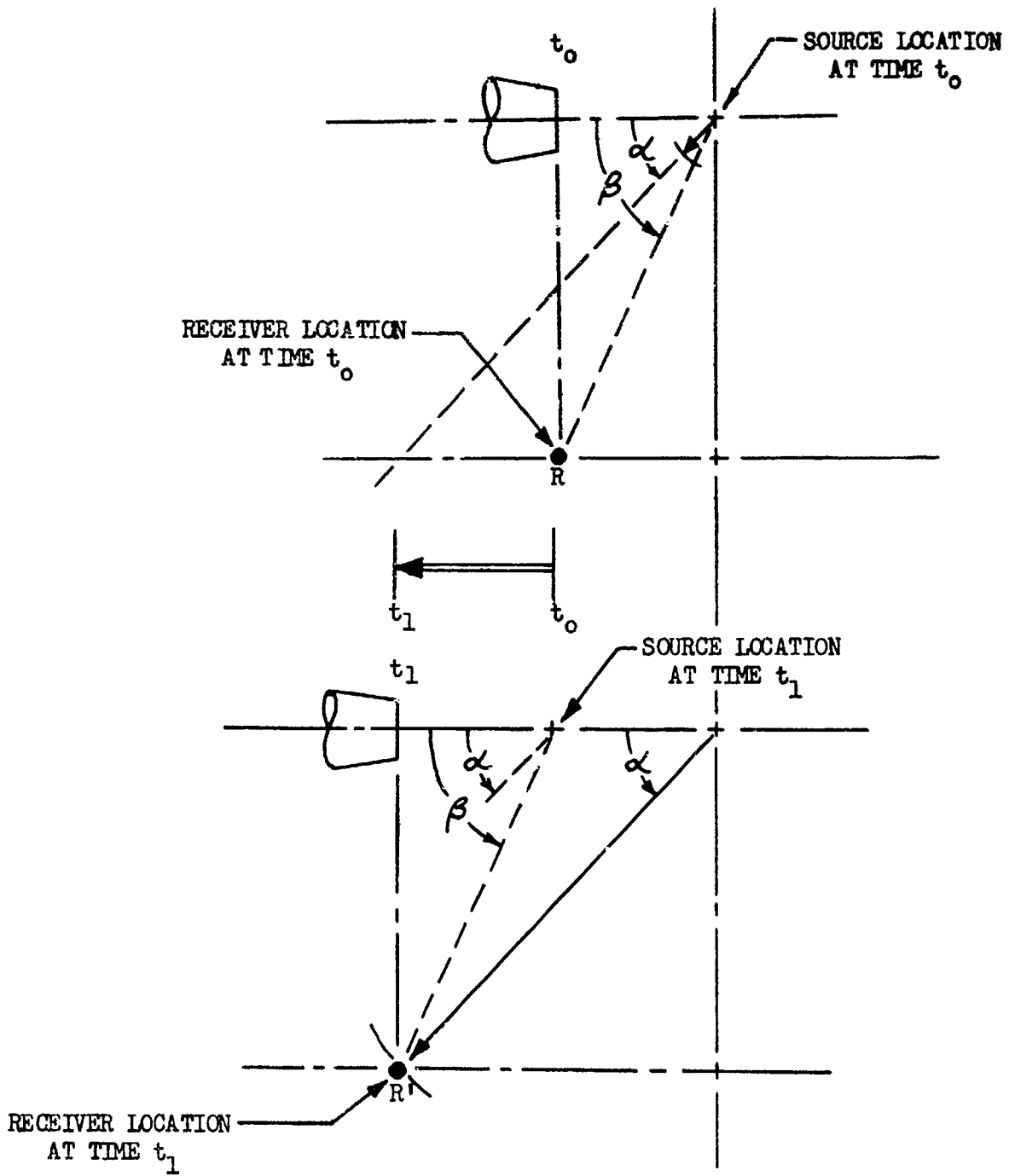


Figure 12. Geometrical relationship between angles α and β for a jet in motion.

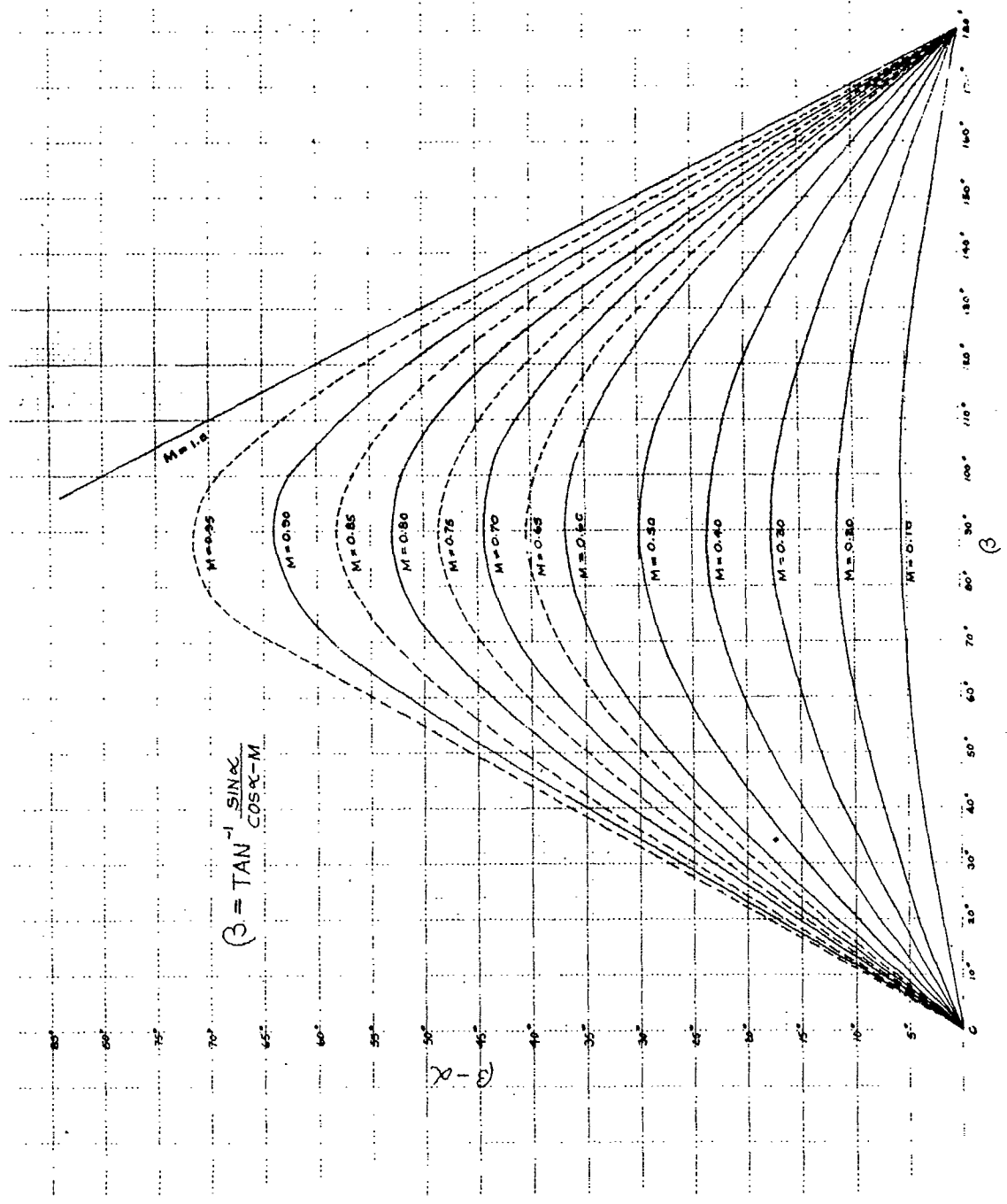


Figure 13. Relationship between angles ($\beta - \alpha$) and β for a jet in motion at various Mach numbers.

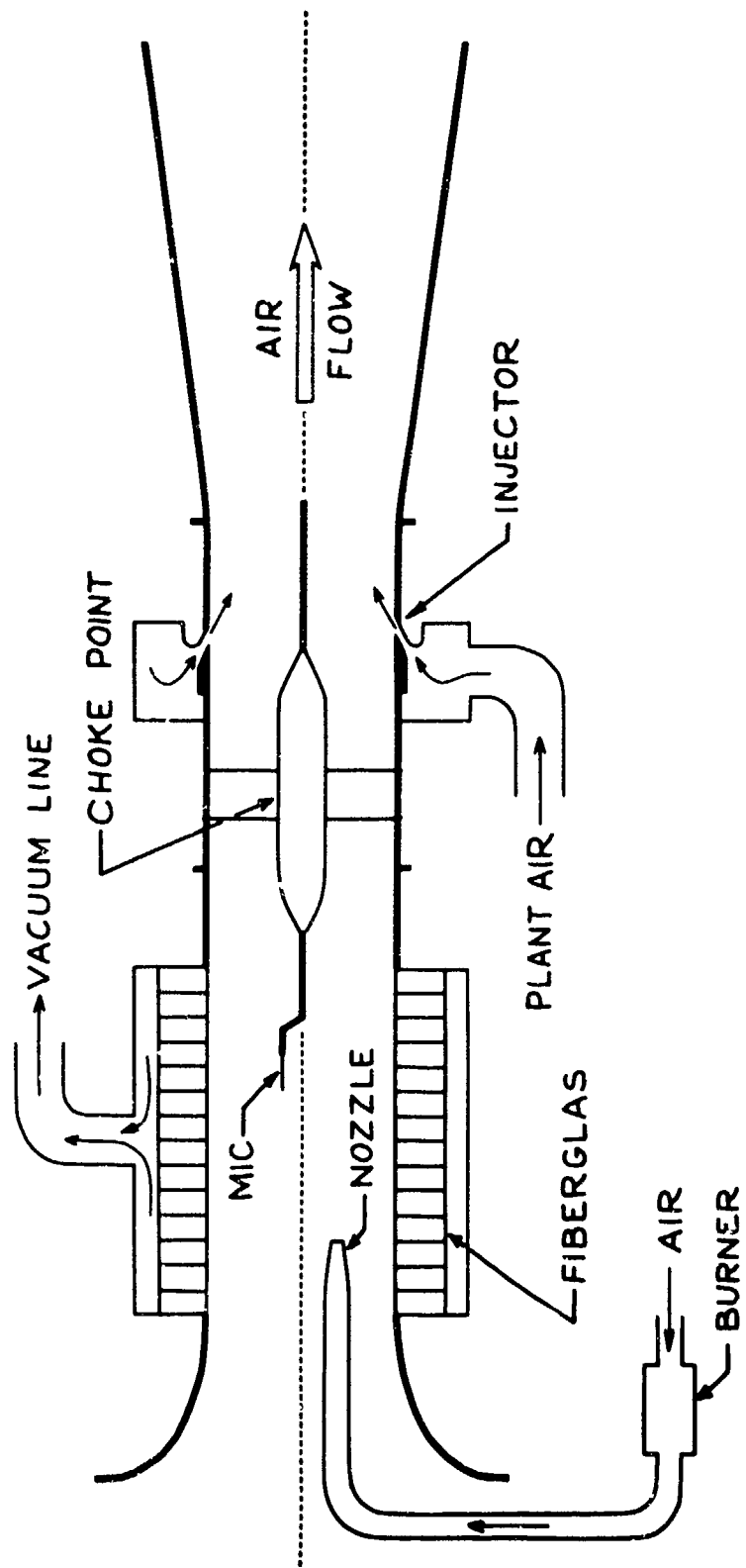
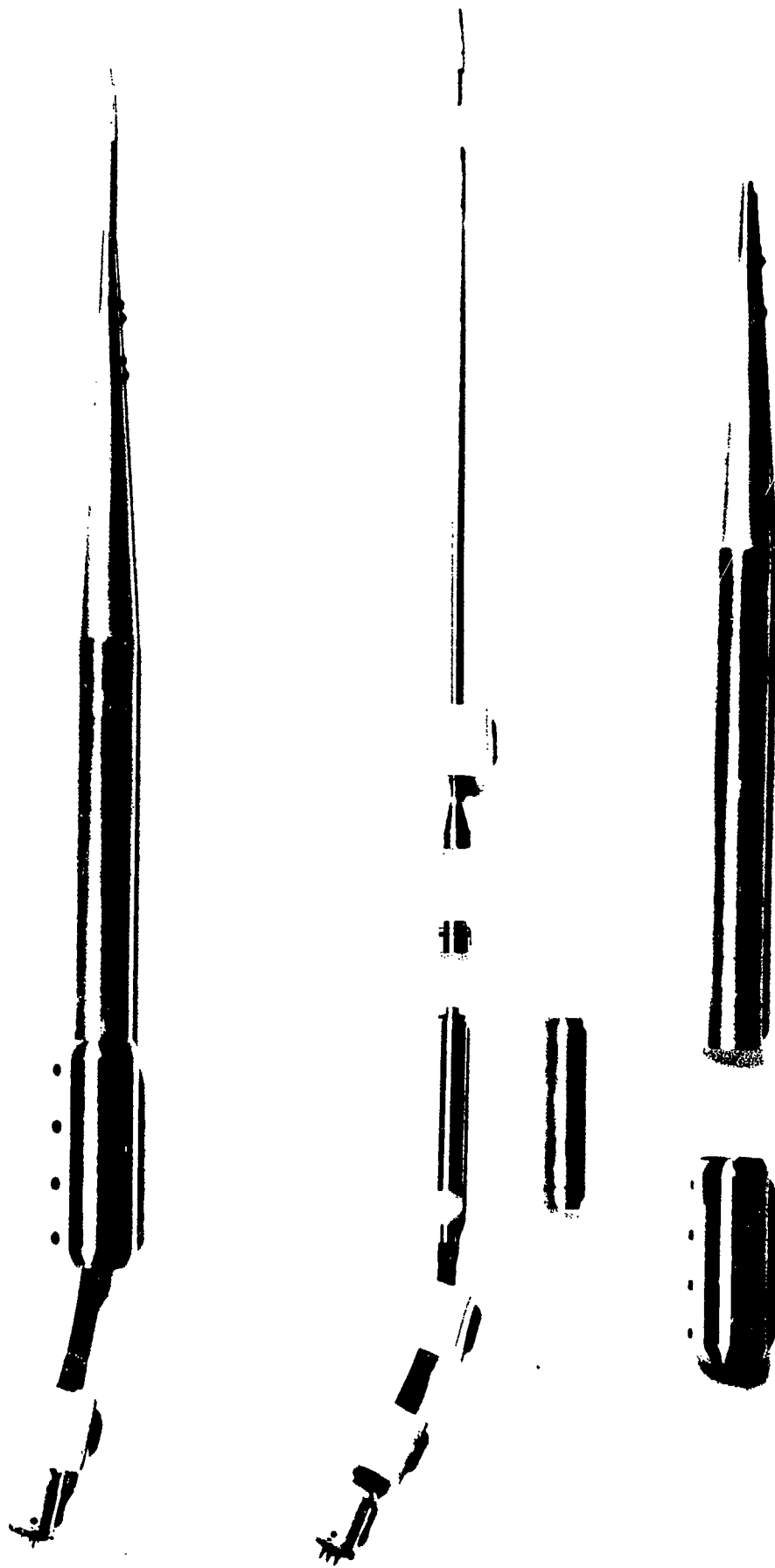


Figure 14. Schematic diagram of 16-inch wind tunnel assembly.



Figure 15. Photograph of 16-inch induction wind tunnel assembly.



ASD-TDR-62-787

Figure 16. Assembled and exploded views of Bruel & Kjaer Type 4134 microphone with probe.

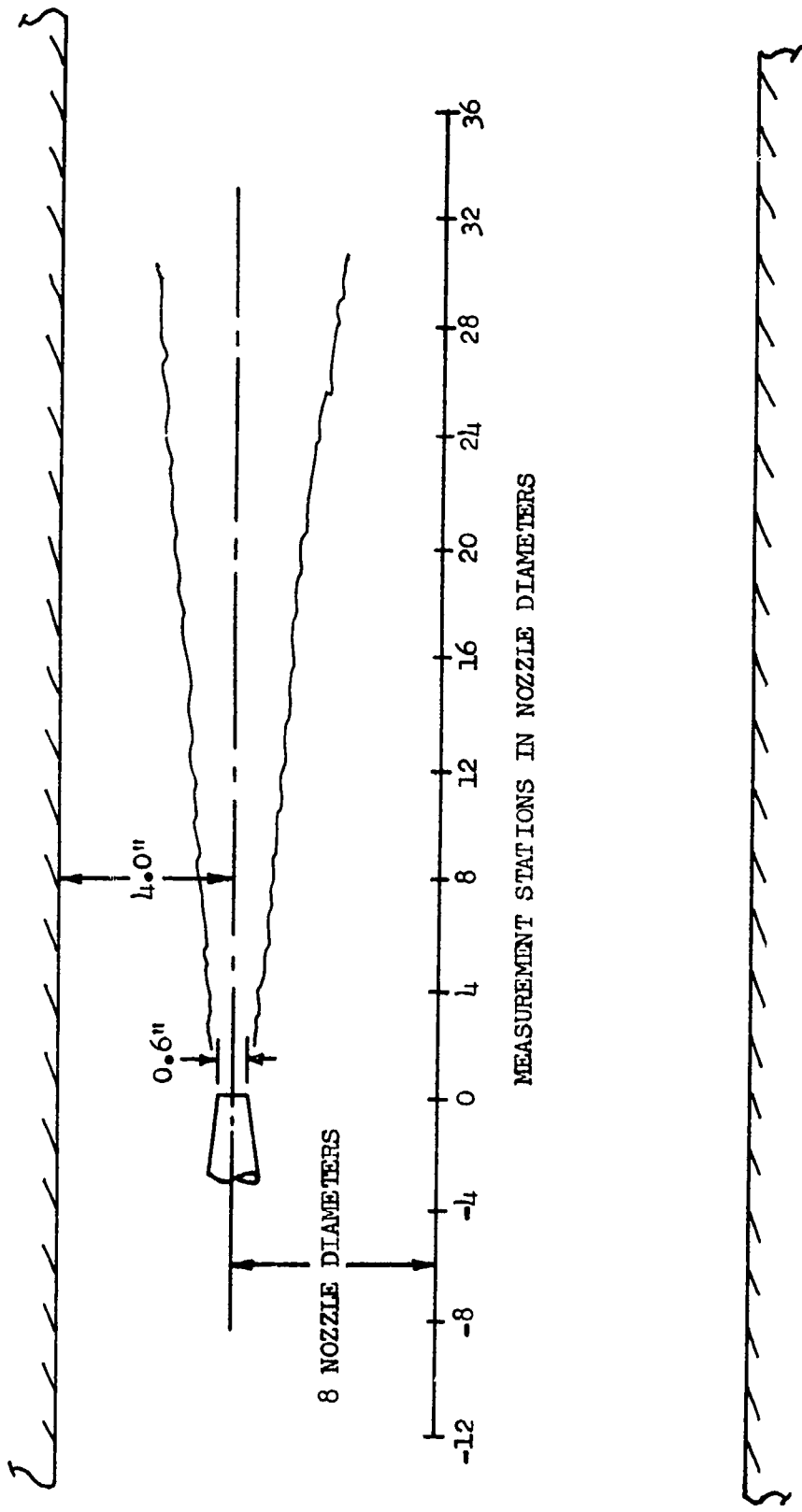


Figure 17. Model jet placement in wind tunnel and microphone locations used in obtaining noise data for both static and wind conditions.

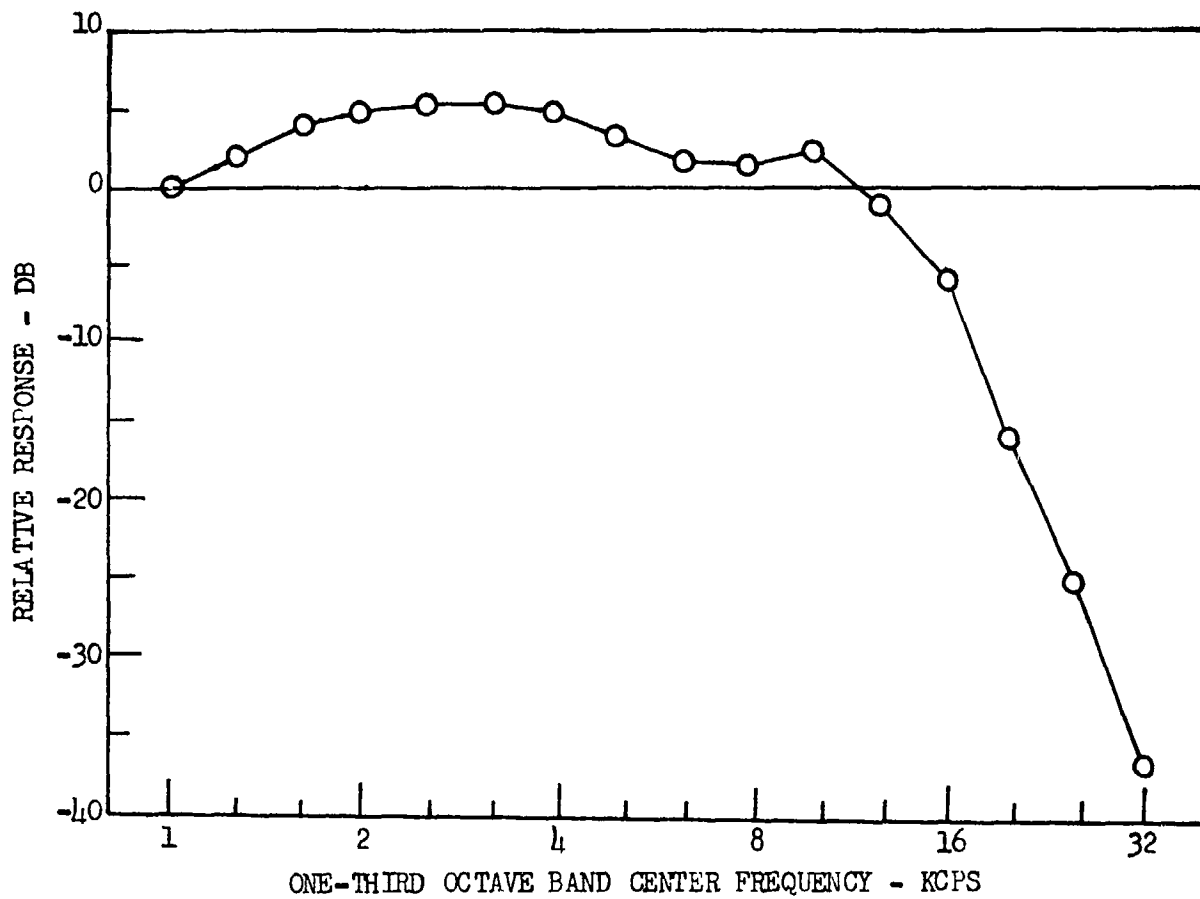


Figure 18. Frequency response of probe microphone with electrical equalization.

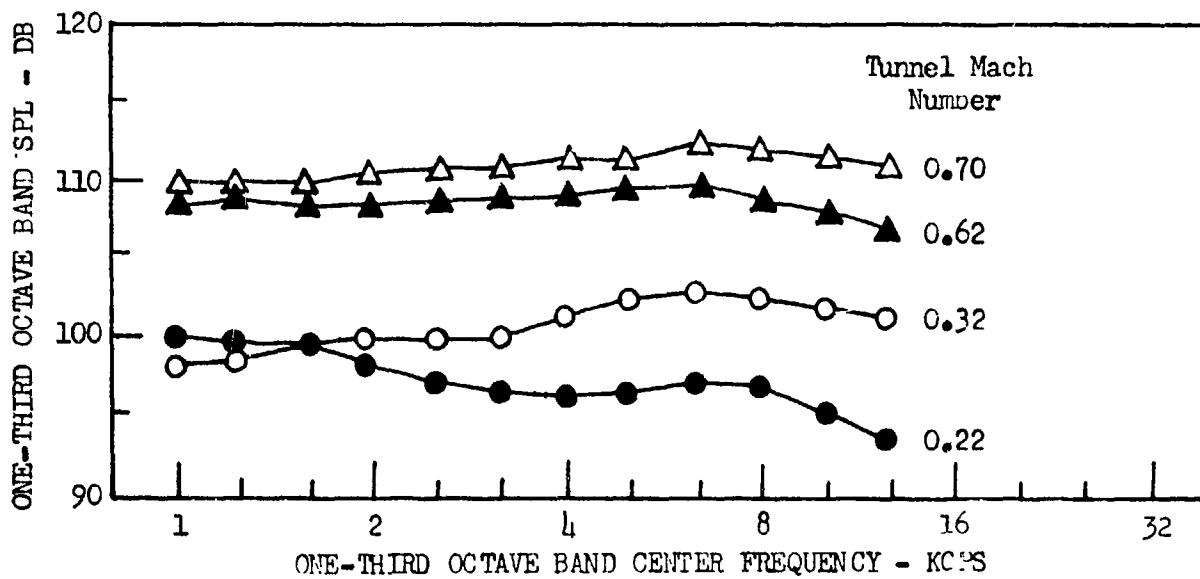


Figure 19. Background noise in wind tunnel test section.

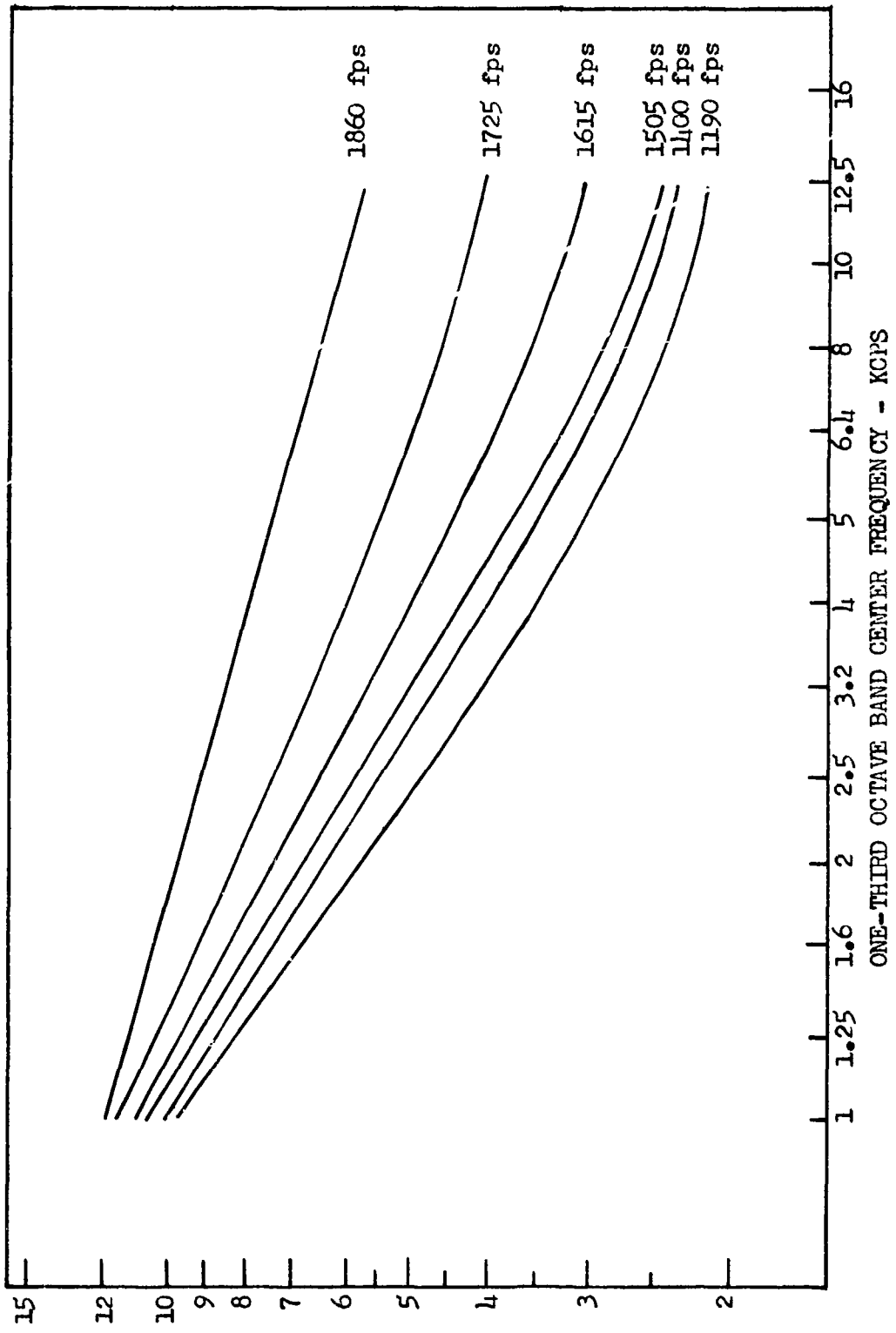


Figure 20. Source locations of various frequency bands of noise generated by the 0.6-inch model jet.

The experimentally determined apparent source locations of noise in one-third octave bands of frequency are shown for various exit velocity conditions of the stationary jet.

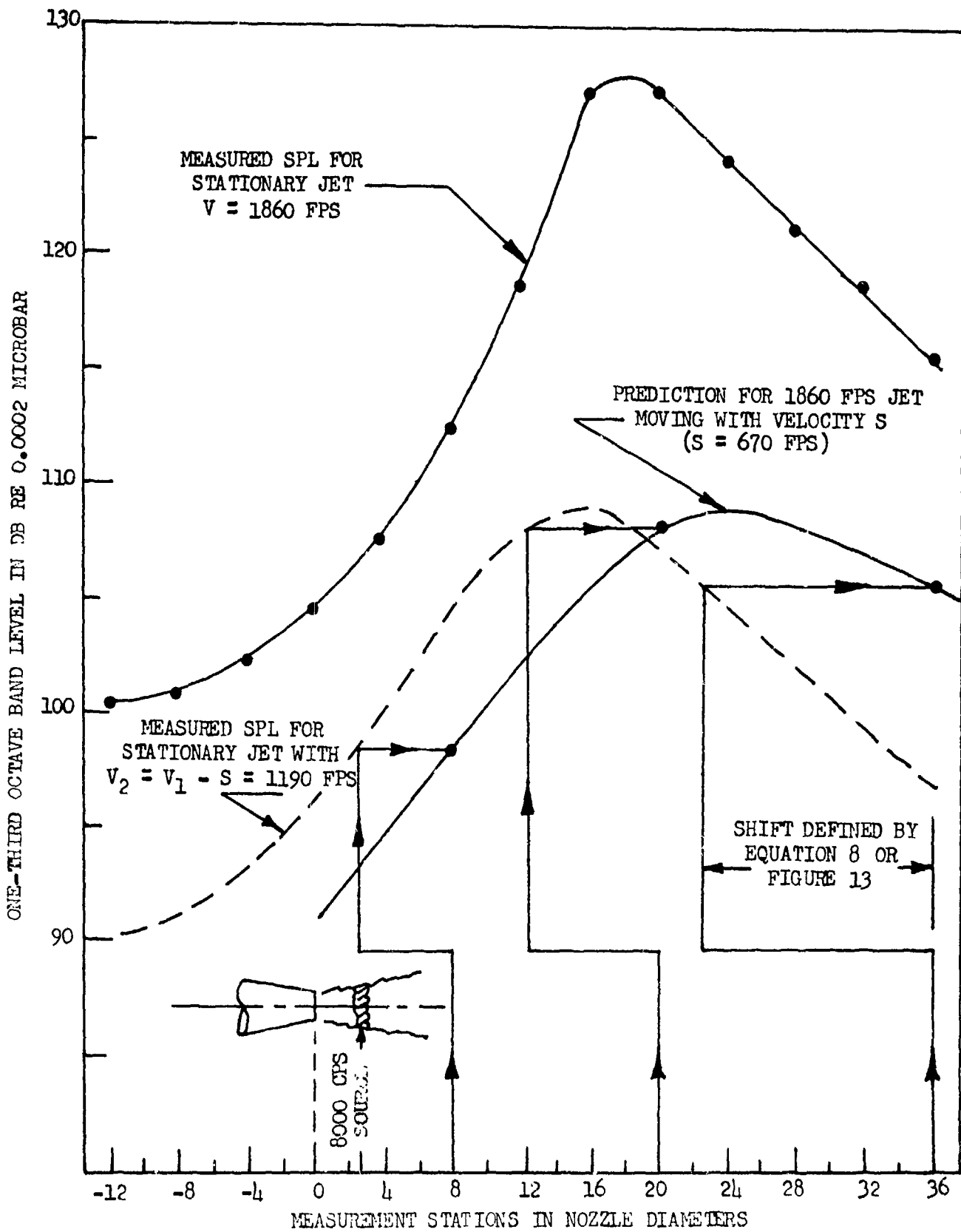
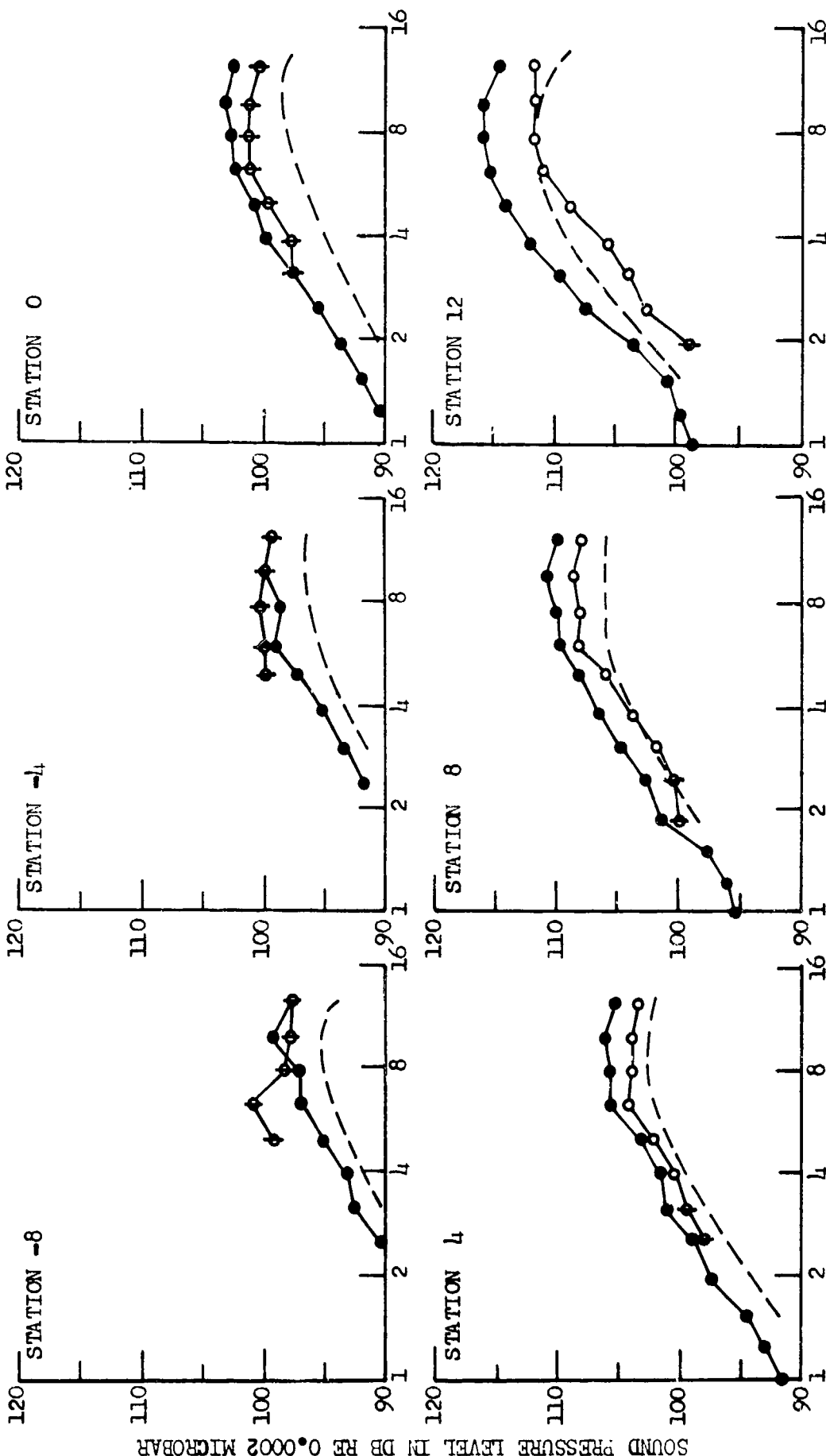


Figure 21. Illustration of method of predicting the change in SPL at a location due to vehicle motion.

Jet Velocity	Tunnel Velocity	Relative Velocity	Measured Measured Predicted
1615 fps	0 fps	1615 fps	Measured
1615 fps	245 fps (M = 0.22)	1400 fps	Measured
1400 fps	0 fps	1400 fps	Predicted



SOUND PRESSURE LEVEL IN DB RE 0.0002 MICROBAR

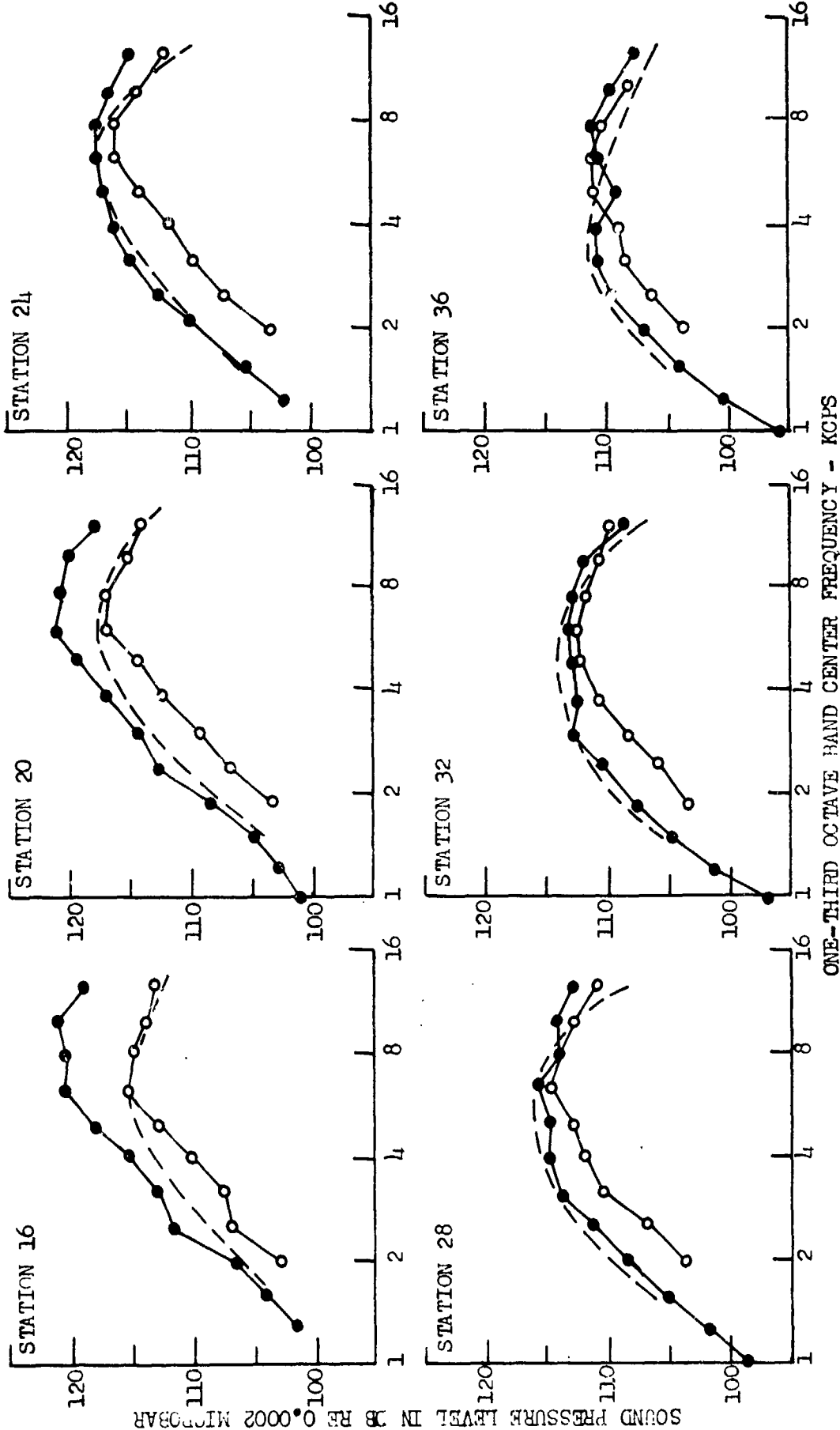
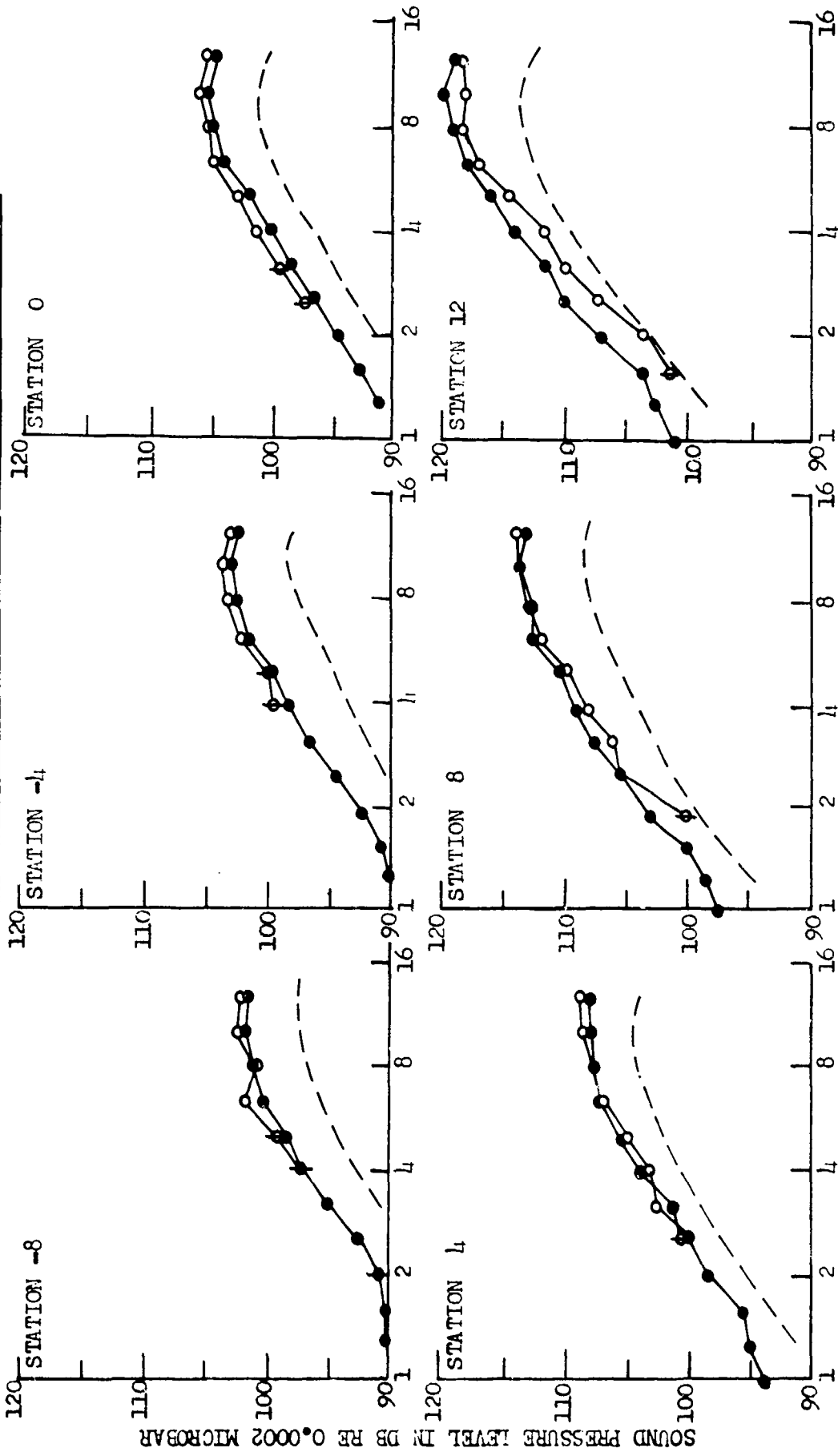


Figure 22 a. Comparison of measured and predicted SPL versus frequency for various measurement stations. Measured SPL data for a 1645 fps jet in motion at Mach 0.22 (245 fps) are compared to SPL values predicted from data measured on an equal relative velocity (1100 fps) static jet. The reference curve (●—●) shows SPL data measured on a 1615 fps static jet.



	Jet Velocity	Tunnel Velocity	Relative Velocity	Measured Measured Predicted
●	1860 fps	0 fps	1860 fps	Measured
○	1860 fps	245 fps (M = 0.22)	1615 fps	Measured
---	1615 fps	0 fps	1615 fps	Predicted



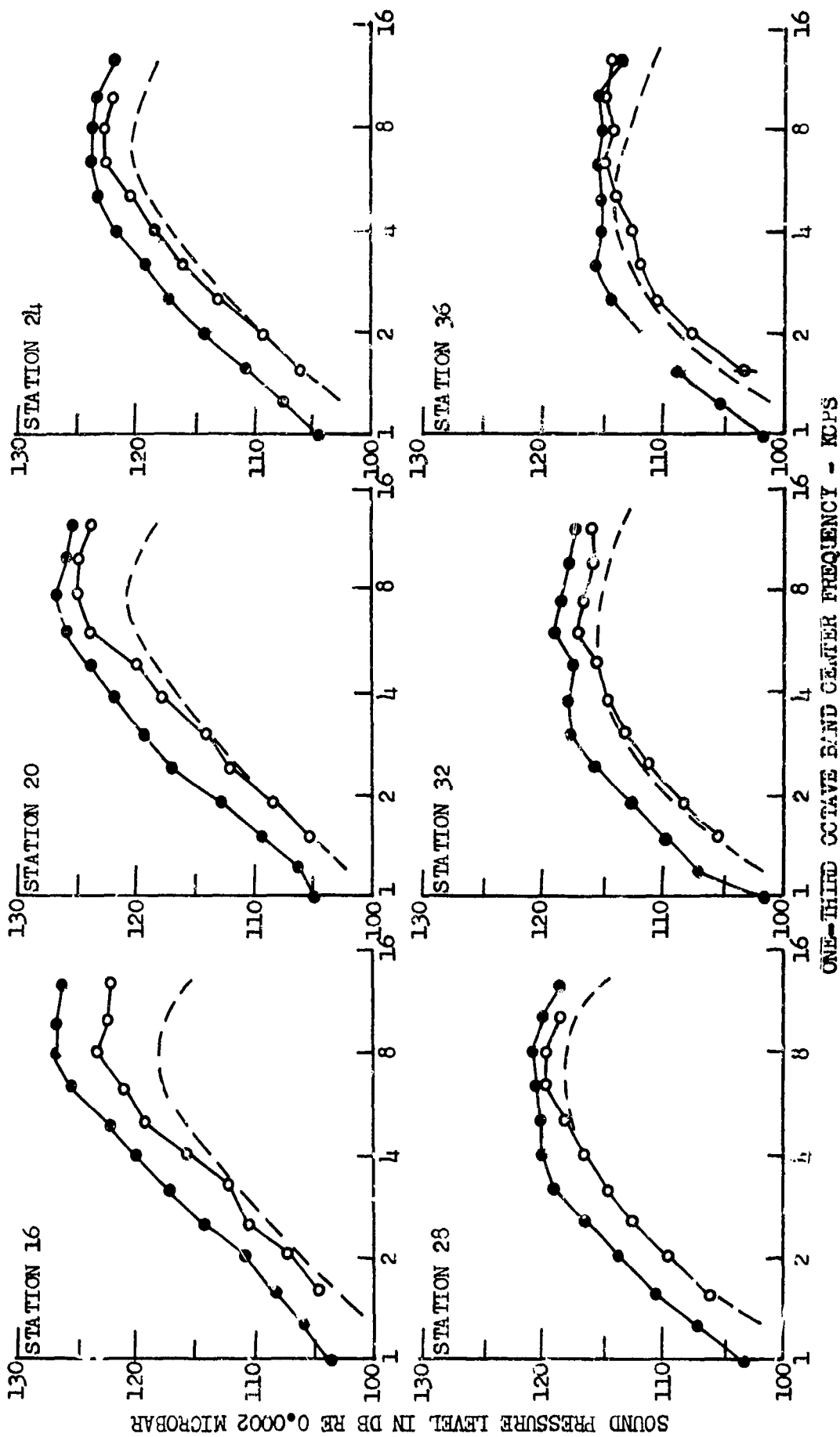
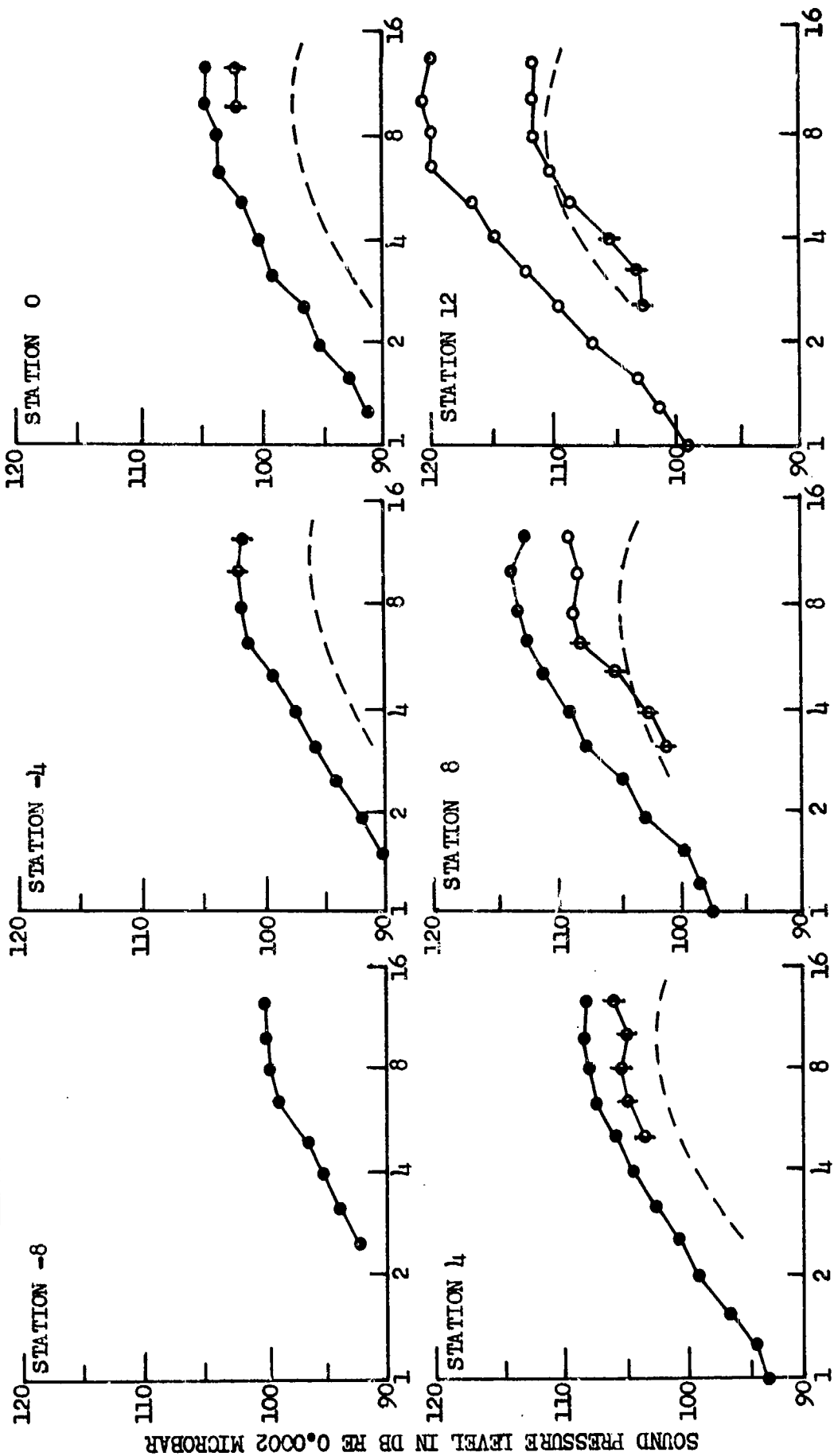


Figure 22 b. Comparison of measured and predicted SPL versus frequency for various measurement stations.

Measured SPL data for a 1860 fps jet in motion at Mach 0.22 (245 fps) are compared to SPL values predicted from data measured on an equal relative velocity (1615 fps) static jet. The reference curve (●---●) shows SPL data measured on a 1860 fps static jet.

	Jet Velocity	Tunnel Velocity	Relative Velocity	Measured Measured Predicted
●	1725 fps	0 fps	1725 fps	
○	1755 fps	355 fps (M = 0.32)	1100 fps	
- - -	1100 fps	0 fps	1100 fps	



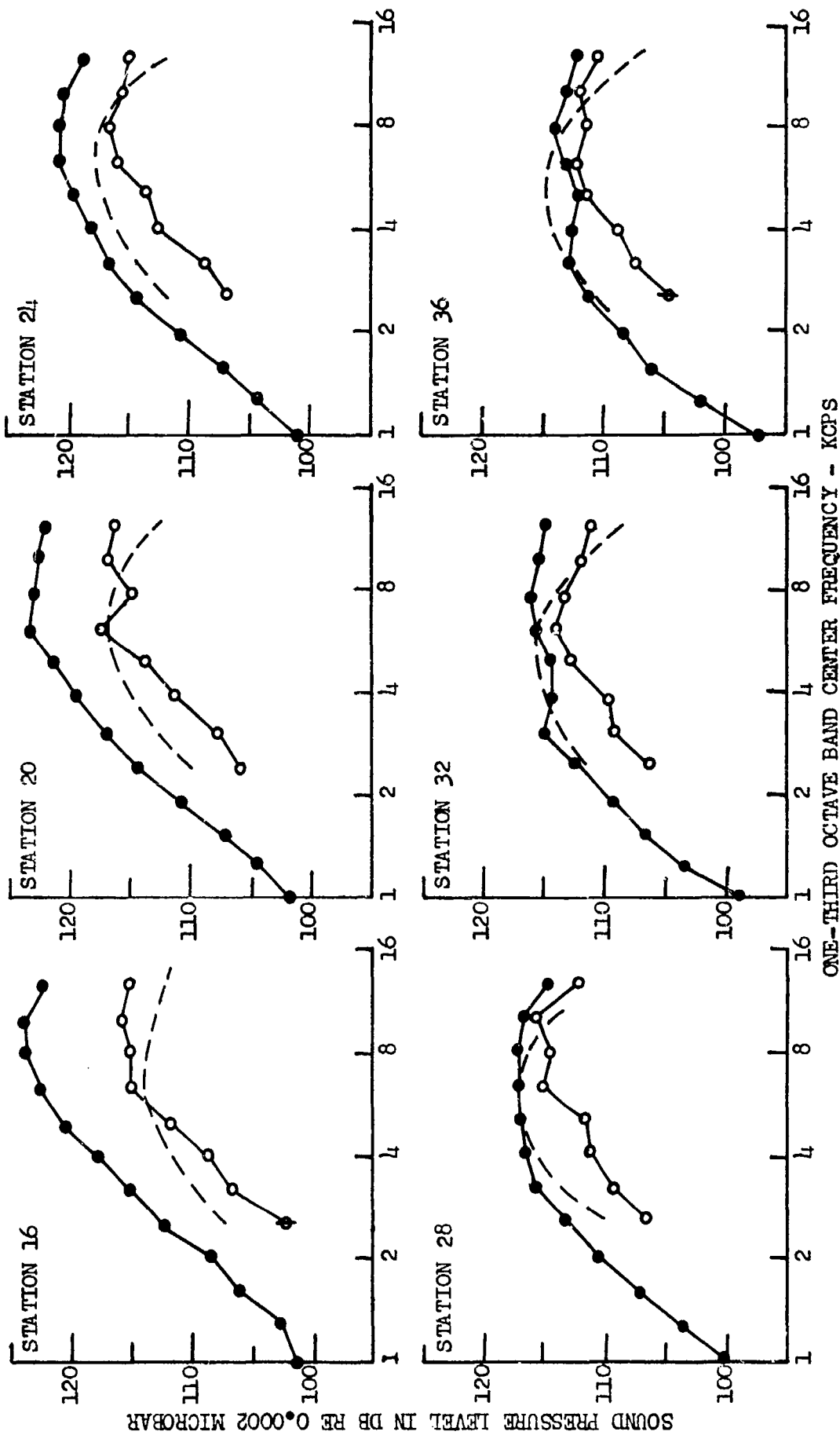
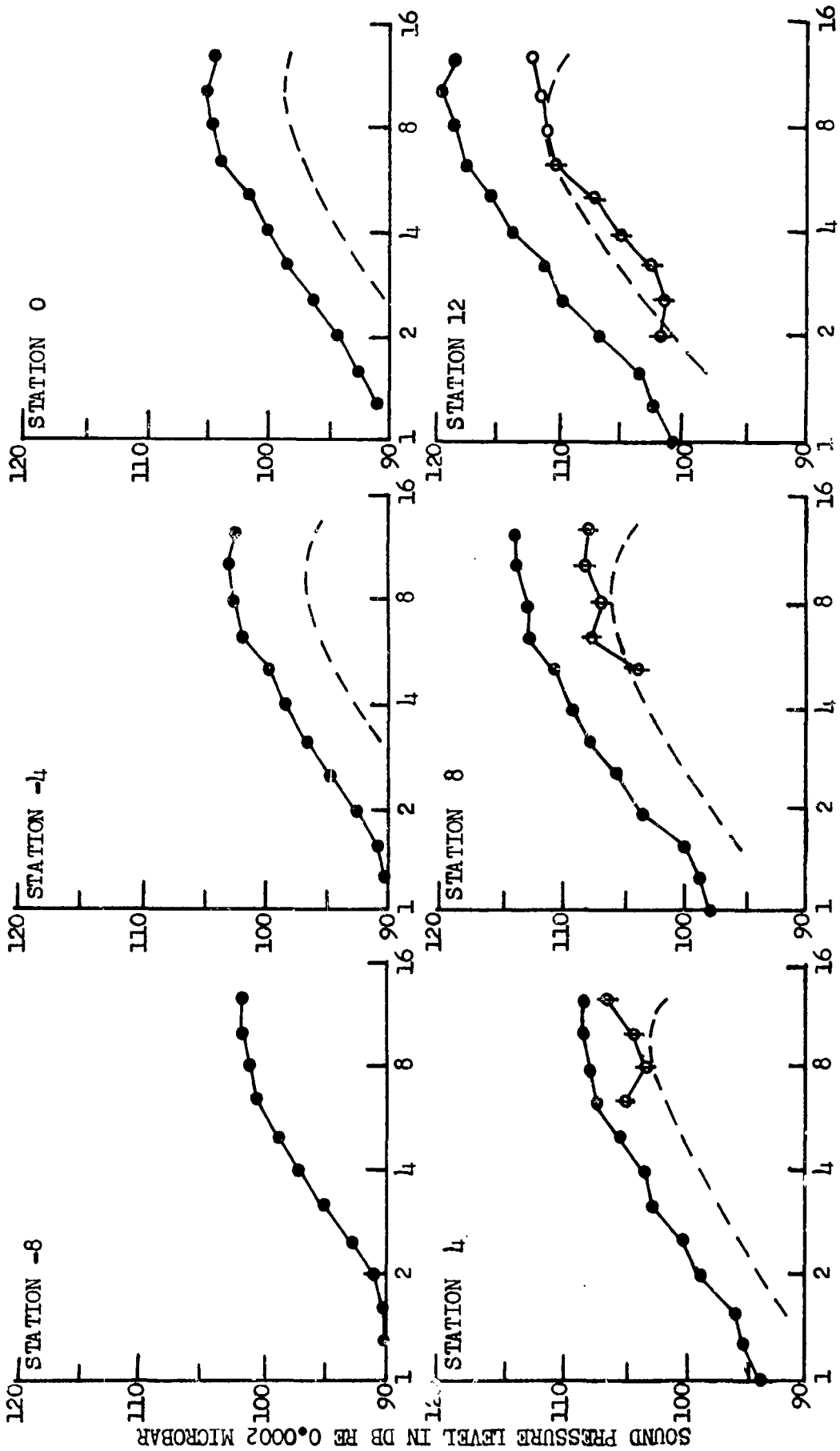


Figure 22 c. Comparison of measured and predicted SPL versus frequency for various measurement stations. Measured SPL data for a 1755 fps jet in motion at Mach 0.32 (355 fps) are compared to SPL values predicted from data measured on an equal relative velocity (1100 fps) static jet. The reference curve (●—●) shows SPL data measured on a 1725 fps static jet.

	Jet Velocity	Tunnel Velocity	Relative Velocity	Measured Measured Predicted
●	1860 fps	0 fps	1860 fps	Measured
○	1860 fps	355 fps (M = 0.32)	1505 fps	Measured
---	1505 fps	0 fps	1505 fps	Predicted



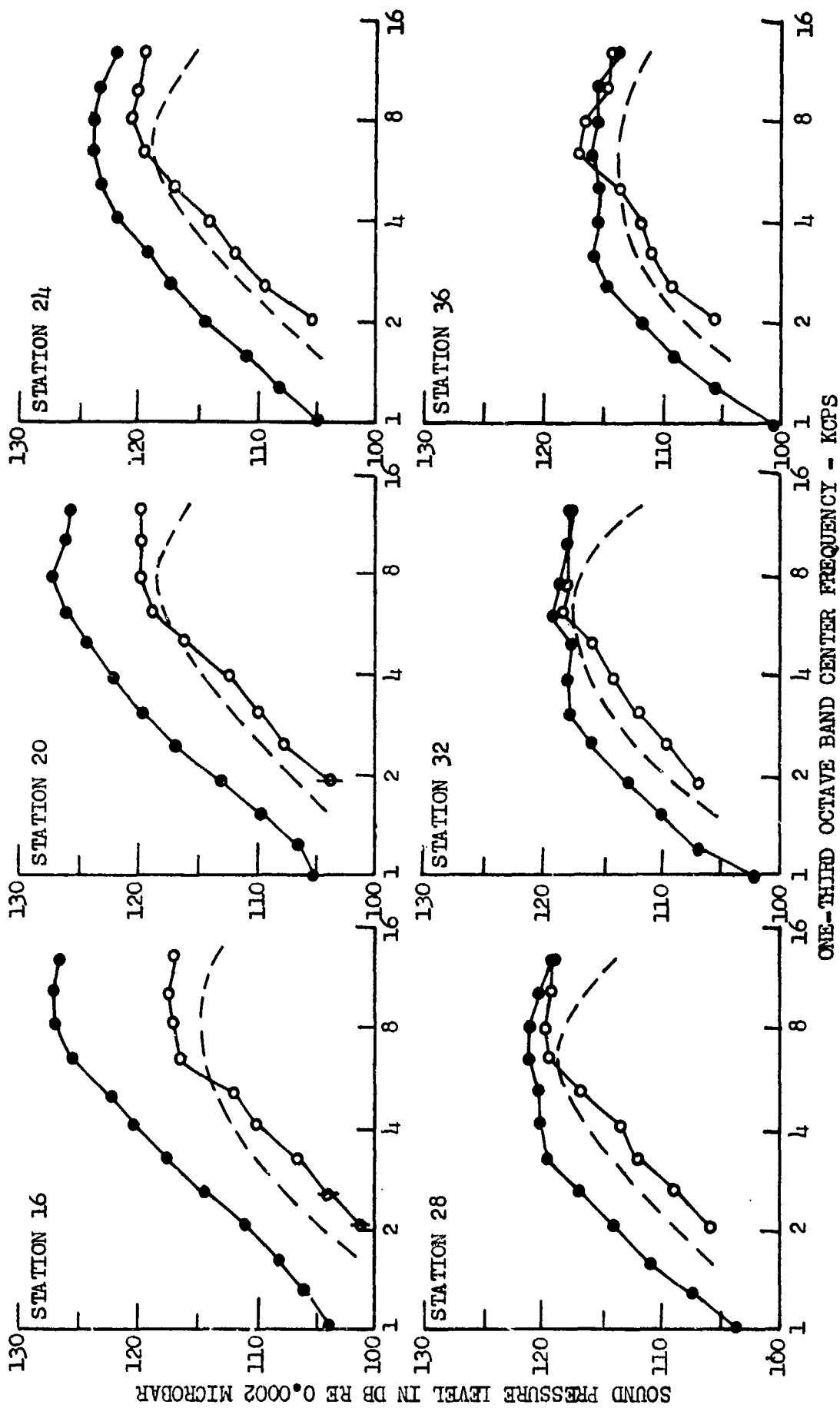
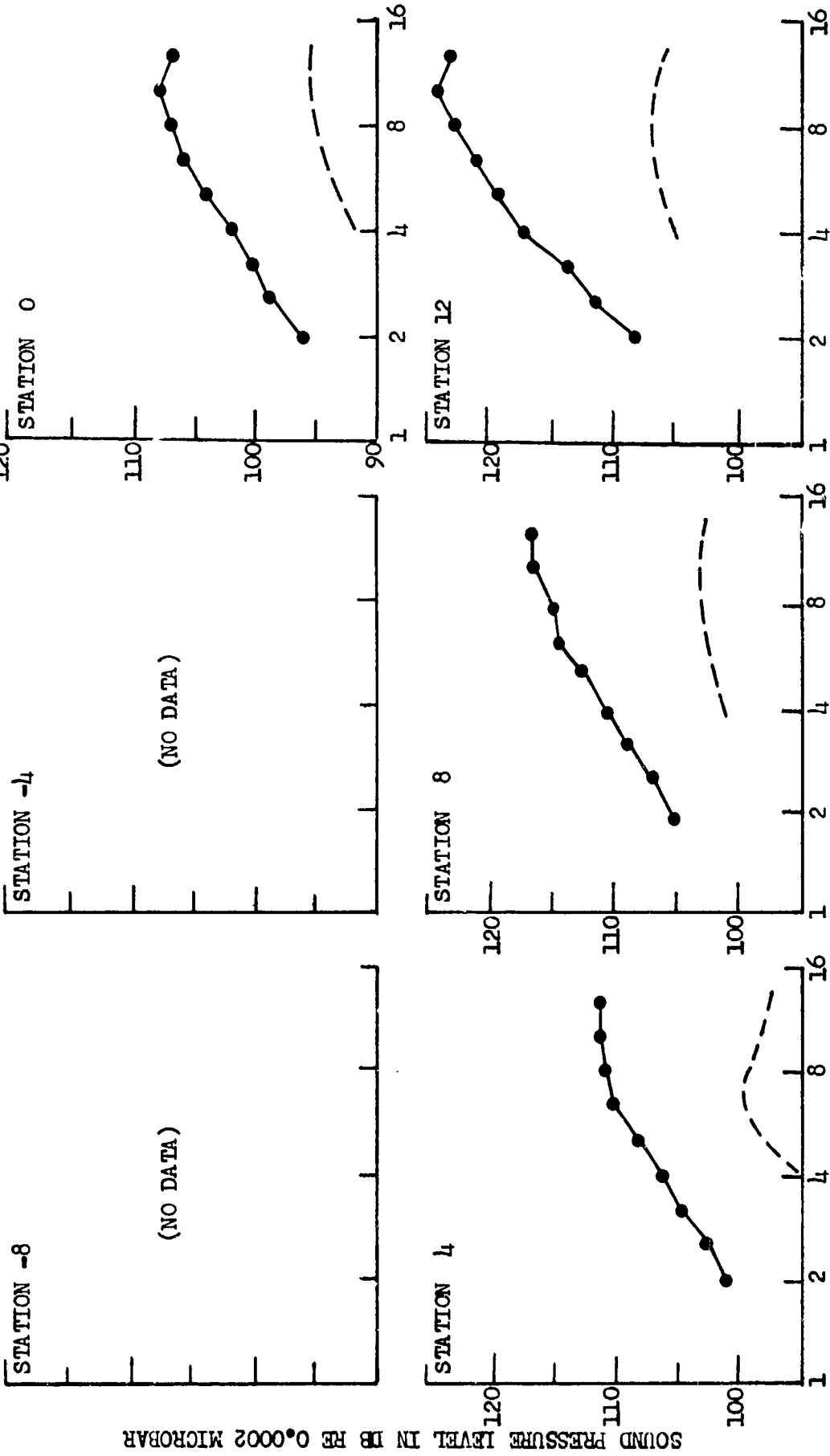


Figure 22 d. Comparison of measured and predicted SPL versus frequency for various measurement stations. Measured SPL data for a 1860 fps jet in motion at Mach 0.32 (355 fps) are compared to SPL values predicted from data measured on an equal relative velocity (1505 fps) static jet. The reference curve (●—●) shows SPL data measured on a 1860 fps static jet.

Jet Velocity	Tunnel Velocity	Relative Velocity	Estimated Measured Predicted
●	0 fps	2070 fps	
○	670 fps (M = 0.62)	1400 fps	
---	0 fps	1400 fps	



SOUND PRESSURE LEVEL IN DB RE 0.0002 MICROBAR

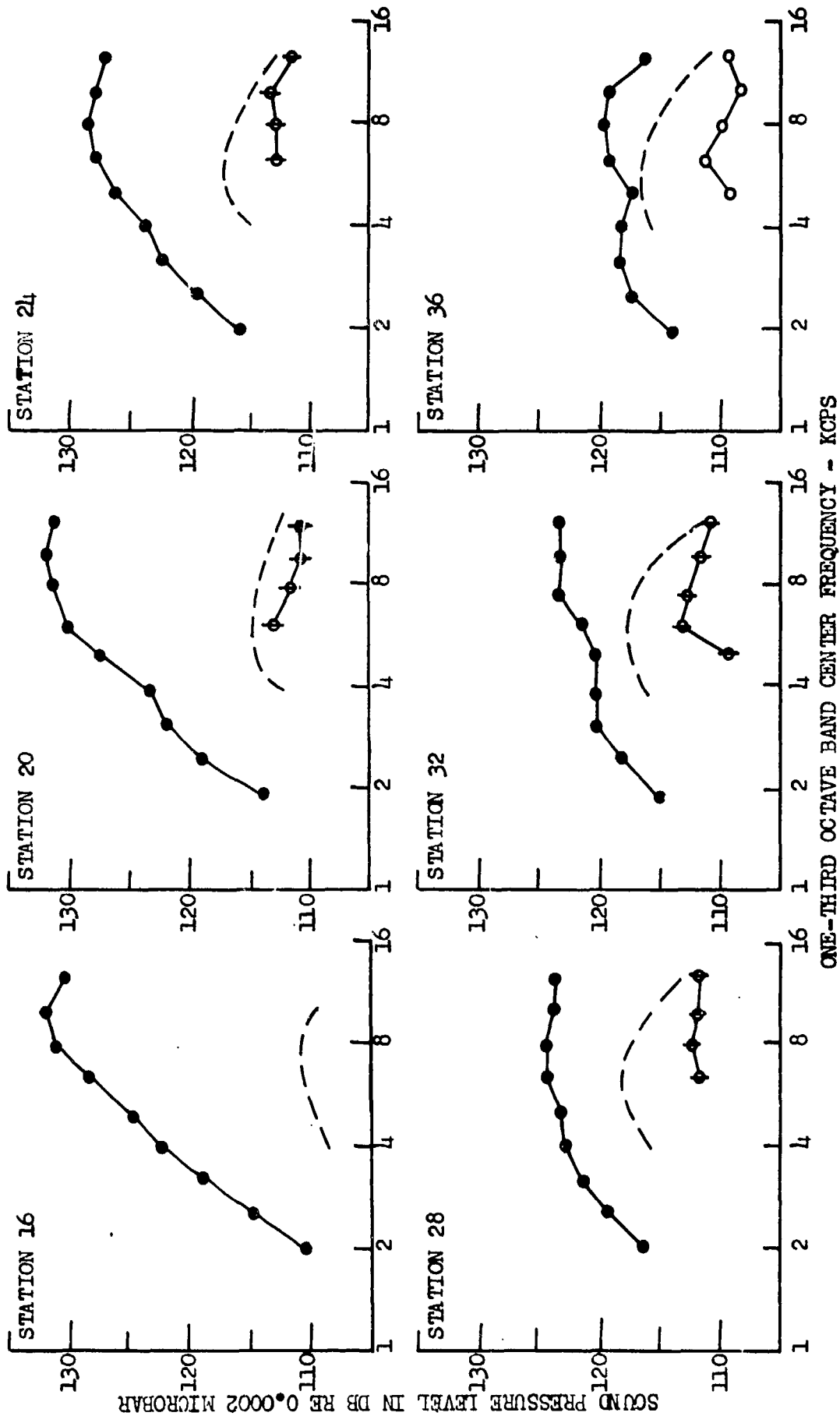


Figure 22 e. Comparison of measured and predicted SPL versus frequency for various measurement stations. Measured SPL data for a 2070 fps jet in motion at Mach 0.62 (670 fps) are compared to SPL values predicted from data measured on an equal relative velocity (1100 fps) static jet. The reference curve (●—●) shows SPL data estimated for a 2070 fps static jet.

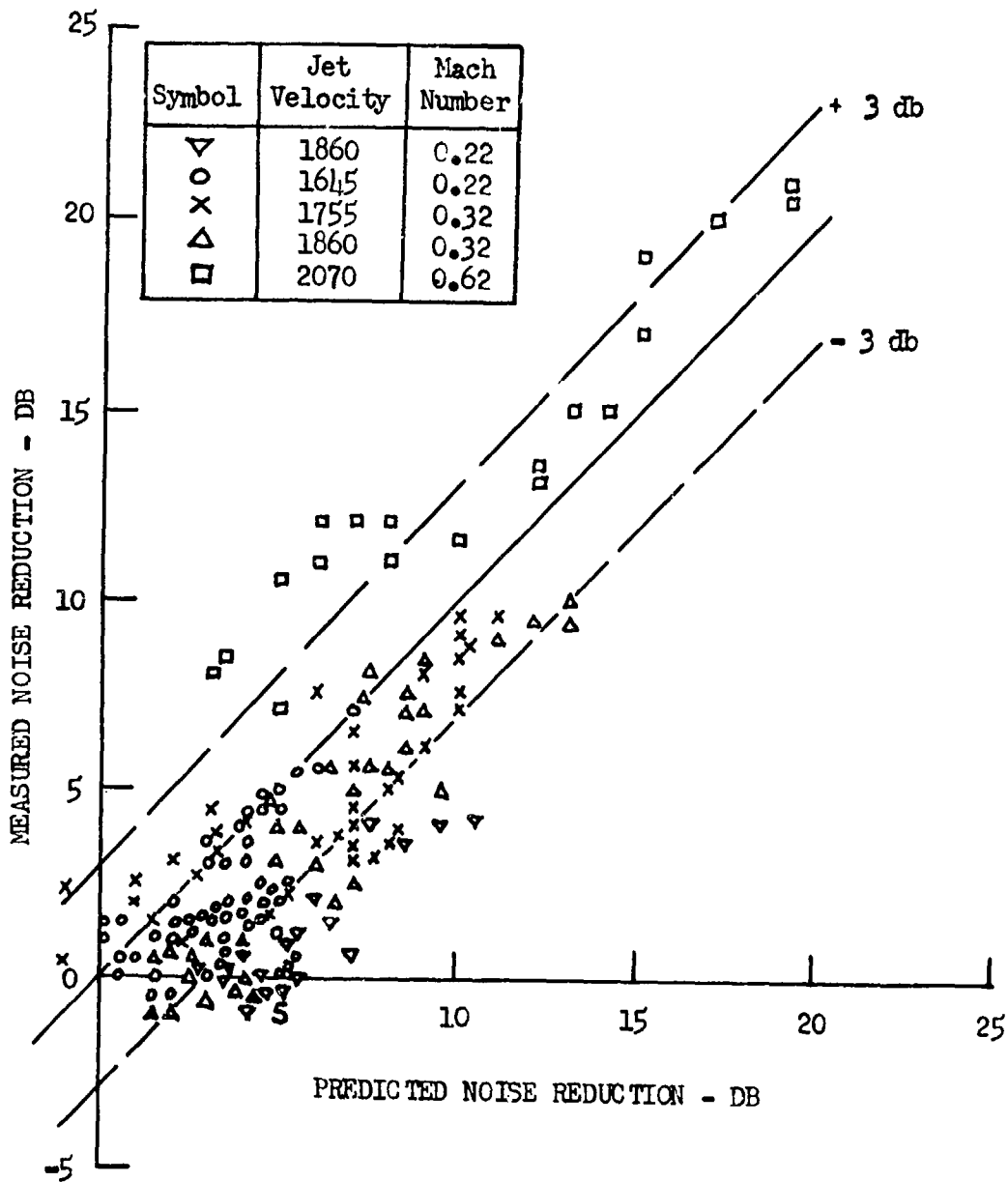


Figure 23. Measured vs. predicted values of noise reduction due to motion.

Plotted symbols indicate the correlation between measured and predicted values of noise reduction (from Figure 22, a-e) for the upper four 1/3 octave bands (6.4, 8, 10, and 12.5 kcps).

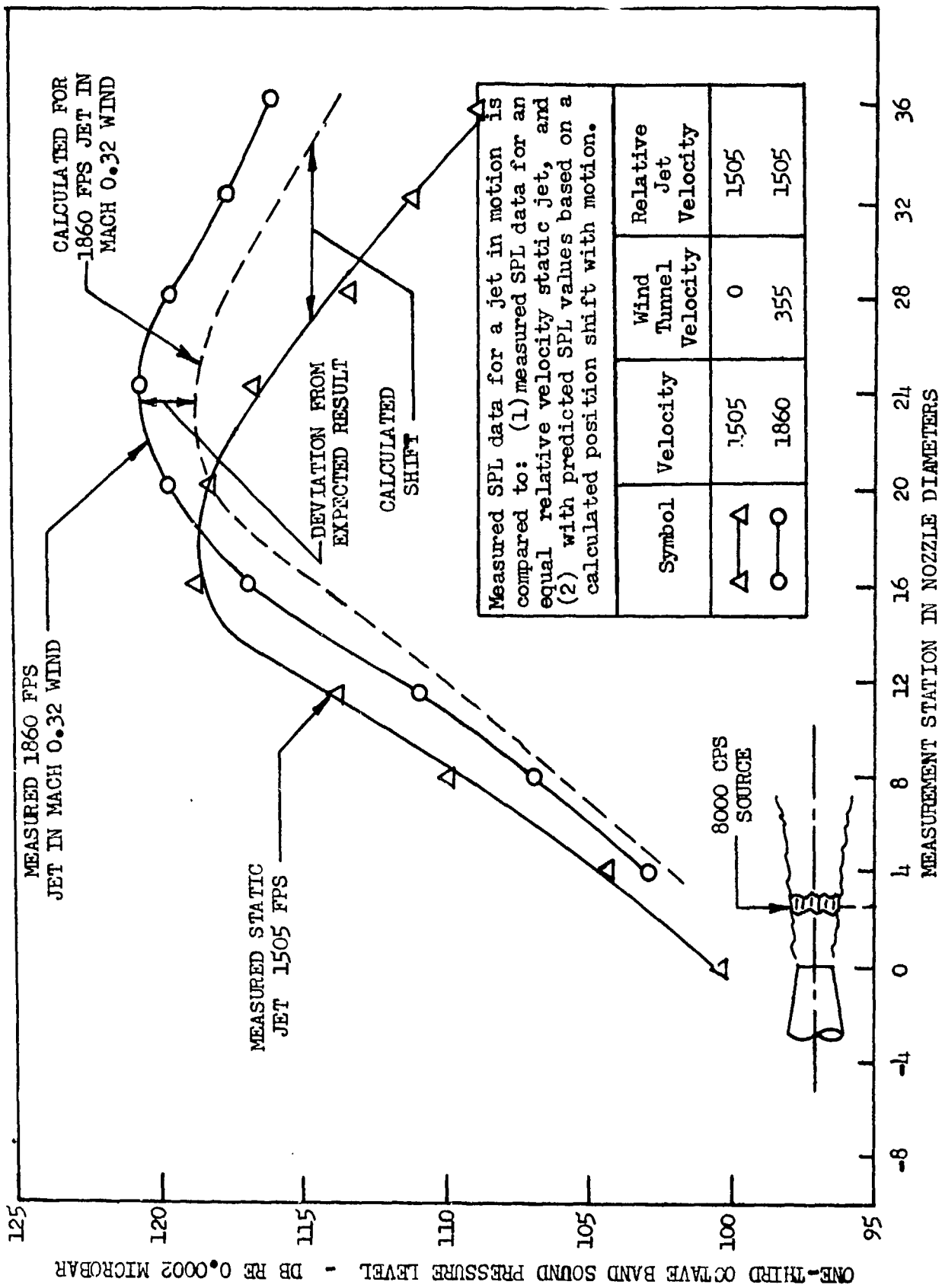


Figure 24. Comparison of measured and predicted SPL versus station for the 8000 cps band (one-third octave).

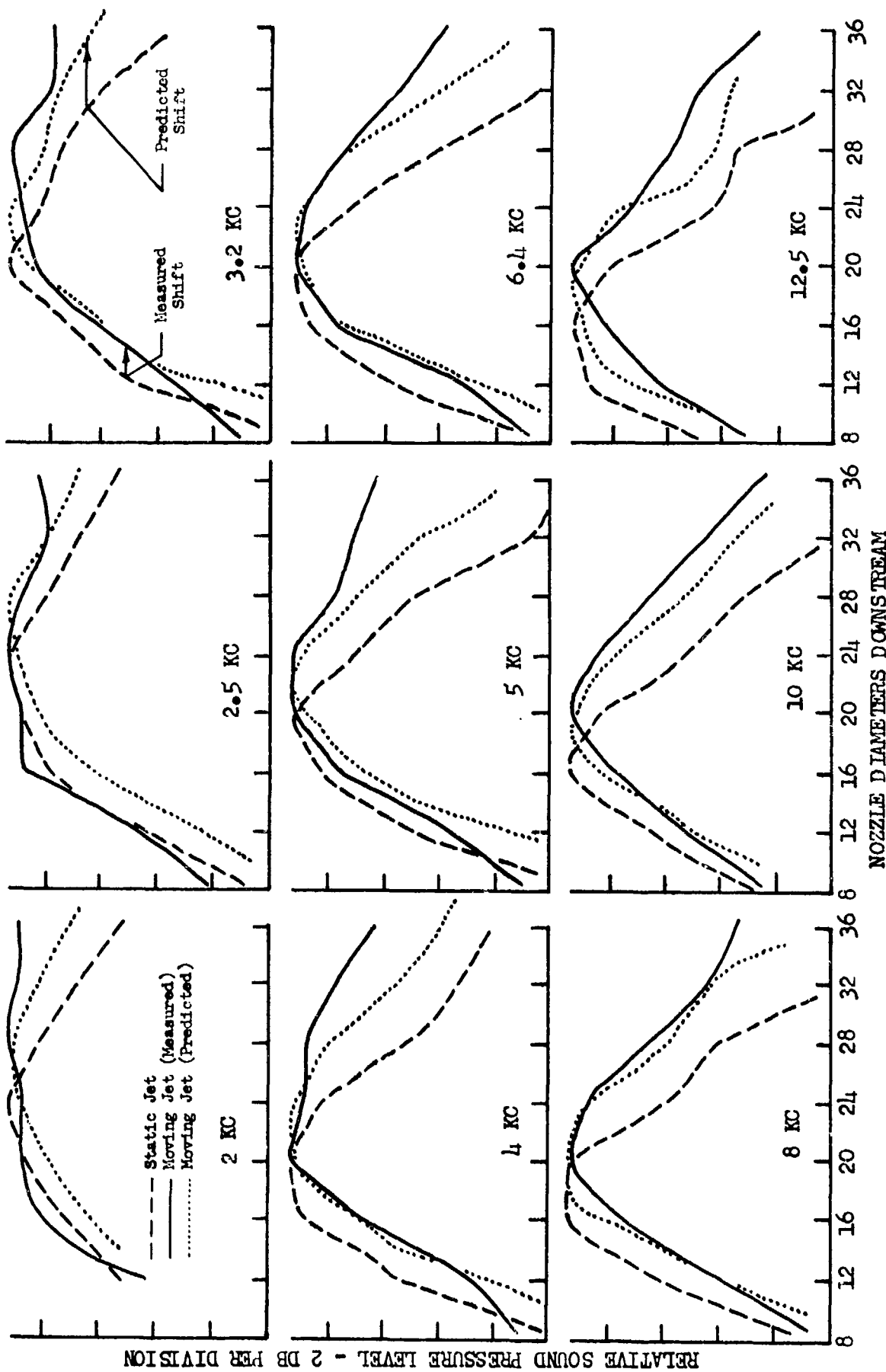


Figure 25 a. Position shift of noise due to motion for various 1/3 octave frequency bands. The downstream shift of position of the noise is indicated by comparing measured noise data for a 1645 fps jet in motion at Mach 0.22 (245 fps) with a static jet (1400 fps) at the same relative velocity (1400 fps). The predicted shift for the same condition is also shown. To facilitate comparison the measured sound levels for the moving jet have been adjusted to agree with the predicted motion and measured static curves at their peaks.

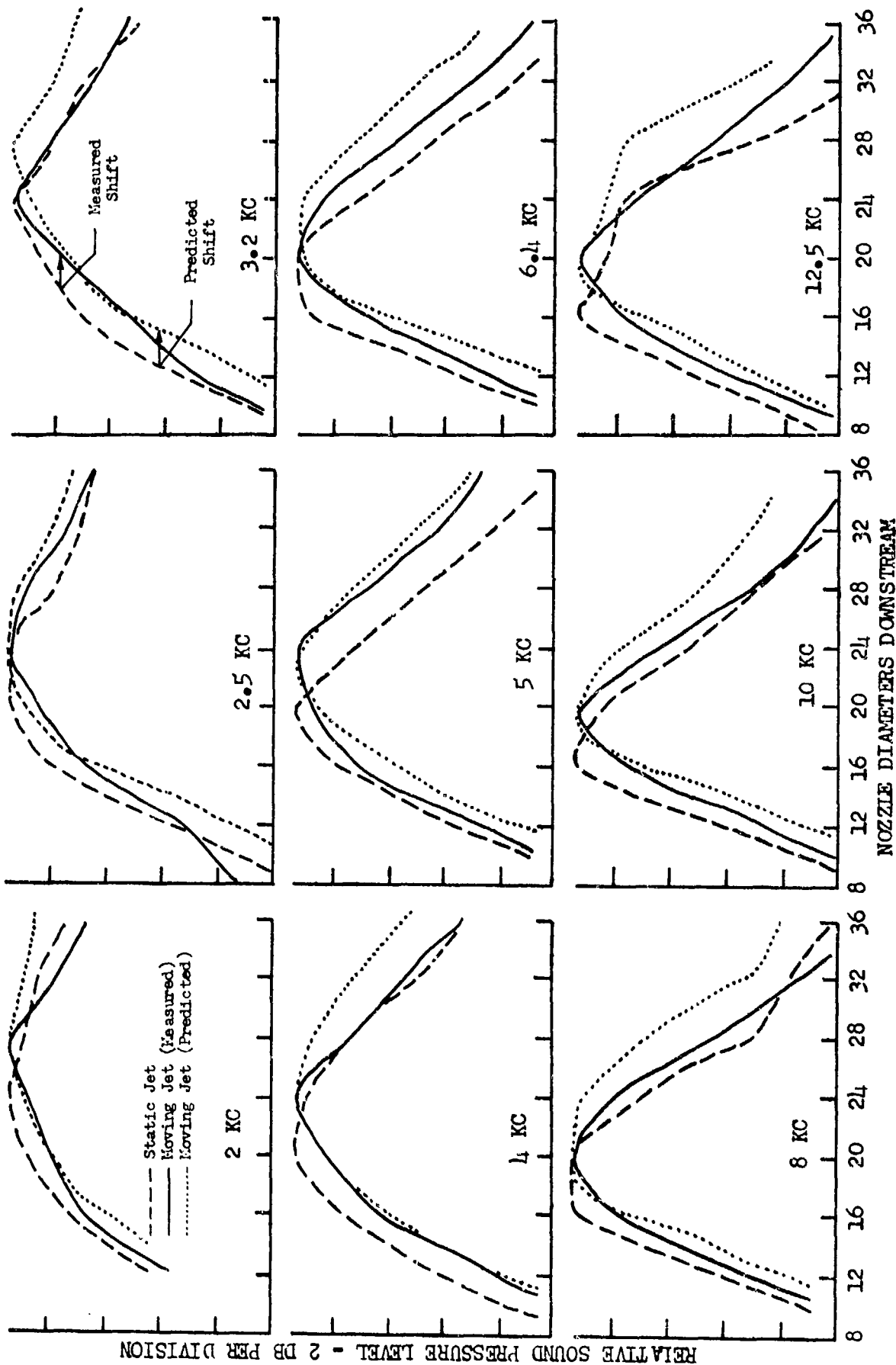


Figure 25 b. Position shift of noise due to motion for various 1/3 octave frequency bands. The downstream shift of position of the noise is indicated by comparing measured noise data for an 1860 fps jet in motion at Mach 0.22 (245 fps) with a static jet (1615 fps) at the same relative velocity (1615 fps). The predicted shift for the same condition is also shown. To facilitate comparison the measured sound levels for the moving jet have been adjusted to agree with the predicted motion and measured static curves at their peaks.

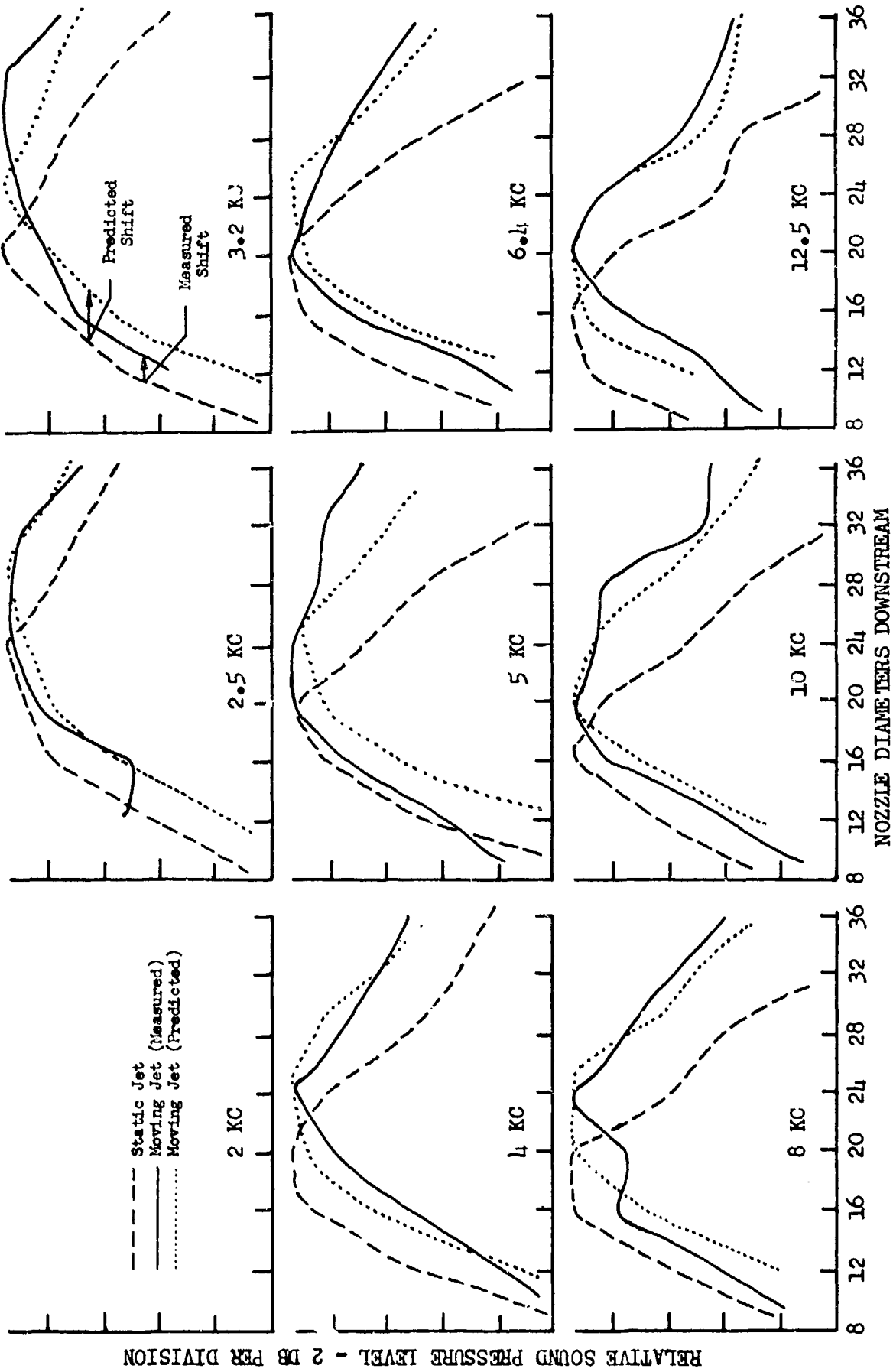


Figure 25 c. Position shift of noise due to motion for various 1/3 octave frequency bands.

The downstream shift of position of the noise is indicated by comparing measured noise data for a 1755 fps jet in motion at Mach 0.32 (355 fps) with a static jet (1400 fps) at the same relative velocity (1400 fps). The predicted shift for the same condition is also shown. To facilitate comparison the measured sound levels for the moving jet have been adjusted to agree with the predicted motion and measured static curves at their peaks.

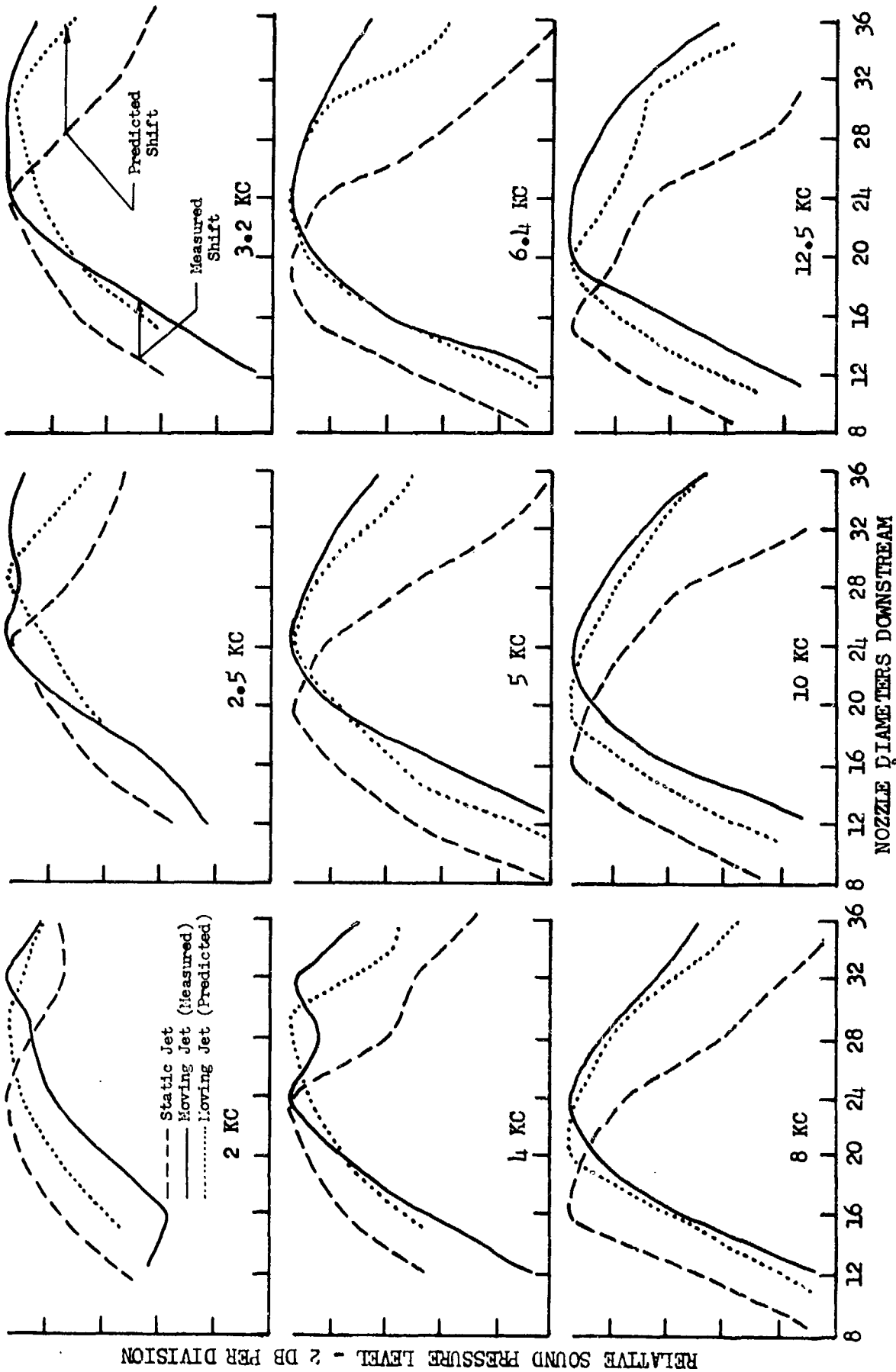


Figure 25 d. Position shift of noise due to motion for various 1/3 octave frequency bands.

The downstream shift of position of the noise is indicated by comparing measured noise data for an 1860 fps jet in motion at Mach 0.32 (355 fps) with a static jet (1505 fps) at the same relative velocity (1505 fps). The predicted shift for the same condition is also shown. To facilitate comparison the measured sound levels for the moving jet have been adjusted to agree with the predicted motion and measured static curves at their peaks.



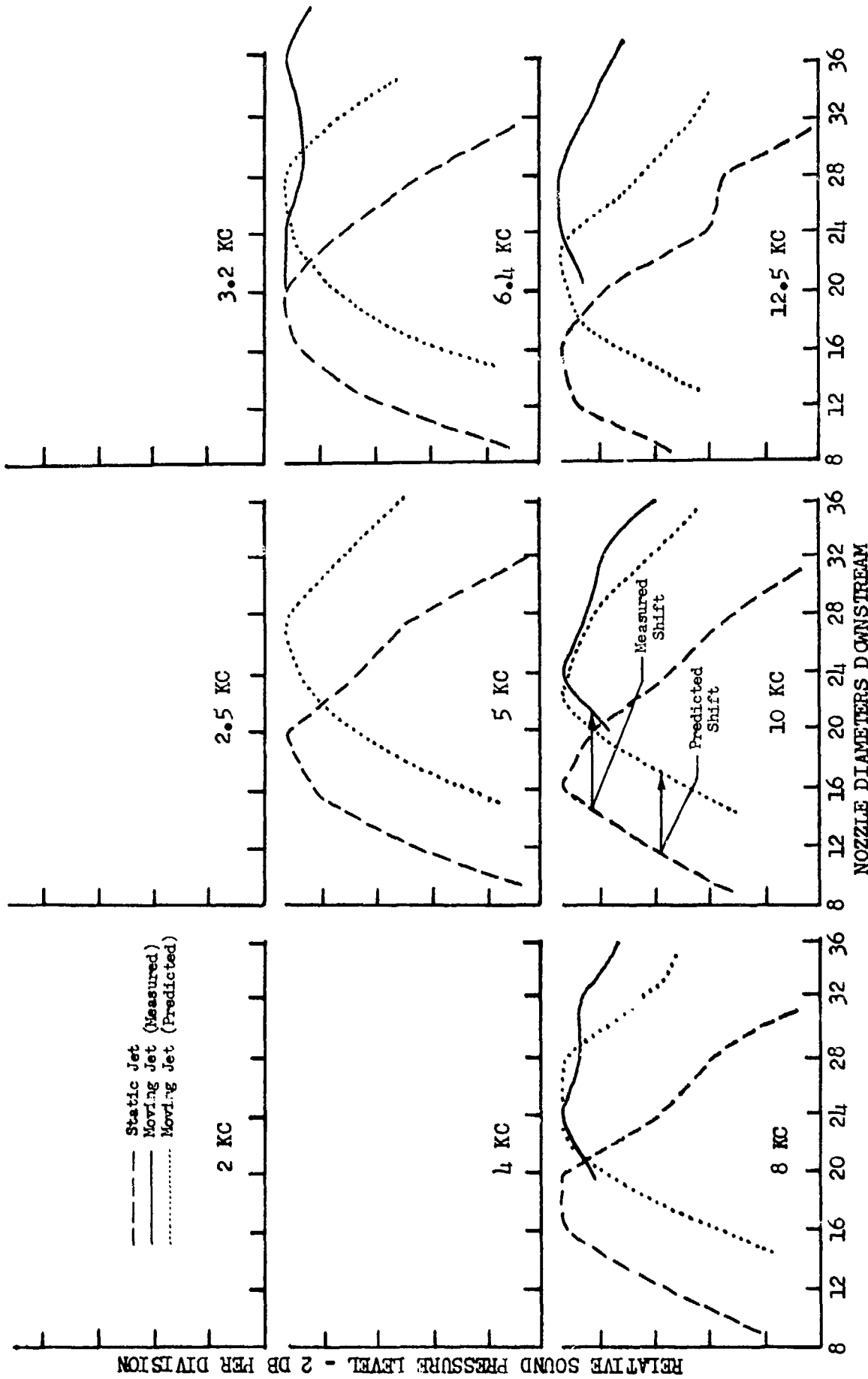


Figure 25 e. Position shift of noise due to motion for various 1/3 octave frequency bands. The downstream shift of position of the noise is indicated by comparing measured noise data for a 2070 fps jet in motion at Mach 0.62 (670 fps) with a static jet (1400 fps) at the same relative velocity (1400 fps). The predicted shift for the same condition is also shown. To facilitate comparison the measured sound levels for the moving jet have been adjusted to agree with the predicted motion and measured static curves at their peaks.

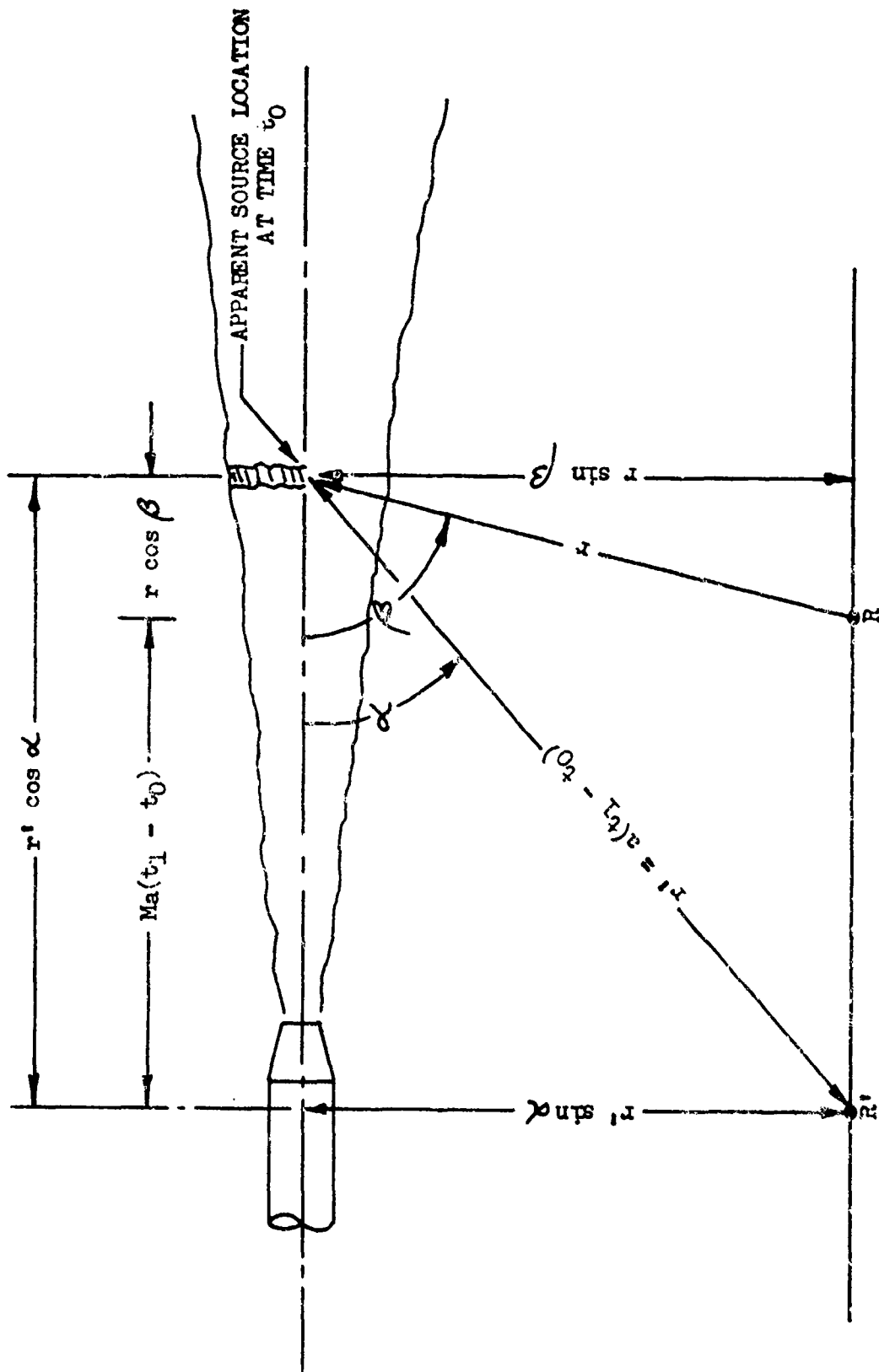


Figure 26. Mathematical relationship between angles α and β for the moving vehicle situation.

LIST OF REFERENCES

1. Morgan, W. V., Sutherland, L. C., and Young, K. J., The Use of Acoustic Scale Models for Investigating Near Field Noise of Jet and Rocket Engines. WADD Technical Report 61-178. Aeronautical Systems Division, Air Force Systems Command, USAF. Wright-Patterson AFB, Ohio. April 1961.
2. Handbook of Toxicology. Vol. I. Edited by W. S. Spector. WADC Technical Report 55-16. Aeronautical Systems Division, Air Force Systems Command, USAF. Wright-Patterson AFB, Ohio. April 1955.
3. Threshold Limit Values for Toxic Chemicals. Air Force Pamphlet AFP 160-6-1. Medical Service, Dept. of the Air Force. February 1959.
4. Handbook of Chemistry. Ninth Edition. Compiled and edited by N. A. Lange, assisted by G. M. Forkner. Handbook Publishers, Inc., Sandusky, Ohio, 1956.
5. Handbook of Chemistry and Physics. Fortieth Edition. Charles D. Hodgman, editor. Chemical Rubber Publishing Co., Cleveland, Ohio, 1958.
6. Sax, N. I., et al, Dangerous Properties of Industrial Materials. Reinhold Publishing Corp., New York, 1957.
7. Lewis, B. and Von Elbe, G., Combustion, Flames, and Explosions. Academic Press, Inc., New York, 1951.
8. Rossini, F. D., et al, Selected Values of Physical and Thermodynamic Properties of Hydrocarbons and Related Compounds. Carnegie Press, Pittsburgh, Pa. 1953.
9. Mayes, W. H., Lanford, W. E., and Hubbard, H. H., Near Field and Far Field Noise Surveys of Solid Fuel Rocket Engines for a Range of Nozzle Exit Pressures. NASA Technical Note D-21. National Aeronautics and Space Administration, Washington D. C., August 1959.
10. Mueller, James N., Equations, Tables, and Figures for Use in the Analysis of Helium Flow at Supersonic and Hypersonic Speeds. NACA Technical Note 4063. National Aeronautics and Space Administration, Washington, D. C. September 1957.
11. Lighthill, M. J., "On Sound Generated Aerodynamically. I. General Theory." Proc. Roy. Soc. (London). Vol. 211, A. March 1952. pp. 564-587.
12. Oestreicher, Hans L., The Field of a Spatially Extended Moving Sound Source. WADC Technical Report 54-223. Aeronautical Systems Division, Air Force Systems Command, USAF. Wright-Patterson AFB, Ohio. June 1955.
13. Cole, J. N., Kyrakis, D. T., and Oestreicher, Hans L., A Method for Calculating the Acoustical Characteristics of Aircraft in Flight. WADC Technical Note 56-488. Aeronautical Systems Division, Air Force Systems Command, USAF. Wright-Patterson AFB, Ohio. December 1956.

14. Powell, Alan, Similarity Considerations of Noise Production from Turbulent Jets, both Static and Moving. Douglas Aircraft Co. Report SM 23246. Douglas Aircraft Co., Inc., Santa Monica, California. 1 July 1958.
15. Franken, Peter A., Kerwin, Edward M. Jr., and the Staff of Bolt, Beranek, and Newman, Inc., Methods of Flight Vehicle Noise Prediction (Section I). WADC Technical Report 58-343. Aeronautical Systems Division, Air Force Systems Command, USAF. Wright-Patterson AFB, Ohio. November 1958.
16. Franken, Peter A., and the Staff of Bolt, Beranek, and Newman, Inc., Methods of Space Vehicle Noise Prediction (Section VI). WADC Technical Report 58-343 (Vol. II). Aeronautical Systems Division, Air Force Systems Command, USAF. Wright-Patterson AFB, Ohio. September 1960.
17. Powell, Alan, "On the Effect of Missile Motion on Rocket Noise." J. Acoust. Soc. Am. vol. 30. November 1958. p.1048.
18. Williams, J. E. Ff., Some Thoughts on the Effects of Aircraft Motion and Eddy Convection on the Noise from Air Jets. U.S.A.A. Report No. 155. Dept. of Aeronautics and Astronautics, University of Southampton, Hampshire, England. September 1960.
19. Eldred, K. M., et al, Investigation of Noise with Respect to the LFC, NB-66 Aircraft. Report No. NOR-61-10, Norair Division, Northrop Corp., Hawthorne, California. April 1961.
20. Knowler, A. E. and Holder, D. W., The Efficiency of High Speed Wind Tunnels of the Induction Type. R. & M. No. 2448, Aeronautical Research Council Reports and Memoranda, Ministry of Supply, London, England. 1954.
21. Fakan, John C. and Mull, Harold R., Effect of Forward Motion on Sound-Pressure Level in the Near Noise Field of a Moving Jet. NASA Technical Note D-61 (Lewis Research Center, Cleveland, Ohio). National Aeronautics and Space Administration, Washington, D. C. October 1959.
22. Ames Research Staff, Equations, Tables, and Charts for Compressible Flow. Report 1135 (Ames Aeronautical Laboratory, Moffett Field, California). National Aeronautics and Space Administration, Washington, D. C. 1953.
23. Ower, E., The Measurement of Air Flow. Chapman & Hall, London, England. 1927.
24. Young, K. J., Sound Level Test of XB-47 Airplane. Boeing Test Report T-28164, The Boeing Company, Seattle, Wash. December 18, 1951.